UC San Diego

UC San Diego Electronic Theses and Dissertations

Title

Effect of a Holliday junction binding peptide, wrwycr, in human cells

Permalink

https://escholarship.org/uc/item/66s9w5x8

Author

Patra, Sukanya

Publication Date

2010

Peer reviewed|Thesis/dissertation

eScholarship.org Powered by the California Digital Library
University of California

UNIVERSITY OF CALIFORNIA SAN DIEGO

SAN DIEGO STATE UNIVERSITY

Effect of a Holliday junction binding peptide, wrwycr, in human cells

A Dissertation submitted in partial satisfaction of the requirements for the degree Doctor of Philosophy

in

Biology

by

Sukanya Patra

Committee in Charge:

University of California, San Diego

Professor Michael David

Professor Matthew D Weitzman

San Diego State University

Professor Anca M Segall, Chair

Professor Kathleen McGuire

Professor Roland Wolkowicz

Professor Robert W Zeller

2010

Copyright

Sukanya Patra, 2010

All rights reserved

The Dissertation of Sukanya Patra is approved, and it is acceptable in quality and form for publication on microfilm and electronically:

_____

_____

_____

_____

_____

_____

Chair

University of California, San Diego

San Diego State University

2010

DEDICATION

To my parents, Benu Binode Patra and Sandhya Patra for their immense love and unconditional support.

আমার জীবনের এই পরিচ্ছদ আমার বাবা ও মাকে উৎসর্গ করলাম।

I am honored to have you as my parents. Thanks for your constant motivation and encouragement that helped me prove and improve myself in this walk of life.

EPIGRAPH

"I am among those who think that science has great beauty. A scientist in his laboratory is not only a technician: he is also a child placed before natural phenomena which impress him like a fairy tale."

Madam Marie Curie

(Physicist, 1867-1934)

TABLE OF CONTENTS

Signature page …….. iii

Dedication ……... iv

Epigraph ……... v

Table of contents ……. vi

List of Abbreviations …….. x

List of Tables ……..... xiii

List of Figures …….. xiv

Acknowledgements …… xvii

Vita …… xix

Abstract …… xx

Chapter I. …… 1

Introduction …….. 1

Background …….. 1

Characteristics of wrwycr …… 4

Control peptides …… 6

Intriguing parallels between CPPs and wrwycr …….. 8

1. Molecular composition and uptake ……... 8

2. Anticancer properties of antimicrobial CPPs …….. 9

Modes of cell death …….. 10

Replication, DNA repair and Holliday junction ……. 13

Cancer versus normal cells ……... 16

Anticancer drugs used in the study …….. 16

Objective and Hypothesis ……. 17

Outline of the dissertation ……. 18

Chapter II. Effect of a DNA repair inhibitor in U2OS cells …….. 20

Abstract …….. 20

Introduction ……. 21

Results …… 23

wrwycr gets in U2OS cells by itself …….. 23

wrwycr exhibits dose-dependent acute toxicity in U2OS cells ……... 27

wrwycr-induced cytotoxicity is permanent …… 31

wrwycr induces early and late apoptosis in U2OS cells …… 32

Effect of wrwycr becomes more severe in the presence of DNA damaging agents ……. 37

wrwycr-induced γ-H2AX foci formation is potentiated upon addition of DNA damaging agents …….. 42

wrwycr mildly inhibits replicative DNA synthesis …….. 46

wrwycr interferes with recovery from replication fork collapse caused by HU ……. 48

IMR-90 cells, a slow-growing, non-cancerous cell line are resistant to wrwycr ……... 57

Discussion ……. 57

Chapter III. Uptake and effects of wrwycr in HeLa cells and a HeLa cell variant 64

Introduction …… 64

Backgound ……... 64

Hypothesis and previous study ……... 65

Summary of results with HeLa cells …… 66

Limitations and current research outline ……. 66

Results ……. 69

Uptake of wrwycr in HeLa cells …… 69

Etoposide potentiates wrwycr-induced cytotoxicity in HeLa cells …. 71

Cytotoxicity induced by wrwycr is irreversible but not cumulative … 78

wrwycr treatment does not induce apoptosis but increases cell size … 82

wrwycr initiates DNA DSB response by generating γ-H2AX foci ….. 88

Discussion ……... 89

wrwycr uptake in HeLa cells is linear ……..... 90

wrwycr treatment elicits a permanent but non-cumulative damage in HeLa cells ……. 90

Concurrent administration of etoposide and wrwycr induces non-apoptotic DNA damage …… 93

Chapter IV. IMR-90 cells are resistant to wrwycr-mediated cytotoxicity ….. 95

Abstract ……... 95

Introduction …….. 96

Results ……. 97

WRWYCR (wrwycr) entry in IMR-90 cells is less efficient than IMR-90 cells …… 97

IMR-90 cells are resistant to wrwycr-mediated acute cytotoxicity …... 98

Concurrent administration of hydroxyurea and wrwycr reduces DNA content of IMR-90 cells …… 102

wrwycr by itself does not induce apoptosis in IMR-90 cells …….. 106

wrwycr treatment does not cause DNA breaks nor induce DSBR ….. 108

Discussion ……. 110

Chapter V. Discussion and Future Work …….. 112

Characteristics of peptide WRWYCR …….. 112

1. Factors affecting intracellular wrwycr concentration ……. 112

2. Relationship between uptake and cytotoxicity …….. 113

3. Co-localization studies with WRWYCR …….. 114

Evaluation of DNA damage response and determining correlation with cytotoxicity …….. 115

Possible mechanisms of cell death …….. 115

Development of a sensitive assay to achieve stepwise synchronization of cells and to measure DNA synthesis ……. 118

Discussion of the queries and suggestions for future work …….. 119

Summary and model of wrwycr action ……. 122

Chapter VI Materials and Methods …… 124

Appendix A.1 …… 137

Appendix A.2 …… 139

Appendix A.3 …… 140

Appendix A.4 …… 142

Appendix A.5 …… 146

Appendix A.6 …… 150

References ……. 151

LIST OF ABBREVIATIONS

AMP	anti-microbial peptide
APC	allophycocyanin
ATCC	American Type Culture Collection
ATM	ataxia telangiectasia mutated
ATR	ATM and Rad3 related
BME	beta mercaptoethanol
CARD	caspase recruitment domain
CDC	Centers for Disease Control and Prevention
CFA	colony forming assay
CPP	cell penetrating peptide
$CuSO_4$	copper sulphate
cytC	cytochrome C
DAPI	4,6-diamidino-2-phenyl indole
DMEM	Dulbecco's modified eagle medium
DMSO	dimethyl sulphoxide
DNA	deoxyribonucleic acid
DSB	double strand break
DSBR	double strand break repair
DTT	dithiothreitol
EDTA	ethylene diamine tetraacetic acid
EdU	5-ethynyl-2'-deoxyuridine

FACS	fluorescence activated cell sorting
FBS	fetal bovine serum
FITC	fluorescin isothiocyanate
FSC	forward scatter
γ-H2AX	histone protein variant H2AX phosphorylated at serine 139
GFP	green fluorescent protein
HJ	Holliday junction
HMG	high mobility group
HRR	Homologous recombination repair
H_2O_2	hydrogen peroxide
HPLC	high pressure liquid chromatography
HU	hydroxyurea
λ-phage	bacteriphage lambda
λ-SSR	lambda phage-mediated site specific recombination
MIC	minimum inhibitory concentration
μM	micromolar
mM	milimolar
MMC	mitomycin C
MMP	mitochondrial membrane potential
MOMP	mitochondrial outer membrane potential
MRR	membrane repair response
MTT	[3-(4,5-dimethylthiazol-2-yl)-2,5-diphenyltetrazolium bromide]
NaCl	sodium chloride
NHEJ	non homologous end joining

PBS	phosphate buffered saline
PE	phycoerythrin
PI	propidium iodide
PS	phosphatidyl serine
RFU	relative fluorescence units
Rho-L8	rhodamine tagged WRWYCR
RT	room temperature
SSC	side scatter
TFA	trifluoroacetic acid
TMRE	tetramethyl rhodamine ethyl ester perchlorate
TUNEL	terminal duTP nick-end labeling
UV	ultraviolet radiation
WRWYCR	peptide composed of L-amino acids
wrwycr	peptide composed of d-amino acids
Z-VAD	caspase family inhibitor

LIST OF TABLES

Table I-1: Relative binding affinity of DNA substrates with wrwycr……... 6

Table II-1: Quantitation of intracellular wrwycr concentration in U2OS cells…… 27

Table II-2: Comparison table of caspase-3 upregulation vs % TUNEL positive cells ... 36

Table II-3: Comparison table of caspase-3 versus % TUNEL following co-treatment of wrwycr and etoposide or hydroxyurea…… 40

Table III-1: Review of all the assays in HeLa cells performed previously in laboratory . 67

Tabel III-2: Quantitation of intracellular wrwycr concentration in HeLa cells…… 75

Table III-3: Comparison of MTT versus Live/Dead assay in HeLa cells…… 77

Table IV-1: Quantitation of intracellular wrwycr concentration in IMR-90 cells …….. 100

Table IV-2: Cell cycle analysis of IMR-90 cells…… 105

Table IV-3: Comparison table of % TUNEL and % γ-H2AX positive IMR-90 cells ….. 109

Table V-1: Comparison of wrwycr uptake in U2OS, HeLa and IMR-90 cells…… 116

Table A.5-1: Quantitation of intracellular dodecapeptide in U2OS cells …… 148

LIST OF FIGURES

Figure I-1 Cellular fates after DNA damage
Panel A Different pathways ……..... 2
Panel B Proteins involved …… 3

Figure I-2 Schematic diagram of various stages of apoptosis …… 12

Figure I-3 DNA DSB response pathways and important players deciding the fate of the cell …… 15

Figure II-1 Uptake of wrwycr (WRWYCR) inside U2OS cells ……. 26

Figure II-2 wrwycr treatment for 24 h induces dose-dependent acute toxicity ……. 30

Figure II-3 wrwycr-induced cytotoxicity is permanent ……... 33

Figure II-4 wrwycr treatment induces apoptosis in some U2OS cells …….. 35

Figure II-5 wrwycr-induced cytotoxicity becomes more severe upon co-treatment with sublethal dose of etoposide ……... 39

Figure II-6 Concurrent administration of DNA damaging agents increases wrwycr-induced DNA breaks ……... 41

Figure II-7 wrwycr-induced γ-H2AX foci formation increases upon co-treatment with sublethal doses of HU or etoposide ……. 44

Figure II-8 wrwycr mildly inhibits replicative DNA synthesis ……... 47

Figure II-9 wrwycr interferes with recovery from HU-mediated arrest …... 51

Figure II-10 DNA synthesis inhibition is not due to cell death …….. 53

Figure II-11 Upregulation of ATR vs. γ-H2AX during recovery from HU-mediated arrest …….. 55

Figure II-12 Upregulation of phospho-ATM during recovery from HU-mediated arrest ……... 56

Figure III-1 Uptake of Rho-WRWYCR in HeLa cells …… 70

Figure III-2 Standard curve of wrwycr by HPLC …… 72

Figure III-3 Representative HPLC trace of wrwycr in HeLa cell lysate …. 73

Figure III-4 Summary graph of HPLC quantitation in HeLa cells …….. 74

Figure III-5 24 h of wrwycr treatment has a modest killing effect in HeLa cells …… 76

Figure III-6 Etoposide mildly potentiates wrwycr-induced killing of HeLa cells …… 79

Figure III-7 wrwycr-induced HeLa cell damage is irreversible ……... 81

Figure III-8 wrwycr treatment with or without etoposide does not induce significant apoptosis but interferes with cell division …….. 85

Figure III-9 Immunofluorescence microscopy of HeLa cells for upregulation of γ-H2AX foci …… 91

Figure IV-1 Uptake of Rho-WRWYCR in IMR-90 cells ……. 99

Figure IV-2 IMR-90 cells are resistant to wrwycr-induced cytotoxicity ….. 101

Figure IV-3 Doubling time of IMR-90 cells increase upon co-treatment with etoposide or HU ……. 103

Figure IV-4 Effect of wrwycr on cell cycle with or without an Intra-S blocker, HU ……. 104

Figure IV-5 wrwycr treatment does not induce apoptosis in IMR-90 cells .. 107

Figure V-1 Comparison of uptake and cytotoxicity of wrwycr in U2OS, HeLa and IMR-90 cells ……... 117

Figure A.1-1 Mass spectrometry of HPLC fraction containing peptide monomer and dimer ……. 137

Figure A.1-2 Confocal microscopy of Rh-WRWYCR treated U2OS cells … 138

Figure A.2-1 Phase contrast microscopy of U2OS cells ……... 139

Figure A.3-1 Rh-WRWYCR localizes in or around mitochondria …… 140

Figure A.3-2 Rh-WRWYCR has some co-localization with ER resident GRP-78 …… 141

Figure A.4-1 wrwycr-treatment upregulates p44 protein in U2OS cells … 142

Figure A.4-2 Co-treatment with HU increases p44 accumulation in U2OS cells ……... 143

Figure A.4-3 wrwycr induces p53-independent apoptosis …… 144

Figure A.4-4 Accumulation of DNA breaks is also p53-independent …… 145

Figure A.5-1 Dodecamer peptide induces dose-dependent toxicity in U2OS cells ……... 149

Figure A.6-1 wrwycr induces some nuclear condensation and membrane damage in U2OS cells ……... 150

ACKNOWLEDGEMENTS

I express my heartfelt gratitude towards my advisor Professor Anca Segall for her co-operation and understanding through the years of my PhD career. I must acknowledge her respect for my urge to do cancer research that led us to explore and design a novel project for a microbiology laboratory involving mammalian tissue culture. Her patience and optimism during the research progress provided me enough encouragement to encounter the queries with boldness. Especially, her non-interfering nature allowed me to train myself as an independent researcher over the years.

Special thanks goes to my committee member, Dr. Matthew Weitzman, first for his immense help at the nascent stage of the project by donating to us the cell lines and also for his crucial advices at different stages of my project. I would also like to appreciate the detailed efforts of Professor Michael David that helped me stay focused at various stages of the project. Constructive feedbacks of Professor Kathie McGuire at important crossroads provided confidence in my analytical strength. Dr Roland Wolkowicz was there to help me in all the different ways. Discussions with him at several occasions have turned fruitful at later stages. I warmly thank Dr Robert Zeller for guiding me with valuable suggestions throughout my dissertation. My advisor and I are extremely honored to have such an interactive committee who has been deeply involved in my dissertation work.

I extend my appreciation to Dr Steve Barlow at the Electron microscopy facility, San Diego State University, for helping me set up the confocal microscopy experiments and for useful discussions. I thank Tong Xu and Brett Hilton for queries regarding flow cytometry. I recognize the help of Leo Su and David Fujimoto provided during my first days of cell culture. Special thanks goes to Nathan Authement who helped me finish off some of my

experiments during the final period of my dissertation. Also I would like to thank Professor Ian Booth for his careful analysis of my dissertation and for fruitful discussions.

Last but most importantly, I cherish the immense love and support of my family without which it would have been impossible for me to reach this point. I deeply appreciate the co-operation and understanding of my husband, Sudipto, who has gone out of his way at several occasions to help me pursue my dream. I extend my love to my three year old daughter, Mrittika, who has been a constant source of solace during the ups and downs of my dissertation life. I acknowledge the friendly discussions we had with my brother, Suman and my sister-in-law, Lopa, in this time. Finally I thank my parents and my parents in-law from the bottom of my heart who have taken turns to take care of my daughter so that I can devote more time in my research work.

Chapter II, in full, is being prepared for a future publication. The dissertation author is the primary investigator and author of this work. Co-authors are Nathan Authement and Anca Segall. I would like to acknowledge Nathan for his great assistance in performing the microscopy experiments under constant supervision of the primary author.

Chapter III, in full, is being prepared for future publication. The dissertation author is a co first author of the work. Only the part performed by the dissertation author is presented in chapter III. The primary author in this paper is Leo Su and the corresponding author is Anca Segall.

VITA

2000	Bachelor of Science, Pharmaceutical technology
2000-2002	Research assistant, Department of Pharmaceutical Technology Jadavpur University, Kolkata
2002	Master of Science, Pharmaceutical Technology
2003-2008	Teaching Assistant, Department of Biology San Diego State University, San Diego
2008-2009	Research Assistant, Department of Biology San Diego State University, San Diego
2010	Doctor of Philosophy University of California, San Diego and San Diego State University

PUBLICATIONS

Patra S, Authement R.N and Segall A.M
Effect of a Holliday junction binding peptide in U2OS cells. To be submitted.

Su L, **Patra S** and Segall A. M
A Holliday junction binding peptide causes accumulation of DNA breaks in Hela cells. To be submitted

Mazumder U.K, Gupta M, Bera A, Bhattacharya S, Karki S, Manikandan L and **Patra S.**
Synthesis, antitumor and antibacterial activity of some $Ru(bpy)_2^{2+}$/4-substituted thiosemicarbazide complexes. Indian Journal of Chemistry (2002)

Gupta M, Mazumder U. K, Chaudhuri I, Chaudhuri R. K, Bose P, Bhattacharya S, Manikandan L and **Patra S**.
Antimicrobial activity of *Eupatorium ayapana* (2002)

ABSTRACT OF THE DISSERTATION

Effect of a Holliday junction binding peptide, wrwycr, in human cells

by

Sukanya Patra

Doctor of Philosophy in Biology

University of California, San Diego, 2010
San Diego State University, 2010

Professor Anca Segall, Chair

Cancer is a life threatening disease characterized by uncontrolled growth and spread of abnormal cells. Extensive research in the field for the last fifty years led to the discovery of diverse classes of drugs called chemotherapeutics. The mode of action of many of these drugs exploits the fact that cancer cells replicate much faster than normal cells. Different classes of drugs target different proteins in the DNA replication and repair pathways and kill cells by interfering with these indispensable life processes. Two major obstacles to successful cancer chemotherapy are the significant cytotoxicity of the chemicals to normal cells and the high

probability of resistance. Combination therapies, in which two or more different drugs are used, may help avoid both these problems.

In this study I investigated the effects of a hexapeptide molecule (sequence wrwycr) in cancer cells versus normal cells with particular emphasis on the cytotoxicity of the peptide, and DNA damage resulting from exposure. Peptide wrwycr was originally isolated in our laboratory in a combinatorial peptide library screen for inhibitors of phage lambda site-specific recombination. Subsequently it was discovered that the peptide stabilizes a transient DNA intermediate, the Holliday junction (HJ) generated in the process of recombination and disrupts the equilibrium of the reaction. Extensive *in vitro* and *ex vivo* characterization of the peptide has revealed that it belongs to the class of broad spectrum antibacterial that induces its bactericidal effect via DNA damage. Since HJs (and other branched DNA substrates) are produced in both prokaryotes and eukaryotes, I tested the effects of wrwycr on human cells by studying two cancer cell lines, U2OS, HeLa and a non-cancerous lung fibroblast, IMR-90 as a control. This is a preliminary step towards exploring the anticancer potential of this peptide.

Our results indicate that the effect of wrwycr in cultured human cells is cell-type dependent. Like natural, cationic, hydrophobic antibacterial peptides, wrwycr can enter cancer cells more efficiently than normal cells. U2OS, an osteosarcoma cell line is more sensitive to wrwycr-induced cytotoxicity than HeLa, a cervical cancer cell line. In U2OS cells, wrwycr produces a non-linear dose-dependent cytotoxicity partly via apoptosis. Concurrent administration of a sublethal dose of etoposide with wrwycr potentiates cell death in U2OS and induces the DNA double strand break response. More specifically, wrwycr interferes with recovery from intra-S arrest in synchronized U2OS cells in a linear, dose-dependent manner with no significant killing. This suggests that the exponential increase in cell death upon linear increase in wrwycr dose could be due to the interaction of peptide wrwycr with other cellular

targets generating different forms of damage like ER stress, membrane rupture or mitochondrial damage.

HeLa cells show more signs of cell cycle arrest than cell death with wrwycr treatment. This becomes more evident upon simultaneous treatment with etoposide. Interestingly, IMR-90 cells are the most resistant to wrwycr lethality and DNA damage. This can be attributed only partly to lesser uptake inside these cells. Taken together, we have starting evidence that wrwycr has potential to be used as an anticancer drug by itself or in combination therapy. Much more basic and clinical research needs to be done before this long term goal can be achieved.

CHAPTER I.

INTRODUCTION

Background

Deoxyribonucleic acid (DNA) contains the genetic instructions specifying the biological development of all cellular forms of life, and many viruses. Fidelity of this information transfer during replication is necessary for maintaining healthy life and occurs mainly through DNA recombination. The error-free repair of DNA damage, too, involves recombination. The importance of understanding this fundamental process can hardly be overstated. In order to study this process, the intermediate structures created during DNA recombination need to be isolated. However, these intermediates are transient in nature. Agents that trap these intermediates are thus very useful for isolating intermediates and for dissecting the pathways.

Deregulation of DNA damage repair can lead to a number of possible cellular fates (Figure I-1A). Functional interplay of an array of proteins accomplishes this critical assignment (Figure I-1B; Zhou and Elledge, 2000). Sensor proteins detect the damage and trigger a wide range of cellular processes to correct the injury. The first step is cell cycle arrest, which gives the cell time to repair its DNA and restart the replication fork. When the cellular machinery fails to correct its DNA in time, the cell expresses specific genes and kills itself in an orchestrated pattern without inflammation. Mutations that result in malfunction of one or more of these vital proteins lead to uncontrolled DNA replication and abnormal growth of cell and tissue referred to as cancer.

Cancer is one of the most life threatening disease of the past and current century. So far, permanent cure of this ailment has been rare. Current chemotherapeutics often target proteins involved in DNA processing during replication and repair at particular stages of cell cycle.

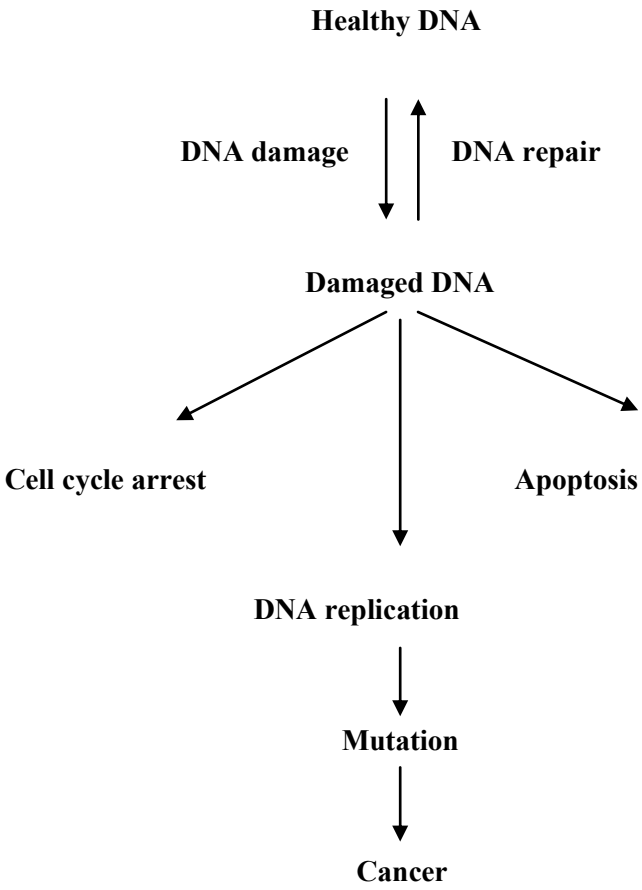

Figure I-1. Cellular fates after DNA damage.
This is a simplified representation of the different directions a cell containing damaged DNA can take. **Panel A** portrays the different pathways that could be taken and their consequences.

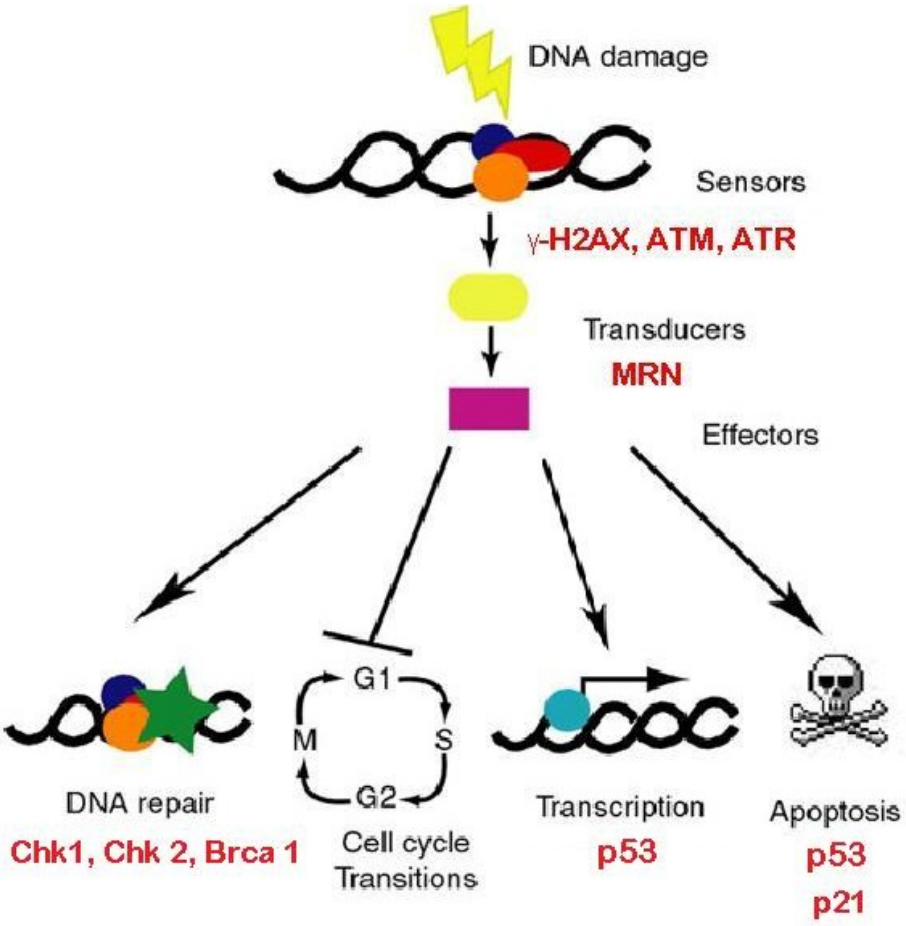

Figure I-1. The cellular fate after DNA damage.
Panel B depicts a few of the proteins that may act on the damaged DNA and dictate its fate. Figure adapted from Zhou and Elledge, Nature, 2000 and *http://www.infobiogen.fr/services/chromcancer/Deep/DoubleStrandBreaksID20008.html*

However, due to significant redundancy and crosstalk between the pathways, cancer cells often survive and become resistant to the drug. Molecules that target transient DNA structures produced during DNA synthesis and repair, and which trap and inhibit their resolution, have a potential to form a category of novel chemotherapeutics, and may be particularly useful in combination with other drugs.

Characteristics of wrwycr

Former members of our laboratory screened a combinatorial peptide library for molecules that inhibit site-specific recombination mediated by the lambda phage tyrosine recombinase, integrase (Cassell et al, 2000, Boldt et al 2004). The most potent peptide with the sequence wrwycr, bears no resemblance with parts of integrase or with any of the helper proteins of the pathway (Cassell et al, 2003, Boldt et al, 2004). Subsequently, it has been shown to bind and trap a common intermediate in the recombination pathway, Holliday junctions (HJs) *in vitro* [Kepple et al, 2005]. This peptide and a related dodecamer can also inhibit tyrosine recombinase-mediated excision of several prophages, in *E. coli* and *Salmonella*, and to stabilize the Holliday junction intermediates of lambda site-specific recombination *in vivo* (Gunderson et al, 2009). More recently, 2-dimensional gel electrophoresis analysis (methods based on Bell and Byers, 1983; Friedman and Brewer, 1995) has shown that peptide treatment increases HJ in bacteria (Medina-Cleghorn and Segall, unpublished results). HJ is a transient DNA intermediate that is produced during DNA repair by homologous recombination (HR) and site-specific recombination. The formation and resolution of HJs, their level within cells, and the enzymes that both generate and resolve them are of great interest. Thus, this peptide inhibitor may have the potential to help dissect both homologous recombination and recombination-dependent repair *in vitro* and *in vivo* [Kepple et al 2005] and perhaps be the lead compound in a novel class of DNA damage repair inhibitors.

Peptide wrwycr is bactericidal and treated cells accumulate DNA breaks. The peptide interferes with segregation of chromosome and is synergistic with UV, MMC and H_2O_2 in bacteria (Gunderson and Segall, 2006; Su et al, manuscript in preparation). Detailed analysis of several mutants defective in various steps of the homologous recombination pathway, like strand invasion, HJ resolution, single strand gap and double strand break processing, have supported the idea that HJ and other branched DNA intermediates are targets of the peptide (Gunderson et al, manuscript in preparation). Thus, at least in bacterial cells, wrwycr acts as a DNA damage repair inhibitor. Since HJs are also produced in eukaryotic cells, it would be useful and interesting to understand wrwycr activity in human cells (cancer and normal) in order to explore its potential as a future antibiotic and chemotherapeutic. Already we have evidence that wrwycr is toxic to HeLa cells at high concentrations presumably by accumulating DNA breaks that cannot be repaired efficiently (Su, Patra and Segall, manuscript in preparation).

The active *in vitro* form of wrwycr is a dimer linked through a disulfide bridge. It loses potency significantly when used in the presence of a reducing agent like DTT (dithiothreitol) or BME (β-mercaptoethanol). Modeling experiments corroborate the above data by providing evidence that the WRWYCR dimer has more stable interactions with the center of the HJ than the wrwycr monomer (Kepple et al, 2008). The interaction of WRWYCR (wrwycr) with DNA is structure-specific. No preference towards particular DNA sequences has been found. The peptide binds protein-free branched DNA intermediates with the hierarchy shown in Table I-1 and inhibits both structurally and mechanistically distinct proteins including RecG, RuvABC, hRad54, etc) that process HJ and other branched DNA structures resembling HJ (Kepple et al, 2005, 2008; Bugreev et al; 2006, 2007; Rajeev et al; 2007).

Table I-1. Relative binding affinity of DNA substrates with wrwycr

Substrate	K_d (nM)[a]
Holliday junction[b]	14.3 ± 3.2
Complete fork	63.5 ± 12.0
Lagging strand fork	79.2 ± 17.3
Leading strand fork	132 ± 32.8
Flayed fork	628 ± 107
Oligomer	731 ± 134

[a] K_d measurements of the relative binding affinity of WRWYCR for various branched DNA substrates are obtained using solution fluorescence quenching assays (Table adapted from Kepple et al, 2008)

[b] Holliday junction is the only DNA substrate that forms a complex stable to electrophoresis.

Control peptides used in the study

In this dissertation, we used two "negative control" peptides, wkhyny and WRWYAR, for investigating the effects of wrwycr in human cells specifically to assess (1) whether wrwycr effect is specific rather than a non-specific response generated by exposure to any cationic peptide of similar size, and (2) whether wrwycr loses potency significantly when its ability to dimerize is compromised. To address the second possibility, in a few of the assays, I also used the peptide, wrwyrggrywrw (dodecamer).

wkhyny : This hexapeptide came out of the first screen of the combinatorial peptide libraries. It accumulates HJ in the λ-phage mediated recombination reaction without affecting the first round of cleavage (Cassell et al, 2000). However, it has significant differences from wrwycr. First, accumulation of HJ in the recombination reaction is about 50-fold less (Boldt et al, 2004, Kepple et al 2005) compared to wrwycr. Second, it cannot bind to protein-free HJ

when either gel electrophoresis or solution quenching assays are used (Kepple et al 2005 and 2008).

WRWYAR (C5A) : This hexapeptide was generated by replacing the cysteine residue of WRWYCR with alanine so that it cannot form a dimer. Use of this peptide demonstrates both the importance of cysteine and the necessity of dimerization for the function of wrwycr. It should be noted that wrwycr and the other two control peptides were the dextro (d-) form, this peptide was in laevo (L-) form because at the time the dextro form of this peptide was not available.

wrwyrggrywrw : It is known that wrwycr is active as a dimer. However, the reducing environment inside cells converts some dimer of wrwycr to wrwycr monomer, thus decreasing the active peptide concentration *in vivo*. With this idea, a dodeca-mer peptide was synthesized with nearly the same sequence as wrwycr, but with the cysteine replaced by glycine such that it mimics a dimer of wrwycr resistant to DTT. Same input concentration is expected to have higher intracellular concentration of wrwyrggrywrw than wrwycr dimer and should be significantly more cytotoxic.

Intriguing parallels between cell penetrating peptides (CPPs) and wrwycr (d8)

1. Molecular composition and uptake

Cell-penetrating peptides belong to a class of short cationic peptides with amphipathic nature. They can enter prokaryotic and eukaryotic cells without the aid of any transporter proteins (Lindgren et al, 2000; Terrone et al, 2003). In fact, CPPs often act as cargo to deliver different classes of impermeant proteins inside cells (Derossi et al, 1998; Scheller et al, 1999; Lindgren et al, 2000; Patel et al, 2009). The mechanism of CPP uptake is quite unclear and highly debated. Some groups have evidence that macropinocytosis is a possible mechanism of uptake (Kaplan et al, 2005, Nakase et al, 2007). Others believe that clathrin-dependent (Richard et al 2005) or independent (Padari et al, 2005, Duchardt et al, 2007) endocytosis is the predominant uptake mechanism. A more recent study has shown that these peptides upregulate the membrane repair response (MRR) in the plasma membrane and help repair the transient damage caused during the peptide uptake (Palm Apergi et al, 2009).

Naturally occurring CPPs are usually at least 20 amino acids long. However, synthetic peptides derived from some naturally occurring peptides are as short as 9 amino acids (Lee et al, 2005). These small peptides are often cytotoxic and induce death to the target cells by interacting with the parent protein. For instance, a peptide derived from granulysin causes hemolysis of erythrocytes when taken up by these cells whereas the parent protein does not (Li et al, 2005).

The dimer of wrwycr is a 12-amino acid cationic peptide containing hydrophobic residues like tryptophan (W) and tyrosine (Y) and charged residues like arginine (R). Thus it might belong to the class of cell penetrating peptides (CPPs) and may translocate across the human cell membrane by one or more of the mechanisms described above.

2. Anticancer properties of antimicrobial, cell penetrating peptides

wrwycr (WRWYCR) is a broad spectrum antibacterial peptide molecule. (Gunderson et al, 2006, 2009) and can be classified as an antimicrobial peptide (AMP). It is known that AMPs have a pronounced effect on membranes and often inhibit bacterial growth by causing membrane perturbation (Lohner et al, 2005; Pistolesi et al, 2007; Palm Apergi et al, 2009). In fact, wrwycr also has a similar membrane effect (Yitzhaki, Rostron, Xu, Authement and Segall, manuscript in prep). However, wrwycr-induced DNA damage is much more pronounced than its effect in bacterial membranes (Gunderson and Segall, 2006, Gunderson et al, 2009). wrwycr causes accumulation of single and double strand DNA breaks (Gunderson et al, 2006; Gunderson et al, manuscript in prep) presumably by interacting with certain DNA repair intermediates including HJ (Gunderson et al, 2009, Cleghorn et al, unpublished results). Thus wrwycr belongs to a novel class of antimicrobial peptides. One important difference between wrwycr and most antibacterial peptides (like defensin, cecropin, etc) is that the latter kill cells mainly by causing cell lysis, while wrwycr does not cause any cell lysis. (Gunderson and Segall, 2006; Su et al, unpublished results).

Several recent studies have suggested a potential anticancer effect of some antimicrobial peptides (Papo et al, 2003; Lee et al, 2005). Healthy eukaryotic cells retain lower membrane potential and their outer leaflet mainly contains zwitterions (Matsuzaki, 1999; Shai, 1999). By comparison, cancer cells maintain a very large membrane potential with a much higher content of anionic phospholipids on the outer leaflet, similar to bacteria (Chan et al, 1998). Thus cationic AMPs disrupt bacterial and cancer cell membranes much more efficiently than normal eukaryotic membranes (Chan et al, 1998). This similarity in membrane composition between bacterial and cancer cells as well as the potential greater need of cancer cells for

DNA repair in tumor compared to normal eukaryotic cells, prompted us to think that it would be interesting to explore the anticancer potential of this peptide.

Modes of cell death

Incubation of cells (prokaryotic or eukaryotic) with certain classes of peptides is growth inhibitory or cytotoxic depending on the time of exposure and concentration of peptide (Saido Sakanaka et al, 1999). The three primary mechanisms of cell death described are apoptosis, necrosis and autophagy (Edinger et al, 2004; Kroemer et al, 2005; Golstein et al, 2006).

Apoptosis or programmed cell death is a normal component of the development and health of multicellular organisms. Here the cell activates an intracellular death program and kills itself in a controlled way. Since the cell itself plays an active role in this process of death, it is often referred to as 'cell suicide' (Kerr et al, 1972). The controlled, orchestrated pattern of signaling that leads to the stepwise demise of the cell makes apoptosis distinct from necrosis. However, recent studies argue that necrosis is also highly regulated, albeit via separate pathways (Arora et al, 1996; Berninghousen and Leippe, 1997; Tavernarakis, 2007). The pathways of apoptosis may be extrinsic (triggered by death ligands binding to death receptors) or intrinsic (e.g., the mitochondrial pathway triggered by several apoptotic stimuli inside the cell like oxidative damage) (Bratton et al, 2001, Danial et al, 2004; Fulda and Debatin, 2006).

A schematic of the various stages of apoptosis are shown below (Fig I-2). Upon receiving an apoptotic stimulus, the genome of the cell will fracture, the cell will shrink and part of the cell will disintegrate into smaller apoptotic bodies (Fig I-2). The apoptotic bodies containing the degenerating materials of the cell are packaged tightly and stay within the cell membrane until phagocytosed by neighboring macrophages (Raff, 1998). The different types of apoptotic stimuli include virus infection, DNA damage repair deficiency, embryonic development, etc.

One of the earliest hallmarks of apoptosis includes phosphatidyl serine (PS) translocation from the inner to the outer leaflet of the plasma membrane without any persistent damage of the plasma membrane (Fadok et al, 1992). This is followed by mitochondrial outer membrane permeabilization (MOMP) that leads to the release of cytochromeC from the inner membrane and intra-cristal space of mitochondria (Green and Kroemer, 2004; Shiozaki and Shi, 2004). This initiates the formation of apoptosomes that recruit and activate the procaspases via the CARD domain (Acehan et al, 2002). The procaspases are activated to initiator caspases which in turn generate the executioner caspases. Caspases belong to a class of cysteine proteases that cleave different cellular proteins at specific aspartate residues (Alnemri et al, 1996).

In the various chapters of this dissertation, we have addressed whether peptide wrwycr induces apoptosis by measuring annexin V as the early response, cytochrome C release and loss of mitochondrial membrane potential (MMP) as the central response, and caspase-3 upregulation as the late response of apoptosis after peptide treatment with or without concurrent administration of agents triggering the DNA damage response.

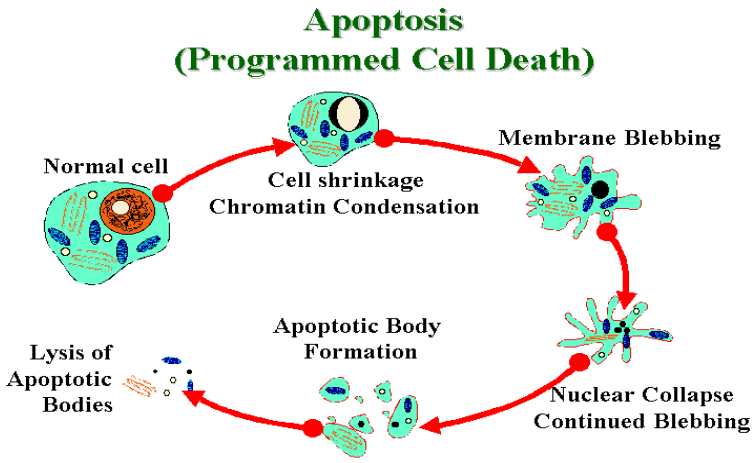

Figure I-2. Schematic diagram of various stages of apoptosis.

Upon receiving a signal of apoptosis, a cell starts to shrink, nuclear material also condenses, cell membrane continues to disintegrate to form small apoptotic bodies that finally undergo lysis. Figure adapted from *www.microbiologybytes.com/virology/kalmakoff*.

Replication, DNA repair and Holliday junction

DNA damage is an inevitable consequence of the normal cell cycle. The genome is particularly sensitive during replication, when several exogenous and endogenous DNA damaging agents target the somewhat relaxed DNA and interfere with replication fork progression (Paulsen and Cimprich, 2007). Every cell has several mechanisms to repair DNA damage (Li and Heyer, 2008). In eukaryotes, this is accomplished by triggering several checkpoints throughout the cell cycle. Activation of cell cycle checkpoints pauses replication and allows the cell more time to repair. Successful DNA repair helps the cell recover from the damage, whereas persistent DNA damage with lack of or insufficient repair causes the cell to enter into permanent senescence or triggers apoptosis. In cases when the cell manages to escape these outcomes by deregulating some essential protein(s) in the pathway, genomic instability, mutagenesis and cancer predisposition ensues. (Figure I-1A, Hoejimakers, 2001; Khanna and Jackson, 2001).

Molecular mechanisms that monitor and regulate replication fork progression are necessary to safeguard the genome from undergoing genomic instability (Paulsen and Cimprich, 2007). This is accomplished by the rigorous interplay of approximately 130 different proteins that are upregulated and may undergo intranuclear redistribution (ATR), (Zou et al, 2002; Zhang et al, 2005) and/or post-translational modification (p53, ATM), (Chehab et al, 1999; van Gent et al, 2001) in response to any DNA damage. These proteins in turn initiate a signal of response to block cell cycle progression, downregulate origin firing, stabilize the affected fork and restart replication. During normal DNA replication, a typical mammalian cell makes about 1.2×10^5 mistakes per cell per division leading to different chemical alterations in the DNA (Pray, 2008). If an active replication fork meets the lesion before it has been repaired, it could lead to replication fork stalling. Persistence of a stalled

fork that is not restarted for certain time ultimately leads to a double strand break (DSB) and thereby triggers a double strand break response (DSBR) which is repaired via homologous recombination repair (HRR).

An intermediate commonly formed in this process is the Holliday junction (HJ). Formation and resolution of HJs are highly reversible and extremely energy efficient. Several other transient, branched DNA structures such as replication forks (other *in vitro* wrwycr substrates mentioned in Table I-1), or D-loops are produced during several pathways of recombination-dependent DNA repair (Figure I-3). Because HJ is an *in vitro* (and bacterial) target of wrwycr, it would be interesting to understand the effect of wrwycr on mammalian cells (cancer versus normal) and try to understand whether the effect (if any) correlates with DNA damage repair. The results may suggest the possibility of wrwycr targeting HJ (and other branched DNA intermediates) in human cells.

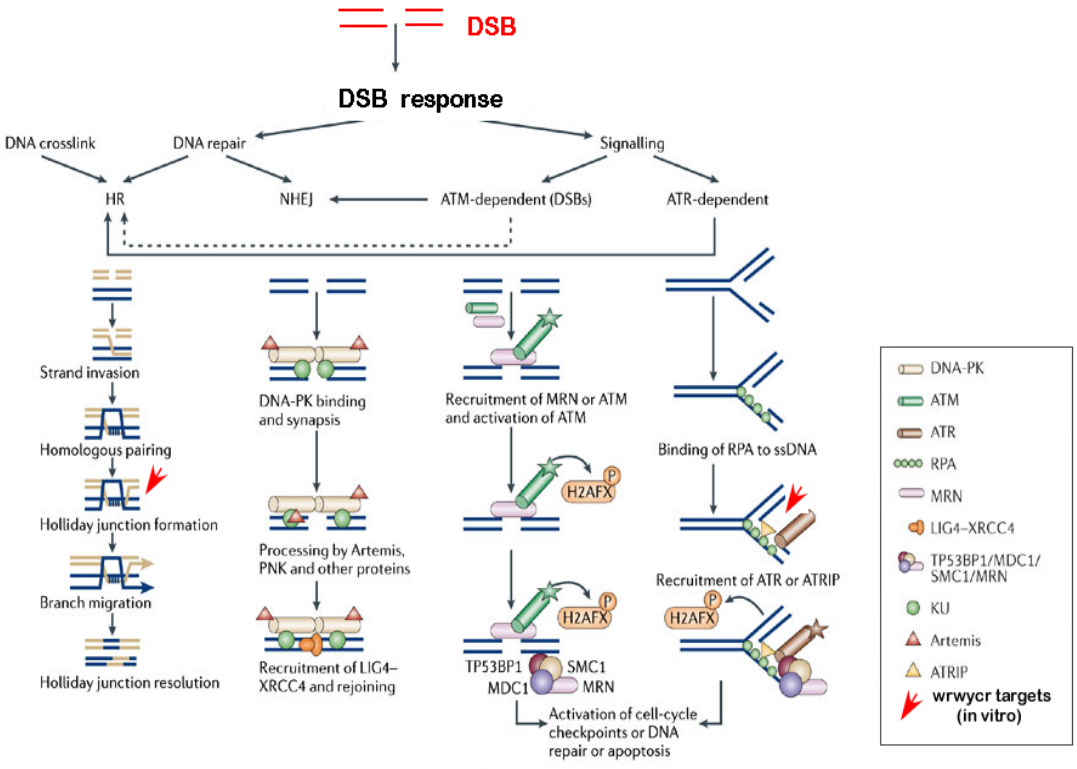

Figure I-3. DNA DSB response pathways and important players deciding the fate of the cell. Figure adapted from O'Driscoll & Jeggo, Nature Reviews Genetics, 2006;7:45-54

Cancer versus normal mammalian cells

Normal human cells regulate their cell cycle stringently for successful maintenance of genomic stability. During immortalization and transformation into a cancer cell, one or more of these pathways become deregulated. Thus cancer cells cycle much faster and are expected to produce more repair and replication intermediates as compared to primary or low passage cells. Also, cancer cells are more permeable to cytotoxic molecules like cell penetrating cationic peptides due to the more anionic nature of their cell membrane (Papo and Shai, 2003, 2005). Normal cells, on the other hand have more zwitterions in their membrane which allow less favorable entry of these peptides (Chan, S. C; 1998)

Anticancer drugs used in the study

I used two chemotherapeutic drugs in the study.

Etoposide is a powerful poison of topoisomerase II-DNA complex that interferes with the cleavage-religation reaction of this mammalian enzyme and stabilizes a cleavable protein-DNA complex producing double strand breaks (Chen et al, 1984; Van Maanen et al, 1988; Tanabe et al, 1991; Treszezamsky et al, 2007). Etoposide-induced DNA damage is usually repaired by homologous recombination repair (HRR).

Hydroxyurea (HU) is a cell cycle specific anticancer drug that inhibits ribonucleotide reductase and depletes cells of their dNTP pool causing intra-S arrest. Prolonged exposure or high concentration of HU can produce DSBs (Saintigny et al, 2001; Lundin et al, 2002; Lundin et al, 2003) and generate ATR-dependent phosphorylation of H2AX (Ward and Chen, 2001; Ward et al, 2004; Chanoux et al, 2009).

Objective and Hypothesis

The overall research goal of my thesis was to investigate the effects of wrwycr in human cells when cultured *ex vivo* with particular emphasis on examining its effects on cancer versus low passage "normal" cells. This would be the first step towards exploring the anticancer potential of an antibacterial peptide. Studying wrwycr effects on a "normal" human cell line might give an idea of the therapeutic index of this peptide. This would be a further step towards testing the plausibility of promoting wrwycr as the lead compound of a new class of anti-tumor drugs.

The hypotheses that were tested in this study are

(1) Peptide wrwycr can enter the cell nucleus and/or mitochondria and demonstrate their cytotoxicity presumably by stabilizing transient branched DNA repair intermediates (like HJ) produced and resolved during DNA damage repair (Figure I-3). These intermediates are also produced during normal replication cycle of a cell as and when errors occur that need to be repaired. Thus, cells with shorter doubling time will generate more wrwycr targets in a given time and be more sensitive to wrwycr treatment. In this regard, we started exploring effect of this peptide in human cells with particular emphasis on testing if any difference in effect is observed between fast-growing and slow-growing cells.

(2) I tested the hypothesis that peptide wrwycr also targets DNA repair intermediates in human cells, by testing whether its effects were synergistic with DNA damaging agents expected to induce repair intermediates that are targets for peptide wrwycr. Although this is not definitive, it served as an early indicator of the potential of the peptide to interfere with DNA repair.

(3) To test whether the mechanism of the peptide in human cells resembles its mechanism *in vitro* or in bacterial cells, I tested the hypothesis that the activity of wrwycr in human cells is largely dependent on its dimerization capacity.

Outline of the dissertation

Cancer comprises a group of diseases characterized by uncontrolled growth and spread of abnormal cells. Current chemotherapeutic agents treat cancer cells mostly by inhibiting their progression. Specifically, they target several essential proteins in the DNA repair pathway. The hexapeptide wrwycr molecule targets transient branched DNA intermediates produced during replication, recombination and repair. Thus concurrent administration of sublethal dose of conventional chemotherapeutics and wrwycr has the potential to target DNA repair proteins and DNA repair intermediates respectively.

This dissertation endeavors to take the first rudimentary step towards exploring the anticancer potential of this antibacterial peptide wrwycr. The main focus of this work is to investigate effects of wrwycr in human cells with particular emphasis on cytotoxicity. This would necessitate development and design of cell-based assays with particular emphasis on DNA damage and repair. Also, assessing possible differences in wrwycr-induced cytotoxicity in cancer versus normal cell lines might throw some light towards its mode of action. Further, wrwycr can be used as tools to dissect replication and/or repair by exploiting its capacity to stabilize transient branched DNA intermediates (like HJ) generated in these pathways.

In **chapter II**, I have described the effects of wrwycr in U2OS cells, an osteosarcoma cell line with wild type p53 expression, and have found that wrwycr induces a dose-dependent acute cytotoxicity that increases significantly upon concurrent administration of DNA

damaging agents. We have also measured upregulation of the DNA damage response and DNA synthesis. More importantly, I have developed a very sensitive method of measuring DNA synthesis during stepwise synchronization followed by recovery from intra-S arrest in the presence or absence of wrwycr. Parallel estimation of persistent repair foci as a hallmark of absence or incomplete recovery provided direct evidence that wrwycr indeed acts as a DNA repair inhibitor in these cells.

Chapter III is a continuation of an earlier study performed on HeLa cells. Specifically, I reinvestigated certain previously addressed questions from a different perspective. In order to test the induction of apoptosis more sensitively, I used a Hela cell variant, Htog1, where cytochrome C is fused to GFP. This construct helped to visualize mitochondrial changes during various stages of apoptosis. Since distribution of rhodamine-tagged WRWYCR is somewhat similar to mitochondrial cytochrome oxidase, this system was especially informative.

The focus of **Chapter IV** is the study of effects of wrwycr in a slow growing non-transformed cell line, IMR-90 cells. This was a step towards testing our first hypothesis that faster growing cancer cells produce more peptide targets compared to slow replicating cells.

In **Chapter VI,** the results of all the chapters are discussed in the context of wrwycr-induced cytotoxicity (and DNA damage) in the various cell lines used in the study. Explanations for the difference in sensitivity for the different cell types are given. In this chapter, certain ongoing studies expected to clarify more ambiguities are also mentioned. A simple model of wrwycr action in human cells is proposed with recommendations of future experiments to test it.

CHAPTER II

EFFECT OF PEPTIDE wrwycr IN U2OS CELLS

Abstract

Fidelity of DNA replication and repair is essential for the maintenance of genome integrity and the health of a cell. We are studying hexapeptides that were originally isolated by screening combinatorial peptide libraries for molecules that inhibit phage lambda site specific recombination. The most potent peptide isolated in the screen is a cationic, hydrophobic peptide with sequence wrwycr. It binds to and inhibits the resolution of Holliday junctions (HJs), intermediate structures generated during replication, recombination and recombination dependent repair. Preliminary studies have shown that this peptide is bactericidal, presumably by causing DNA damage. Since HJs are also intermediates of DNA repair in eukaryotic cells, it would be interesting to understand wrwycr activity in human cells, cancer and normal, in order to explore its potential as a future antibiotic or chemotherapeutic. In this study, we evaluated the cytotoxic effects of wrwycr in the moderately differentiated human osteosarcoma cell line U2OS. We demonstrated that wrwycr enters the U2OS cell cytoplasm and to a lesser extent enters the nucleus. Further, wrwycr exhibits a permanent, dose-dependent acute cytotoxicity with an induction of apoptosis in some U2OS cells. The toxic effect is synergistic with sublethal concentration of etoposide, a known topoisomerase II poison. Subsequently, we have shown that wrwycr treatment causes accumulation of DNA breaks, at least some of which are double strand breaks based on induction of γ-H2AX. Click-iT EdU incorporation assay results indicate that wrwycr inhibits replicative DNA synthesis only 15-20% but has a much more pronounced effect on DNA synthesis in cells recovering from HU-mediated intra-S arrest. Persistence of repair foci of γ-H2AX and phospho-ATM in cells allowed to recover in presence of wrwycr suggests that wrwycr interferes with DNA

repair in U2OS cells. Use of two control hexapeptides in the assays has indicated that the effect of wrwycr is peptide sequence-specific.

Keywords Holliday Junction, DNA repair, DNA synthesis, cancer, U2OS, wrwycr

Introduction

Cells are constantly under DNA damage stress, both endogenous (e.g., metabolic oxidative damage) and exogenous (e.g., radiation), and have several mechanisms to correct the damage. Many of these insults have detrimental effects on the genome, resulting in a number of different types of DNA damage, including chromosomal double stranded breaks (DSBs). The diverse response to this damage, in turn, results in a wide range of cellular consequences, the immediate being an attempt to repair the damage. In a majority of cases, mammalian cells opt for homologous recombination repair (HRR). Homologous recombination is very important in pathways of DNA damage repair, so much so that there is significant redundancy among different routes of recombination-dependent repair (McGlynn and Lloyd, 2002; Michel et al., 2004; Kreuzer, 2005; Heyer, 2003, Li and Heyer, 2008). In both prokaryotes and eukaryotes, homologous recombination comprises of a number of interacting pathways that generate and resolve a number of DNA intermediates by the co-ordination of diverse classes of repair proteins. (Tsaneva et al, 1993; Gray et al, 1997; Karow et al, 2000; Guy and Bolt, 2005; Wen et al, 2005). One frequent intermediate formed during recombination is a four way DNA junction, also called Holliday junction (HJ). Failure to resolve HJs is detrimental to cell viability (Michel et al., 2004; Kreuzer, 2005; Wyman and Kanaar, 2006; Heyer et al, 2003, Heyer 2007, Li and Heyer, 2008). However, studying the recombination process in detail in an *in vivo* context is challenged by the reversibility and the transient nature of intermediates like

D-loops or HJs. Reagents that stabilize and prolong the half-life of such transient intermediates would be useful.

The hexapeptide, WRWYCR, and its d-amino acid isoform wrwycr were isolated as the most potent peptide to inhibit λ-phage mediated integration (and excision) into (and out of) the *Escherichia coli* genome (Boldt et al, 2004). Subsequent studies have shown that these peptides inhibit recombination by binding to protein-free HJs and inhibiting their resolution (Kepple et al, 2005; Kepple et al, 2008), In bacteria, these peptides are bactericidal (Gunderson and Segall, 2006, Gunderson et al, 2009). WRWYCR (wrwycr) dimerizes via its cysteine residue and its *in vitro* potency to trap HJ and inhibit its resolution is lost significantly upon addition of a reducing agent like DTT (Boldt et al, 2004; Kepple et al, 2005, 2008). This peptide is thus of great interest in the field of antibiotic development. A significant step towards achieving this would be to study the effect of wrwycr in human cells. The homologous recombination repair (HRR) process is highly conserved between prokaryotes and eukaryotes both at the mechanistic and protein levels. DNA polymerases are conserved, intermediate DNA structures generated are very similar and many, though not all, of the proteins involved maintain share sequence homology. Given this conservation of DNA repair, we wanted to explore the peptide's effects particularly in faster dividing cancer cells. In order to determine whether the effect is specific to the peptide sequence, we used two control peptides, wkhyny and WRWYAR in most of the assays.

Since *in vitro* and bacterial targets of wrwycr are HJs, DNA intermediates produced during replication, recombination or repair in both prokaryotic and eukaryotic cells, wrwycr may also be cytotoxic to human host cells. Indeed, studies with human HeLa cells have shown that wrwycr is toxic at high concentration (above 150 μM, refer to chapter III, Figure III.5). In this project, we have studied the effect of wrwycr in human osteosarcoma cells (U2OS). Our hypothesis is that rapidly dividing cells (cancer cells) will undergo more rounds of replication,

suffer more DNA damage and thus create more wrwycr targets *in vivo* as the cells try to repair the damage (Bielas et al, 2000). Moreover, they will have less time to repair the damage before DNA replication is completed when compared to slow growing normal cells (Bielas et al, 2000). If this is true, then cancer cells (and other fast replicating cells) will be significantly more sensitive to wrwycr than normal cells. We have identified effects of wrwycr on a cancer versus a non-cancerous human cell line to better understand its mechanism of cytotoxicity. In this chapter, we have shown that wrwycr enters U2OS cells and induces dose-dependent acute cytotoxicity partly by apoptosis. Concurrent use of DNA damaging agents like etoposide and hydroxyurea makes the effect more severe, both by aggravating wrwycr-mediated cytotoxicity and increasing the peptide-induced accumulation of DNA breaks. This is the first, albeit indirect, evidence that wrwycr might act in the DNA damage repair pathways. Further, we have directly assessed the effect of wrwycr on DNA synthesis, both during replication in asynchronous U2OS cells and during recovery from HU-mediated Intra-S arrest. The results indicate that the presence of wrwycr interferes with the restart of stalled replication forks and repair of HU-induced DNA damage. This evidence was supported by the persistence of DNA repair protein foci like phospho-ATM and γ-H2AX in wrwycr-treated cells, additional evidence that wrwycr inhibits DNA repair in U2OS cells. Taken together, we can categorize wrwycr as an anticancer cell-penetrating peptide with a novel mechanism of action.

Results:

WRWYCR (wrwycr) enters U2OS cells by itself

wrwycr is a cationic, hydrophobic hexapeptide that can form a dodecapeptide by oxidation of the cysteine. Cationic peptides can traverse the plasma membrane without causing any membrane damage or without the help of any transporter protein molecules

(Derossi et al, 1994, 1996, Lundberg and Johanson, 2002; Terrone et al, 2003) and belong to the class of cell penetrating peptides (CPPs). We tested whether WRWYCR (wrwycr) can do the same by measuring its uptake into U2OS cells under normal growth conditions (37°C, 5% CO_2) using two approaches.

First, confocal laser microscopy with Liss Rhodamine-tagged WRWYCR (Rho-WRWYCR) was performed to detect the presence and determine the intracellular distribution of the peptide. U2OS cells incubated with different concentrations of Rho-WRWYCR for varying lengths of time were washed and observed under the microscope. PicoGreen was used as a nuclear counter stain. Z series images were taken through the thickness of the cell to analyze peptide entry inside the cells. The obtained images suggest that Rho-WRWYCR is distributed in the cytoplasm within 3 h of incubation (Figure II-1). However, peptide staining is not uniform throughout the cell; rather the peptide seems to concentrate in particular regions of the cytoplasm (Figure II-1.A.g, top panel). The peptide enters the nucleus to a lesser extent and seems to concentrate in small bodies (possibly nucleolus, Figure II-1.A.g top panel). To obviate the possibility that rhodamine is aiding the entry of the peptide, we incubated similar concentrations of rhodamine B by itself (10 μM) with cells for 3 h. At the same voltage settings (see Materials and Methods), neither rhodamine B alone (Figure II-1.A.d top panel) nor unstained cells (Figure II-1.A.a top panel) showed any significant staining. We have also tested a much higher concentration of Rho-WRWYCR, 150 μM, for 24h (conditions for measuring acute toxicity). The peptide distribution is very similar (Appendix A.1-2) but we start seeing non-specific binding of the peptide around the cell, denoted by the arrowhead in Appendix A1-2.

Since the rhodamine tag is almost 60% of the molecular weight of the peptide, it is possible that it is influencing the intracellular distribution of the peptide. Also, quantitation

from microscopy is difficult and error prone. In order to get an independent quantitative estimate, we used a High Pressure Liquid Chromatography (HPLC) assay to analyze U2OS cell lysates after 24 h incubation with wrwycr. There were two peptide-dependent peaks with elution times of 17.567 and 17.867 min (Figure II-1.B right panel) when the chromatograms of the protein elution profile from DMEM-treated and 2% DMSO-treated samples were overlaid on top of 200 μM wrwycr (d8) treated samples. Mass spectrophotometry (Appendix A.1(ii)) confirmed that the two peaks correspond to the hexapeptide (17.567 min) and the dodecapeptide (17.867 min).

Quantitation of intracellular wrwycr concentration reveals two interesting aspects of peptide uptake. First, the final intracellular peptide concentration depends on the initial input concentration (Table II-1), but the relation is not linear. This is true both for the total (monomer +dimer) as well as the dimer concentration inside cells. For instance, the average intracellular dimer concentration after 24 h of incubation increases from 0.2 mM to 1.77 mM (8.8 fold) when the initial input concentration increases from 100 μM to 200 μM wrwycr (2 fold). Second, wrwycr concentrates inside U2OS cells 10x-350x, to mM concentrations, also evidenced in microscopy (Figure II-1.g and data not shown).

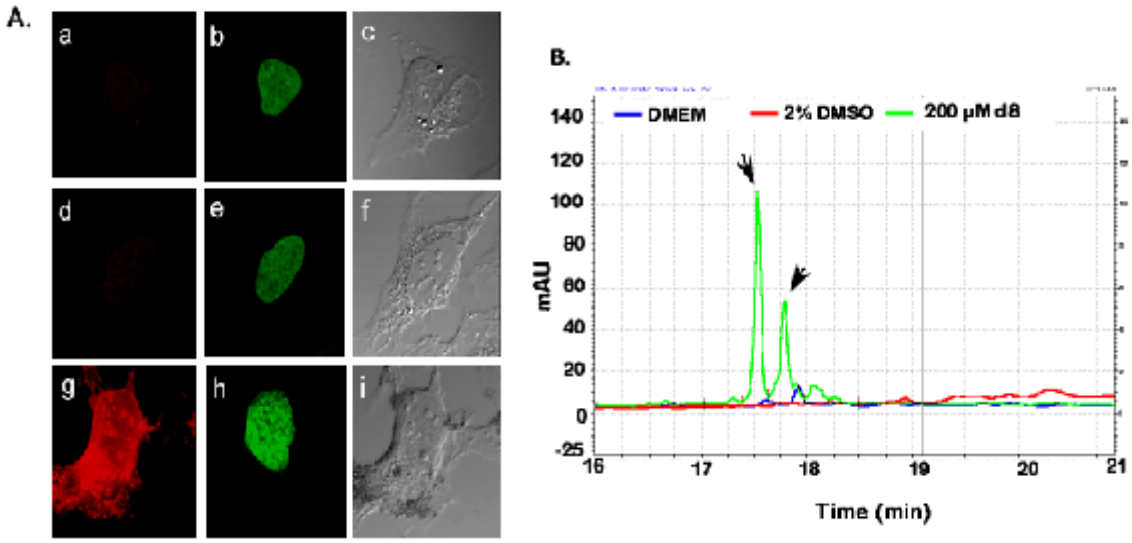

Figure II-1. Uptake of wrwycr (WRWYCR) inside U2OS cells

A. Detection of Rho-WRWYCR in U2OS cells by confocal laser scanning microscopy.

a-c. Control stained only with nuclear stain, PicoGreen. PicoGreen (1 µM) after 10 min of incubation at 37°C. a, Rhodamine channel; b, Pico green channel, c, bright field image of the cell.
d-f. Rhodamine only control. Rhodamine B (10 µM) after 3 h of incubation counterstained with PicoGreen (1 µM) for the last 10 min at 37°C. d, PicoGreen channel; e, Rhodamine channel; f, bright field image of the cell.
g-i. Rhodamine-labeled WRWYCR. Rhodamine (10 µM) WRWYCR after 3 h of incubation counterstained with PicoGreen (1 µM) for the last 10 min at 37°C. g, Pico green channel; h, Rhodamine channel; i, bright field image of the cell.

Each image represents an optical slice near the center of the cell. The confocal microscopy experiment was performed 4 times.

B. Quantitation of uptake in U2OS cells. U2OS cells were incubated with 200 µM wrwycr (d8) or 2% DMSO (solvent) for 24 h at 37°C and the cell lysates were analyzed by HPLC. Shown here is a representative HPLC trace of cell lysates without wrwycr (DMEM treated, red, or solvent 2% DMSO treated, blue) overlaid with 200 µM wrwycr (green). There are two wrwycr dependent peaks with retention time 17.567 min and 17.867 min (arrowheads), corresponding to the monomer (left) and the dimer (right) peaks respectively (confirmed by mass spectrophotometry).

Table II-1. Quantitation of intracellular wrwycr concentration in U2OS cells

Intracellular conc (mM)[c]	Input monomer conc (μM)		
	100	**150**	**200**
monomer	**1** ± 0.28	**2.2** ± 0.7	**6.9** ± 1.6
Dimer[a]	**0.2** ± 0.06	**0.38** ± 0.04	**1.77** ± 0.6
fold change	***1***	***1.9***	***8.85***
Total[b]	**1.4** ± 0.4	**2.97** ± 0.77	**10.4** ± 2.4
fold change	***1***	***2.12***	***7.4***

[a] wrwycr is active as a dimer
[b] Total concentration is determined as monomer (total = monomer + (dimer * 2)
[c] The mean is the average of at least three independent experiments

wrwycr exhibits dose-dependent acute cytotoxicity in U2OS cells

To test our hypothesis that the peptide to be cytotoxic in faster dividing cells, U2OS cells were incubated with increasing concentrations of wrwycr (50 – 200 μM) and corresponding concentrations of DMSO (solvent used to dissolve wrwycr) for 24 h. Acute cytotoxicity was measured by using Live /Dead /Viability / Cytotoxicity kit for mammalian cells and counting individual live vs. dead cells within a population using flow cytometry. The dyes discriminate between live and dead cells based on both membrane integrity and enzymatic activity. Live cells have functional serum esterases that cleave the non-fluorescent membrane-permeant calcein AM compound to produce the green fluorescent membrane impermeant molecule calcein; their intact membranes also exclude the membrane-impermeant red dye, ethidium

homodimer. Dead cells, conversely, allow entry of ethidium homodimer which binds nucleic acids and undergoes a 40 fold enhancement of red fluorescence (Levesque et al, Cytometry, 1995) but lack active esterases to generate calcein. Thus, healthy, live cells will distribute in the Calcein+, PE^{--} quadrant (Q4, Figure II-2A) and dead cells will be in the Calcein-, PE+ quadrant (Q1, Figure II-2A) in the bivariate scatter distribution plot of FITC vs. PE (Figure II-2A). As expected, the media (DMEM) or solvent control (2% DMSO) has most of the cells in Q4 [95.7 and 95.2 respectively, Figure II-2A (i) and (ii)]. On the other hand, wrwycr treatment increases the dead cell population with a corresponding decrease in the live cell population [Figure II-2A (iii) and (iv) and Figure II-2B]. Cytotoxicity of wrwycr starts from 50 μM as compared to DMSO. However, the difference between wrwycr-treated and the solvent-treated samples becomes significant ($p<0.05$) at 100 μM and highly significant ($p<0.005$) at 150 μM. Similar to peptide uptake, acute toxicity is dose dependent but not linear (Figure II-2B, compare % of live or dead cells in 100 μM, 150 μM and 200 μM). We have used the highest concentrations of the control peptides wkhyny and WRWYAR to test the possibility that the cytotoxic effect is non-specific. Neither of the control peptides have any significant cytotoxicity, suggesting that the effect of peptide wrwycr is specific. (Figure II-5B, last two treatments).

Figure II-2. **wrwycr treatment for 24 h induces dose-dependent acute toxicity**

A. Representative FACS dot plots showing the relative distribution of live vs. dead cells after treatment with (i) DMEM (media only), (ii) 2% DMSO (solvent control), (iii) 150 μM, and (iv) 200 μM wrwycr (d8). The numbers indicate the percentage of total cells (10,000) in that quadrant.
   It should be noted that cells in quadrant Q1 are dead, cells in Q4 are live and cells in Q2 or Q3 are sick but not dead.
B. Bar graph representation of live (upper panel) and dead (lower panel) cells as percentage of total cells. Each dose of wrwycr is preceded by the corresponding DMSO concentration (solvent) to consider the solvent effect. Statistical analysis of the results was performed using student's t test and confirmed by non-parametric test.
   ($p < 0.05$ is considered significant and $p < 0.005$ is considered highly significant). The mean is an average of at least three independent experiments.

A.

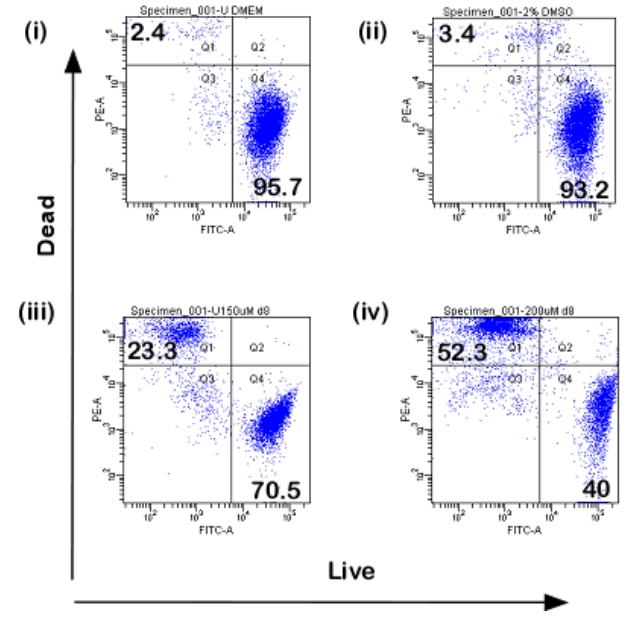
(i)
Specimen_001-U DMEM
2.4
95.7
(ii)
Specimen_001-2% DMSO
3.4
93.2
(iii)
Specimen_001-U150uM d8
23.3
70.5
(iv)
Specimen_001-200uM d8
52.3
40
Q1
Q2
Q3
Q4
PE-A
FITC-A
Dead
Live

B.

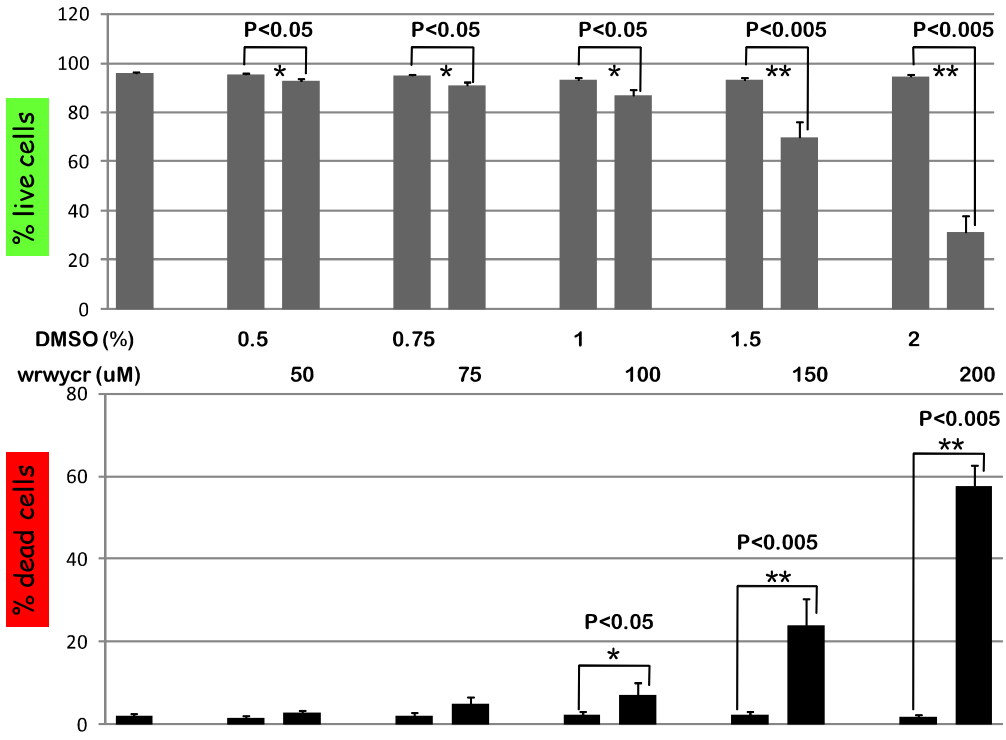
% live cells
120
100
80
60
40
20
0
P<0.05
P<0.05
P<0.05
P<0.005
P<0.005
*
*
*
**
**
DMSO (%)
0.5
0.75
1
1.5
2
wrwycr (uM)
50
75
100
150
200
% dead cells
80
60
40
20
0
P<0.05
*
P<0.005
**
P<0.005
**

wrwycr-induced cytotoxicity is permanent

We examined the wrwycr effect on U2OS cells using the colony forming assay (CFA) to test how the cells respond once the peptide is removed. This would indicate whether the effect of wrwycr on cells is transient or permanent. This is particularly interesting because in the Live/Dead assay, a fraction of wrwycr treated cells was found in the double positive or unstained quadrant (Figure II-2A, cells in Q2 or Q3, respectively) which were considered sick but not dead. In the CFA assay, an individual cell (or a colony of two cells) was exposed to wrwycr (or solvent DMSO) for 24 h after which the treatment was washed off and the cells were allowed to recover in peptide-free medium and form distinct colonies (of 50 or more cells). The representative pictures of the plates (Figure II-3A) show that individual colonies can be stained and counted subsequently. Quantitation of the results indicates that there may be a dose-dependent decrease in the number of colonies with increasing concentration of DMSO (Figure II-3B, compare 86.1% in 1% DMSO to 76.7% in 2% DMSO). DMSO may cause a late (or cytostatic) effect on U2OS cells such that most of the cells are viable after 24 h exposure (Figure II-2A and II-2B), but a significant fraction of those are unable to grow and form colonies even when DMSO is washed away (Figure II-3A and II-3B). The control peptides, wkhyny and WRWYAR, also, do not seem to have any effect on the colony forming ability of the cells by themselves. The reduction in number of colonies is only due to the mild solvent effect (Figure II-3B, compare 84.3% in 1.5% DMSO versus 82.4 and 80.3% in wkhyny and WRWYAR respectively). wrwycr, on the other hand, has a more pronounced effect in reduction of colony number and the inhibition is dose-dependent (Figure II-3B, compare % reduction of wrwycr-treated versus the corresponding concentration of DMSO-treated samples). At lower concentration (100 μM), wrwycr also had a late (or cytostatic) effect on a fraction of cells, such that they were viable after 24 h (87% live at 100 μM exposure, Figure II-2B) but could not form viable colonies (65% cells form viable colonies,

Figure II-3B). At a higher concentration of wrwycr, 200 μM, the effect was similar to the Live / Dead assay and ~55% of cells formed colonies. Taken together, the CFA results indicate that wrwycr-induced cytotoxicity in U2OS cells is permanent but not cumulative. This suggests that interaction of wrwycr with its *in vivo* targets is not irreversible and the peptide can be washed away.

wrwycr induces early and late apoptosis in U2OS cells

In order to understand the mode of cell death, early and late apoptosis were measured using AnnexinV and caspase-3 assay respectively. Early apoptotic cells are AnnexinV positive (Koopman et al, 1994; Vermes et al, 1995) since reversal of phosphatidyl serine (PS) from the inner to the outer leaflet of the plasma membrane is one of the earliest events of apoptotic commitment (Fadok et al, 1992, Hammill et al, 1999). At this point, the redistributed PS is available for AnnexinV to bind to. The plasma membrane, however, retains its integrity and membrane impermeable dyes like propidium iodide (PI) are excluded. In this assay, we counterstained each sample with PI to distinguish between early (Annexin +, PI --; quadrant Q4 in Figure II-4A) and late apoptotic or necrotic (Annexin +, PI +; Q2, or Annexin -, PI +; Q1, Figure II-4A) cells. The maximum concentration of DMSO (2%) has a baseline Annexin V (~6%) and PI (~5%) staining at all the different time points tested (Figure II-4A, top left panel, 18 h data shown). Increasing concentrations of wrwycr increased the fraction of cells undergoing early and late apoptosis. At 100 μM wrwycr, we observed only marginal apoptosis (Figure II-4A) even at 18 h. Higher concentrations of wrwycr, on the other hand, show significant increases in Annexin V staining as early as 6 h (Figure II-4A, the top middle, 150 μM, and top right panel, 200 μM). The results indicate that a higher concentration of peptide wrwycr treatment induces apoptotic signal at an earlier time point (200 μM) and does not increase

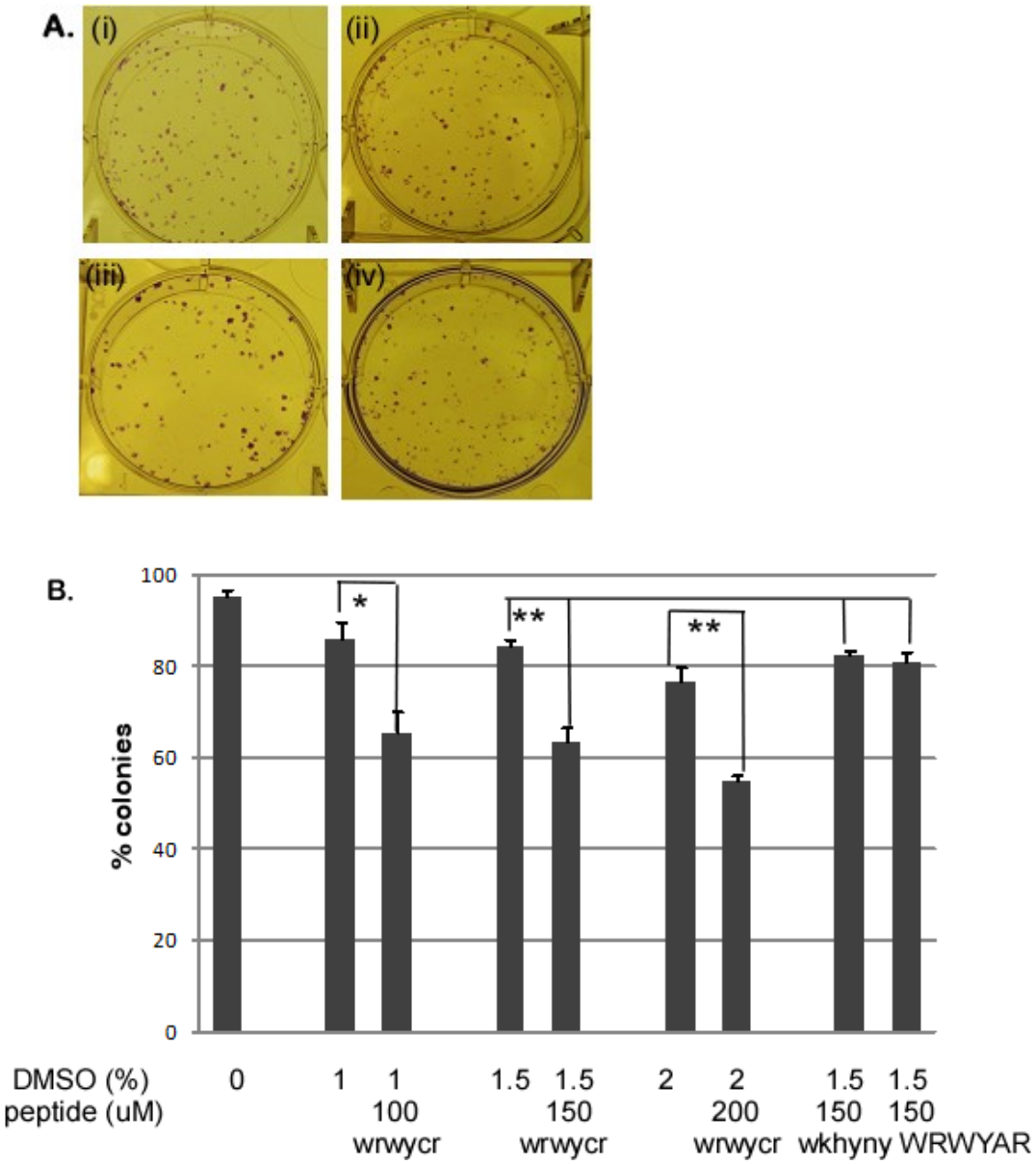

Figure II-3. **wrwycr-induced cytotoxicity is permanent.**

A. Representative colony pictures after treatment with (i) DMEM (ii) 1.5% DMSO (iii) 150 µM wrwycr and (iv) 150 µM wkhyny for 24 h and recovery for 5 days. Each purple dot represents a single colony of cells stained with crystal violet.

B. Scatter distribution of % surviving colonies considering DMEM as 100%. Mean is the average of at least 3 independent experiments each done in triplicates. * indicates significant difference with $p<0.05$ and ** indicates highly significant difference with $p<0.005$.

over time (Figure II-4A, compare 6, 12 and 18 h for 200 μM wrwycr). In contrast, an intermediate peptide concentration (150 μM) increases apoptosis induction up to a certain time and then levels off (Figure II-4A, compare 6, 12 and 18 h for 150 μM wrwycr).

A possible explanation for this variability may be due to peptide entry into U2OS cells and its apparent co-operativity. We have preliminary evidence from HPLC results that intracellular total and dimer wrwycr concentration after 6 h of incubation increases exponentially with input concentration (100 μM input results in 90 μM intracellular wrwycr while 200 μM results in 1000 μM dimer, data not shown).

An independent measure of late apoptosis is the induction of caspase-3. Caspase-3 is an effector protease, a member of the cysteine protease family that cleaves over 400 proteins within cells programmed for apoptosis (Lu¨thi and Martin, 2007, Timmer and Salvesen, 2007). Exposure to wrwycr for 24 h caused a dose-dependent caspase-3 induction (Table II-2, right panel) compared to the solvent control. This was parallelled by a corresponding increase in TUNEL (**T**erminal transferase-mediated d**U**TP **n**ick-**e**nd **l**abeling) positive cells with increasing doses of wrwycr (compare Table II-2, left versus right panel). The TUNEL assay measures the % of cells with fragmented DNA. This may be due to direct DNA damage (Carre and Guilloton, 1997) or a secondary event due to apoptosis (Renvoize et al, 1998). In our hands, the TUNEL response is not reduced in presence of a caspase family inhibitor (data not shown) suggesting that the accumulation of fragmented DNA is not a secondary response of apoptosis. The magnitude of apoptosis and/or DNA damage response is lower than wrwycr-induced cytotoxicity (compare Figure II-4 and Table II.2 with Figure II.2B) suggesting that wrwycr-mediated loss of U2OS cell viability is partly due to apoptosis.

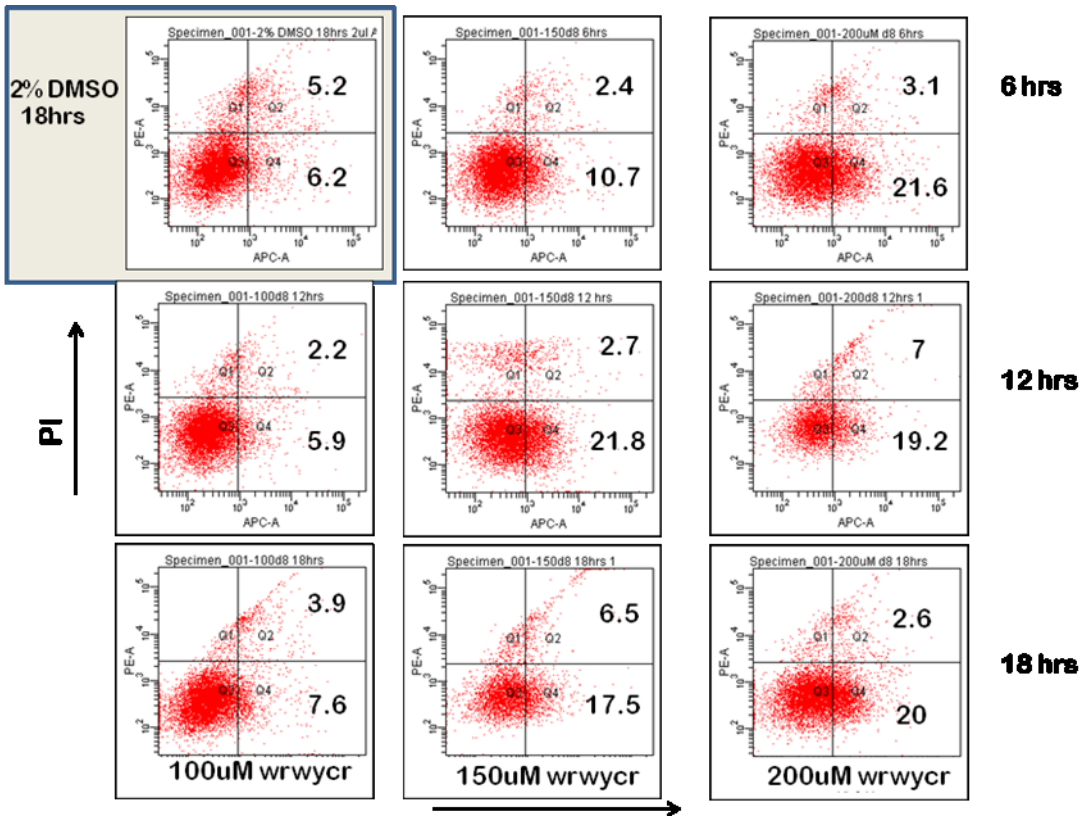

Figure II-4. Treatment with wrwycr induces apoptosis in some U2OS cells.
Flow cytometric analysis of Annexin V binding at different time points (6, 12 and 18 h) with increasing concentrations of wrwycr [100 µM; panel (i), 150 µM; panel (ii), 200 µM; panel (iii).]. The inset contains the solvent control 2% DMSO treated for 18 h. It should be noted that 2% DMSO is the highest concentration of solvent used in all the different assays.

Table II-2. Comparison table of caspase-3 upregulation versus % TUNEL positive cells

	TUNEL	caspase-3
Treatments	**% TUNEL + cells**	**RFU/µg protein[a]**
DMEM	0.5± 0.3	
Sorb (400mM)[b,e]	NT	1.4 ± 0.2
DNAse I[c]	84 ± 8.3	17.4 ± 6.5
Etopo (150uM)[b,e]		NT
		67.8 ± 12
DMSO (%)	NT[d]	
1.5	1.6 ± 0.7	4 ± 1
2		5.8 ± 2.1
wrwycr (d8, µM)	2.9 ± 1	
150	16.5 ± 8.8	4.8 ± 1.3
200		15.04 ± 4.2

[a] RFU per treatment is obtained by subtracting the blank reading from the sample RFU reading

[b] Positive controls for TUNEL is DNaseI as it generates DNA breaks by an enzymatic reaction. But it does not induce apoptosis

[c] Two positive controls for caspase-3 assay are classical apoptosis inducers, sorbitol (400mM) and etoposide (150uM)

[d] NT = Not tested

[e] sorb = sorbitol; etopo = etoposide

Effect of wrwycr becomes more severe in the presence of DNA damaging agents

In order to test whether the *in vitro* and *in vivo* target of wrwycr are similar, we asked whether the cytotoxicity is accompanied by any DNA damage of the cells. First we took an indirect approach. In this study, we used etoposide and hydroxyurea, two classes of DNA damaging agents that activate two distinct but overlapping DNA repair pathways in human cells. Etoposide is a topoisomerase-II poison that stabilizes the DNA-topoisomerase complex generating double strand breaks (DSB), and HU is a ribonucleotide reductase inhibitor that causes replication fork stalling and inhibits DNA synthesis. HU-mediated DNA damage response mimics the Ultra Violet (UV) and etoposide mimics the Ionizing Radiation (IR) repair pathways. These are the two main pathways that repair via homologous recombination.

The basic principle was that compounds acting in same or similar pathways should have more than additive (or synergistic) effect. When administered in sublethal doses, DNA damaging agents should generate DNA lesions and activate specific DNA repair pathways. If any of these pathways produces wrwycr targets, then co-treatment of wrwycr with that drug should have more than additive response. We tested this by measuring cytotoxicity (Live/Dead), accumulation of DNA breaks with or without apoptosis (TUNEL versus caspase-3 upregulation) and persistence of a DSB marker, γ-H2AX.

First, we performed the Live/Dead assay after 24 h of incubation with either wrwycr alone or with sublethal concentration of etoposide. We titrated a range of etoposide concentrations and found that 1.3 μM etoposide treatment for 24 h does not cause significant cell death (Figure II-5A panel (i) and data not shown) in U2OS cells. As mentioned earlier, 150 μM and 200 μM wrwycr by themselves cause the death of ~23% and 57% cells respectively. However, upon addition of 1.3 μM etoposide, the dead cell population increases significantly, to ~38% and 83% respectively, and the response is more than additive. This suggests that etoposide and

wrwycr are somehow potentiating each other's cytotoxic action. Calling this effect synergistic would require more statistical analysis. In order to obviate the possibility that DMSO (2%), the solvent used, might by itself have a synergistic effect when administered with etoposide, we used 1.3 μM etoposide + 2% DMSO as a control in this experiment. The results indicate that DMSO (2%) and etoposide (1.3 μM) bear no synergy when administered together (Figure II-5B).

Caspase-3 upregulation follows a similar trend. Here we used both etoposide and hydroxyurea in conjunction with 150 μM and 200 μM wrwycr and found that the combination treatment with etoposide elicits more caspase-3 activity than with hydroxyurea (Table II-3, right panel). The TUNEL response, however is increased more upon concurrent administration of wrwycr with HU than with etoposide (Table II-3, left panel, Figure II-6). Interestingly, the presence of the caspase inhibitor in the treatments does not reduce the TUNEL signal both in case of wrwycr alone or with HU and etoposide suggesting that the accumulation of DNA breaks is not a secondary event of apoptosis.

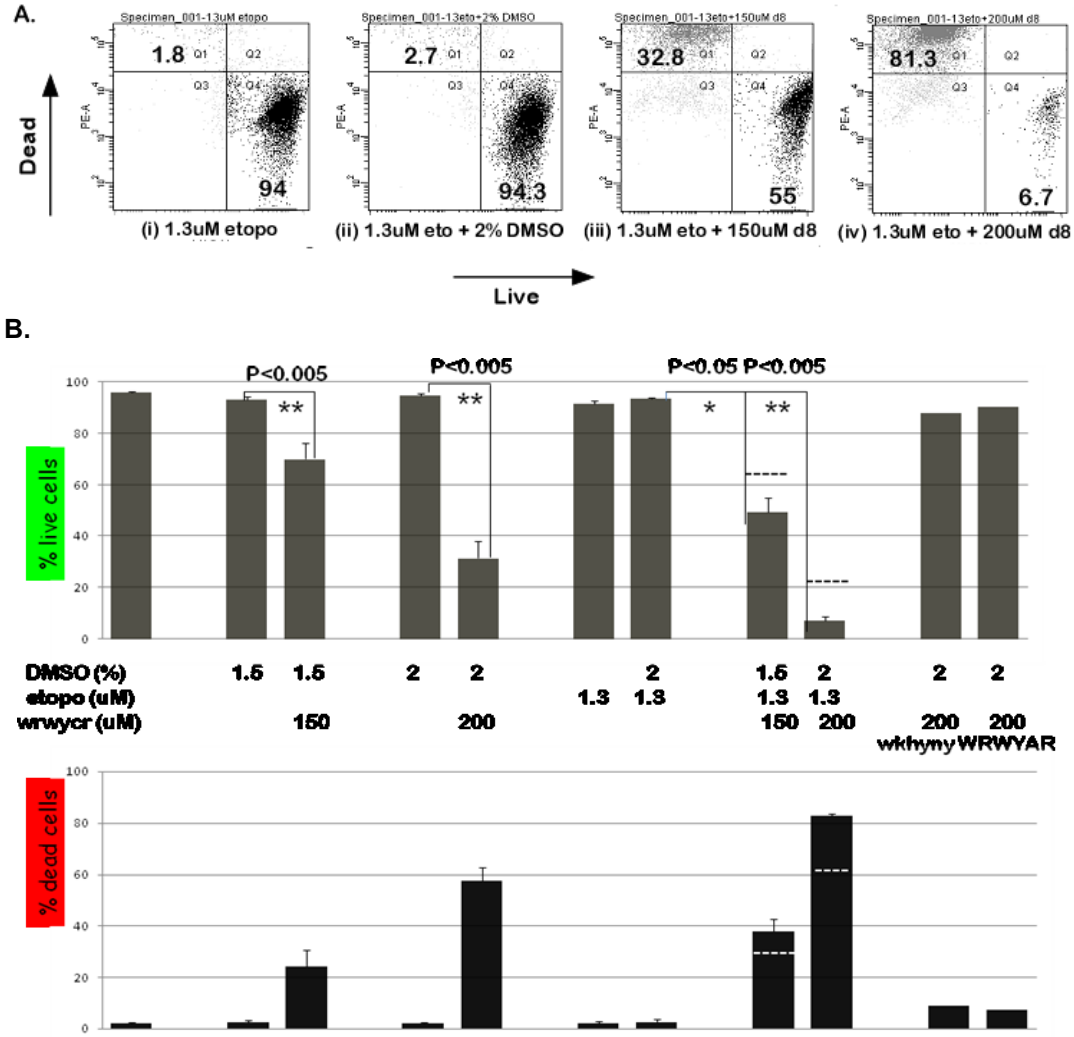

Figure II-5. wrwycr- induced cytotoxicity becomes more severe upon co-treatment with a sublethal dose of etoposide

A. Representative FACS dot plots of Live/Dead assay showing the relative distribution of live vs. dead cells after treatment with (i) 1.3 µM etopo (ii) 1.3 µM etoposide + 2% DMSO (iii) 1.3 µM etoposide + 150 µM and (iv) 1.3 µM etoposide + 200 µM wrwycr (d8). The numbers indicate the percentage of total cells (10,000) in that qµadrant.

B. Bar graph representation of live (upper panel) and dead (lower panel) cells as percentage of total cells. Statistical analysis of the results are performed by student's t test and confirmed by non-parametric test. $p < 0.05$ is considered significant and $p < 0.005$ is considered highly significant. The dotted line represents the % of cells if the action of wrwycr and etoposide was additive.

Table II-3. Comparison table of caspase-3 upregulation versus. % TUNEL positive cells following co-treatment of wrwycr and etoposide or HU

	TUNEL	caspase-3
Treatments	**% TUNEL+ cells [h]**	**RFU/µg protein[b, h]**
DMEM	0.5± 0.3	1.04 ± 0.2
Sorb (400mM)[c, g]	NT	17.4 ± 6.5
DNAse I[d]	84 ± 8.3	NT
Etopo (150uM)[c, g]	NT	67.8 ± 12
DMSO (%)		
1.5	NT[e]	4 ± 1
2	1.6 ± 0.7	5.8 ± 2.1
wrwycr (d8, uM)		
150	2.9 ± 1	4.8 ± 1.3
200	16.5 ± 8.8	15.04 ± 4.2
etopo [g] (uM)		
1.3[f]	2.2 ± 1.5	1.27 ± 0.2
1.3 + 150d8	5.9 ± 2.6	9.7 ± 1.4
1.3 + 200d8	18.4 ± 1.8	31.4 ± 6.9
HU (mM)		
5[f]	4.7 ± 3.9	0.73 ± 0.16
5 + 150d8	6.3 ± 2.4	5.3 ± 0.7
5 + 200d8	31.5 ± 6	19.3 ± 3.4

[a] The d8 effect is calculated by subtracting out the effect of corresponding concentrations of DMSO

[b] RFU per treatment is obtained by subtracting the blank reading from the sample RFU reading

[c] Positive controls for TUNEL is DNAseI as it generates DNA breaks by an enzymatic reaction. But it does not induce apoptosis

[d] Two positive controls for caspase-3 assay are classical apoptosis inducers, sorbitol (400mM) and etoposide (150uM)

[e] NT = Not tested

[f] 1.3uM etoposide and 5mM HU treatment for 24 h are sub-lethal to U2OS cells

[g] etopo = etoposide; sorb = sorbitol

[h] In TUNEL assay, Mean is the average of 3 independent experiments; In caspase-3 assay, Mean is the average of 4 independent experiments each done in duplicate

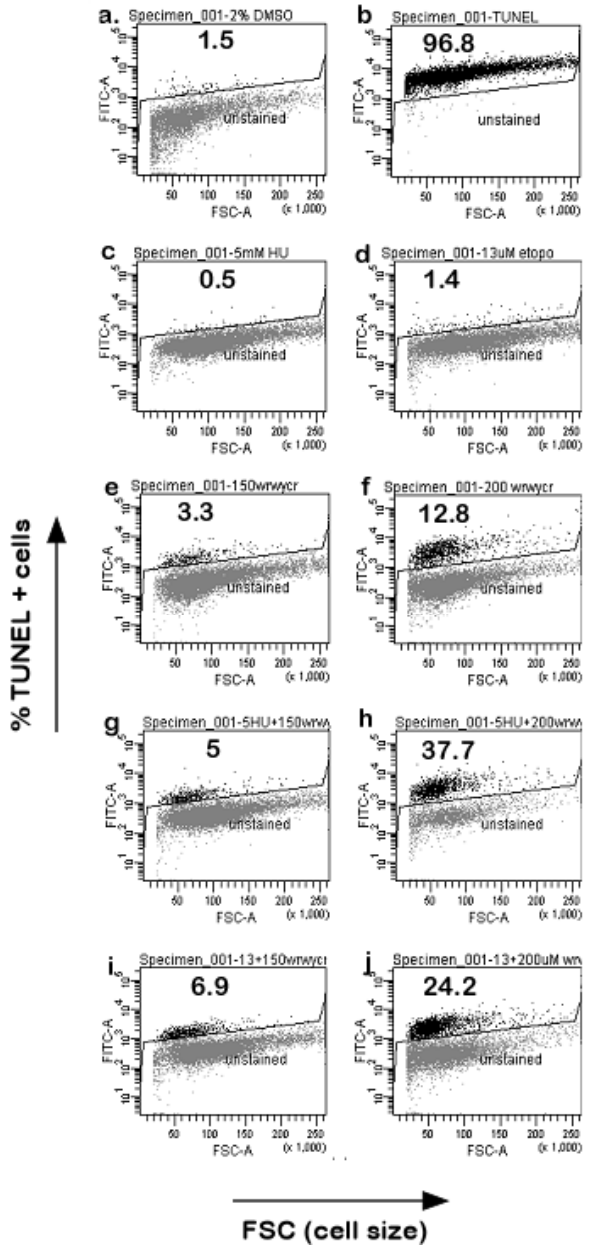

Figure II-6. Concurrent administration of DNA damaging agents increases wrwycr-induced DNA breaks.

U2OS cells were exposed to wrwycr in presence or absence of HU and etoposide for 24 h and assayed for fragmented DNA by TUNEL analysis and flow cytometry. Shown here is a representative dot plot of % TUNEL + cells versus FSC. Panels of treatment are (a) 2% DMSO (solvent control), (b) DNAseI (positive control), (c) 5mM HU, (d) 1.3 µM etoposide, (e) 150 µM wrwycr, (f) 200 µM wrwycr, (g) 5 HU + 150 µM wrwycr, (h) 5 HU + 200 µM wrwycr, (i) 1.3 µM etopo + 150 µM wrwycr and (j) 1.3 µM etopo + 200 µM wrwycr.

wrwycr induced γ-H2AX foci formation is potentiated upon addition of DNA damaging agents

γ-H2AX is an activated form of a histone variant, H2AX, phosphorylated at Ser 139. This histone variant is generated as a first response to a DNA double strand break (Vafa et al, 2002). γ-H2AX forms the repair foci and recruits various repair proteins (ATM, Brca2, etc) at the site of damage (Paull et al, 2000). After the cell has completed DNA repair, the protein gets dephosphorylated (Chowdhury et al, 2005; Tsukuda et al, 2005, Keogh et al, 2005). Thus γ-H2AX is an important hallmark of the DSB repair response. Persistent γ-H2AX foci are a sign of unrepaired DNA damage specifically DSBs. We tested γ-H2AX foci formation using increasing concentration of wrwycr alone or in conjunction with the sub-lethal dose of etoposide or hydroxyurea. The peptide by itself produces γ-H2AX foci only in a small fraction of cells (Figure II-7A, 4.5% and 13.3% for 150 μM and 200 μM wrwycr respectively). This increases upon concurrent administration of 1.3 μM etoposide (5.2% and 22.5% for 150 μM and 200 μM wrwycr respectively) and 5 mM HU (~7% and 32% for 150 μM and 200 μM wrwycr respectively). The FACS results indicate that only a subpopulation of the cells affected by wrwycr actually retain γ-H2AX (compare Figure II.5B lower panel and Figure II.7A). The same is true for the combined treatment of wrwycr and etoposide (Figure II.7A). This suggests a few possibilities. One, DNA damage is not the main cause of cell death. Secondly, the cells having a few foci are gated out (only cells beyond a particular fluorescence intensity score positive in flow cytometry, see Materials and Methods).

A limitation of flow cytometry is that it cannot show the distribution pattern of foci within a population of γ-H2AX positive cells, every cell has a distinct number of foci but both score positive in flow cytometry. This difference is revealed more easily via microscopy. Fluorescence microscopy was performed with cells treated with wrwycr alone or wrwycr and

5mM HU treated for 18 h to detect γ-H2AX foci. The results agree with the FACS (and are more informative). As expected, the media-treated or the solvent-treated controls did not have many foci [Figure II-7B (a)]. Peptide wrwycr showed a few foci per nucleus only when used at the highest concentration [Figure II-7B (b)]. As expected, HU (5mM) by itself also produced a few foci per nucleus [Figure II-7B (c)]. HU at this concentration inhibits DNA synthesis in U2OS cells (Figure II-9A). This provides supporting evidence that γ-H2AX foci formation is not a direct outcome of replication arrest. Etoposide (51 μM), however, known to induce apoptosis via DSB formation (Van Maanen et al, 1988; Tanabe et al, 1991; Treszezamsky et al, 2007), produces numerous foci in almost 100% of treated cells [Figure II-7B (f)]. The combination of 150 μM or 200 μM wrwycr and 5mM HU, elicited profuse γ-H2AX foci formation when compared to either single treatment suggesting that the effect is synergistic [Figure II-7B, compare (b) & (c) with (d) & (e)].

The microscopy results were quantified using Image J. The mean green fluorescence intensity per cell was calculated as the average of approximately 50 nuclei per treatment. The results indicate that 200 μM wrwycr acts in synergy with 5mM HU to produce γ-H2AX foci (Figure II-7C; 117 instead of 29.9 + 23.4; intensity measured as arbitrary units). Taken together, this experiment indirectly suggests that the wrwycr-induced accumulation of DNA damage particularly double strand break response is increased both upon co-treatment with HU and etoposide. It is known that HU-mediated damage interferes with DNA synthesis. A more-than-additive response upon co-treatment with wrwycr and HU could thus imply that wrwycr substrates are also generated during replication arrest or processing of stalled replication forks, and is consistent with the peptide's affinity for substrates that mimic replication forks.

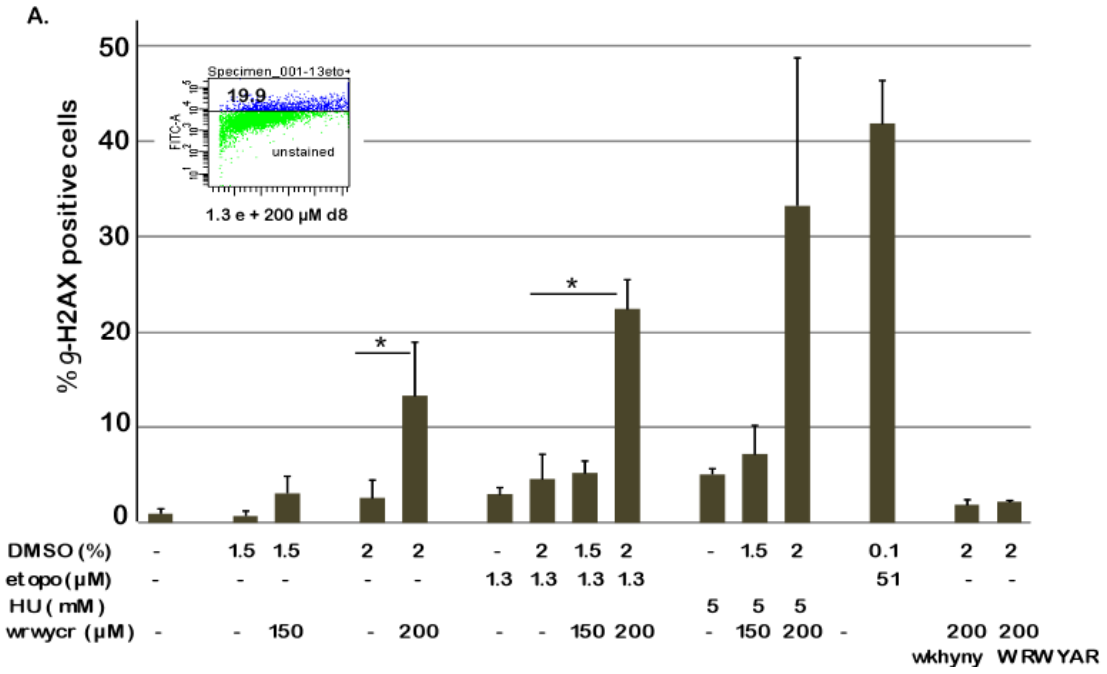

Figure II-7. wrwycr-induced DNA DSB response measured by formation of γ-H2AX foci is more severe upon concurrent treatment with hydroxyurea or etoposide.

A. Measurement of DNA DSB response by counting % of cells with persistent γ-H2AX foci using flow cytometry. Bar graph representation of the flow cytometry results. $P<0.05$ (*) is considered statistically significant. The inset contains a representative dot plot of FSC (forward scatter) vs. FITC (anti γ-H2AX is tagged to FITC) showing the gating of the cells.

B. U2OS cells were grown and treated in cover slips inside 12 well plates for 18 h. Fixed and permeabilized cells were stained with γ-H2AX antibody and analyzed for foci formation using immunofluorescence microscopy. Shown here are the representative images after (a) 2% DMSO, (b) 200 µM wrwycr, (c) 5 mM HU, (d) 5 mM HU + 150 µM wrwycr, (e) 5 mM HU + 200 µM wrwycr and (f) 51 µM etoposide treatment.

C. Quantitation of γ-H2AX foci using the Image J program. Bar graph representation of the mean green fluorescence intensity (γ-H2AX) inside the nucleus as a measure of the number of foci in the nucleus (it is hard to count individual foci for certain treatments). The result indicates the distribution of foci formation on a per cell basis.

B.

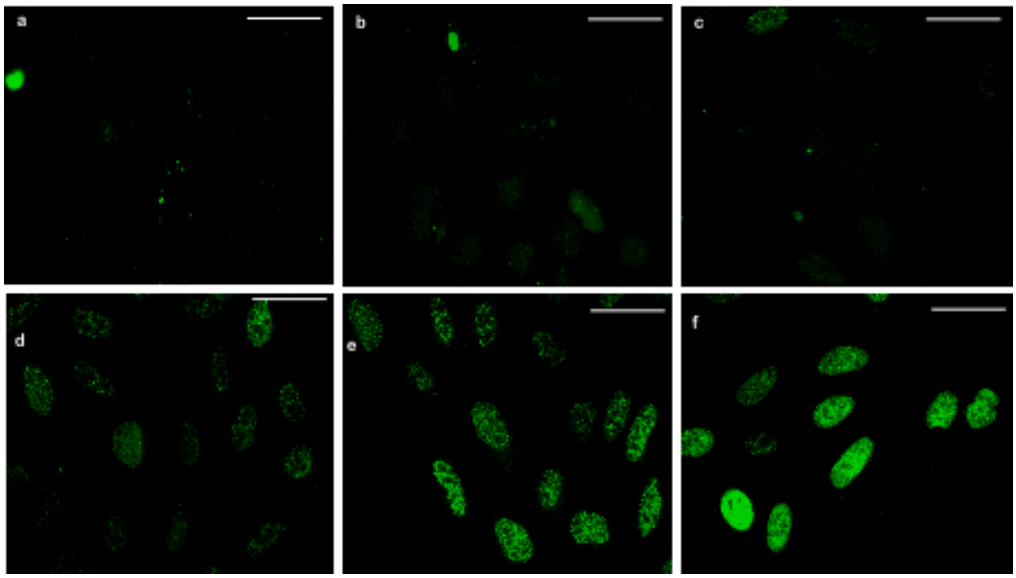

C.

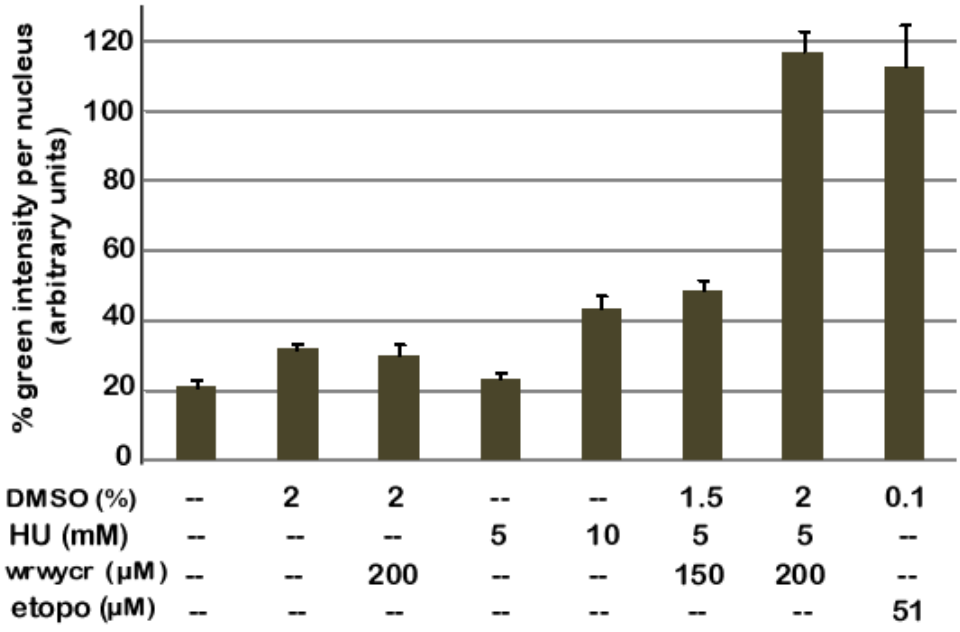

Figure II-7 Continued

wrwycr mildly inhibits replicative DNA synthesis

Cancer cells undergo more rounds of replication than healthy cells. Based on the *in vitro* activities of the peptide, our hypothesis is that wrwycr targets replication and DNA repair intermediates and prevents their resolution. If this is true, then DNA synthesis may be affected upon wrwycr treatment. I used a derivative of the classical BrdU incorporation assay, the Click-iT EdU assay. Total incorporation of EdU into DNA during DNA synthesis was measured directly over time. Shown here are the results of the 18 h time point. Sample treated with DMSO (2%) was used as the negative control and had minimal effect on replication (Figure II-8A, Panel (i) and graph in Figure II-8B). On the other hand, 10 mM HU arrests 100% of cells from synthesizing DNA (Figure II-8A, Panel (ii) and graph in II.8B) without killing them (data not shown). The results indicate that wrwycr exhibits a linear dose-dependent inhibition of DNA synthesis (Figure II-8A, Panel (iii); Figure II-8B, 11%, 16% and 24% respectively for 100 μM, 150 μM and 200 μM wrwycr). Similar to the DNA damage response, wrwycr-mediated DNA synthesis inhibition is lower than the peptide-mediated cell killing (compare Figure II-8B with Figure II-2B). This suggests that direct inhibition of DNA synthesis is only partly responsible for wrwycr-induced cell death. If wrwycr induced cytotoxicity was solely due to DNA damage and inhibition of DNA synthesis, we would expect a much larger % of live cells unable to synthesize DNA. However, when the entire population of cells is gated, the reduction in DNA synthesis is similar to the cytotoxicity (~48% cells are unable to synthesize DNA and 57% cells dead, data not shown). The control peptides did not have any significant effect on DNA synthesis (Figure II-8B). In this experiment, we confirmed that using a peptide that mimics a dimer of wrwycr in a single chain, wrwyrggrywrw, referred to as the dodecamer. Essentially, wrwyrggrywrw should have 100% *in vivo* dimer concentration since it is a single polypeptide, and thus should be more potent.

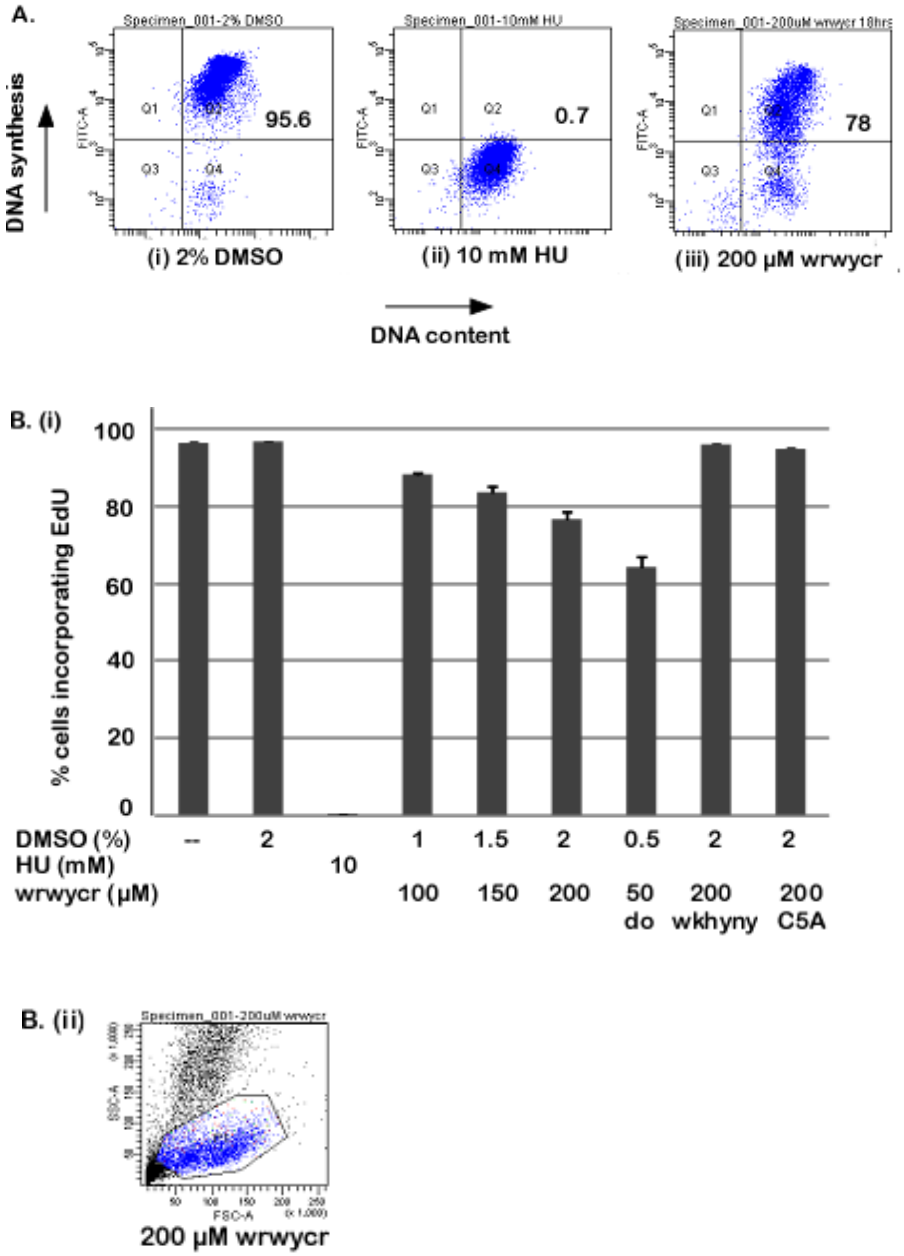

Figure II-8. wrwycr mildly inhibits replicative DNA synthesis

A. Representative FACS dot plots of FITC (DNA synthesis) vs. APC (DNA content) after 18 h of 1 µM EdU incubation. (i) 2% DMSO (ii) 10 mM HU (iii) 200 µM wrwycr

B. (i) Bar graph representation of % of cells incorporating EdU in 18 h.
(ii) FACS dot plot contains the gating of the cells based on their FSC and SSC pattern; only the live cells were gated. and the population of cells already dead is gated out. Note that, in this assay, we included 50 µM dodecamer, a peptide that mimics a wrwycr dimer with sequence wrwyrggrywrw and is resistant to reduction in vivo.

This is indeed the case. The 50 μM dose of wrwyrggrywrw inhibits DNA synthesis in about 40% of live cells (Figure II-8B). In summary, wrwycr seems to reduce bulk DNA synthesis only mildly.

wrwycr interferes with recovery from replication fork collapse caused by hydroxyurea (HU)

Measuring DNA synthesis within an asynchronous population can lead to ambiguity in data interpretation as seen in the previous experiment. After 18 h, it is difficult to conclude whether DNA synthesis inhibition is the cause or effect of cell death. This is because, by the time wrwycr-induced DNA synthesis inhibition becomes prominent, a substantial fraction of the cells show signs of death. Prolonging the cell cycle by arresting cells at particular stages might delay wrwycr-mediated cell death. Depending on the mode of arrest, the recovery phase might produce plausible targets of wrwycr. To address this, we tested recovery from stalled replication by stepwise synchronization of U2OS cells. We developed a synchronization procedure based on a report that used hydroxyurea to cause intra-S arrest without cell death in U2OS cells (Martin and Ouchi, 2008).

Following overnight adhesion, cells were first grown in RPMI supplemented with 2% FBS for 18 h, a regimen that arrested around 50% of the cells in G1/S phase (Figure II-9A). The cells were subsequently grown in regular media (DMEM with 10% FBS) with 5 mM HU for 5 h arresting 100% of the cell population in S phase. (Figure II-9A, diagram). Each stage of arrest was confirmed by testing DNA synthesis using the Click-iT EdU assay. The inset histogram shows that no cells are able to synthesize DNA at this point (no EdU incorporation). The cells were then allowed to recover in regular media in the presence or absence of wrwycr upto 16 h. During recovery all the collapsed replication forks will need to be restarted. In the absence of wrwycr, most of the cells should be able to recover either by directly restarting

forks or after DNA repair. However, we predicted the presence of wrwycr to target the repair intermediates that will be generated in this process and to delay or interfere with the recovery. The results supported the prediction.

We measured two parameters in parallel to test whether wrwycr interferes with recovery from intra-S arrest.

First, we measured DNA synthesis during recovery (2, 4, 8, 12 and 16 h) phase adding EdU with the recovery media (DMEM + 10% FBS with or without the different treatments). wrwycr effect starts at 12 h and becomes more pronounced at 16 h (recovery time course, Figure II-9B). As expected, DMEM and DMSO-treated samples recovered much better than the wrwycr-treated samples (representative histogram in Figure II-9C and Figure II-9D, ~ 86% and 83% for DMEM and DMSO versus. 60% and 53% for 150 μM and 200 μM wrwycr, respectively). We have gated only the live cells based on the FSC and SSC parameters (Figure II-9C, inset dot plot). Also, each sample was tested using the Live / Dead assay to confirm that the inhibition of DNA synthesis is not due to cell death (Figure II-10). Indeed, wrwycr treatment at concentrations that interfered significantly with recovery (150 μM and 200 μM) did not cause any significant cell death (4.5% and 5% respectively), suggesting that inhibition in recovery is not a secondary response of cell death. This is the first evidence that wrwycr can interfere with recovery from stalled replication in U2OS cells.

In conditions where cells are unable to repair DNA damage, distinct foci of DNA repair proteins should persist at sites of damage for several hours before signals for cell death pathways are triggered (Paull et al, 2000). Distinctively, successful DNA repair will dissolve

Figure II-9.wrwycr interferes with recovery from HU-mediated arrest

A. Design and prediction of DNA damage and repair. Shown here is a schematic of a step by step synchronization of a population of U2OS cells. The Y axis represents % cells synthesizing DNA and is shown as an inset histogram in each section. The X axis shows the different treatment and timing of those treatments to arrest the cells in particular phases of cell cycle. The final phase of recovery shows the expected results.
B. Three dimensional FACS histograms showing several time points of recovery in presence or absence of wrwycr. The arrow represents the population of cells unable to incorporate EdU. The effect becomes evident no earlier than 12 h and is prominent at 16 h. The treatments in each panel are color coded as follows: DMEM (red), 2% DMSO (green), 200 μM wkhyny (turquoise), 100 μM wrwycr (blue), 150 μM wrwycr (brown), 200 μM wrwycr (purple) and 5mM HU (grey).
C. FACS histogram of the 16 h recovery phase showing the fraction of cells that are able to recover from the Intra-S arrest caused by the replication fork collapse and synthesize DNA. The color coding in the inset legend shows the different treatments. The right half of the dotted line gates cells that have incorporated EdU and the left half gates cells unable to incorporate EdU (or synthesize DNA). The inset FACS dot plot shows that only live cells are gated based on FSC vs. SSC pattern to obtain the histogram.
D. Quantitation of the 16 h recovery phase in presence or absence of wrwycr. Bar graph representation of % of cells synthesizing DNA in arrest and recovery phase after different treatments.

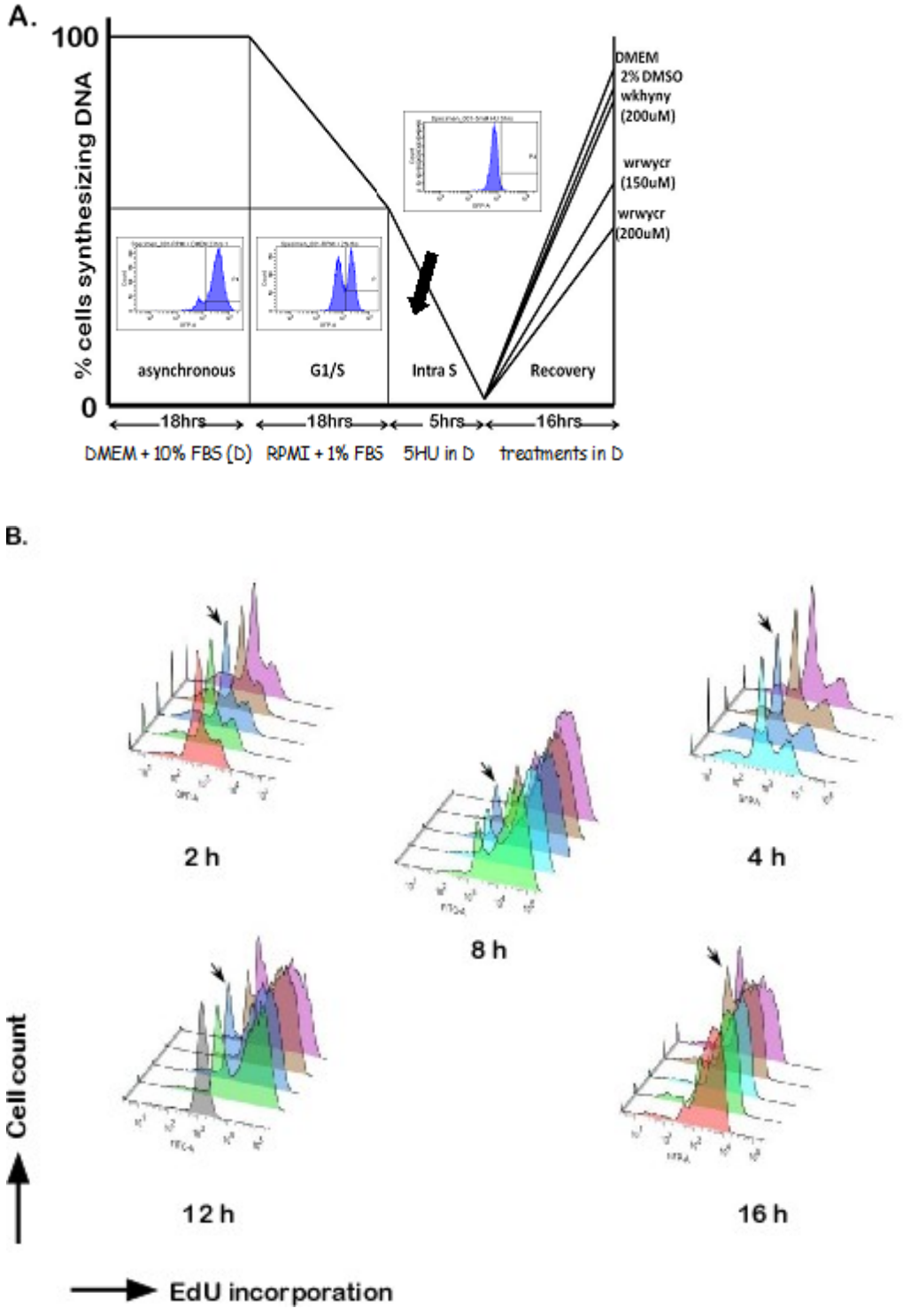
A.
100
% cells synthesizing DNA
0
asynchronous
G1/S
Intra S
Recovery
DMEM
2% DMSO
wkhyny
(200uM)
wrwycr
(150uM)
wrwycr
(200uM)
18hrs
18hrs
5hrs
16hrs
DMEM + 10% FBS (D)
RPMI + 1% FBS
5HU in D
treatments in D
B.
2 h
8 h
4 h
12 h
16 h
Cell count
EdU incorporation

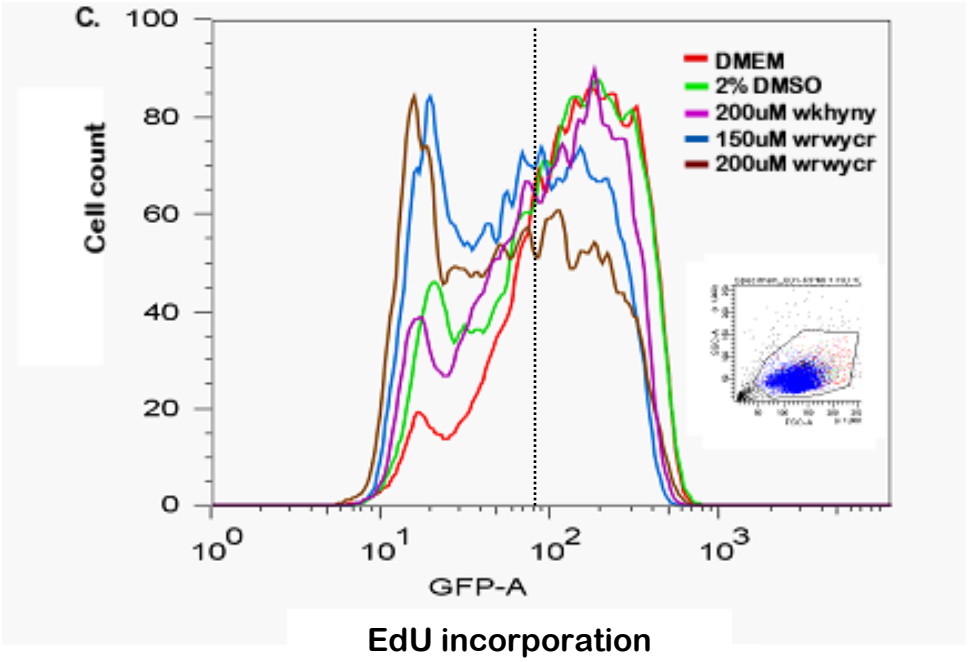

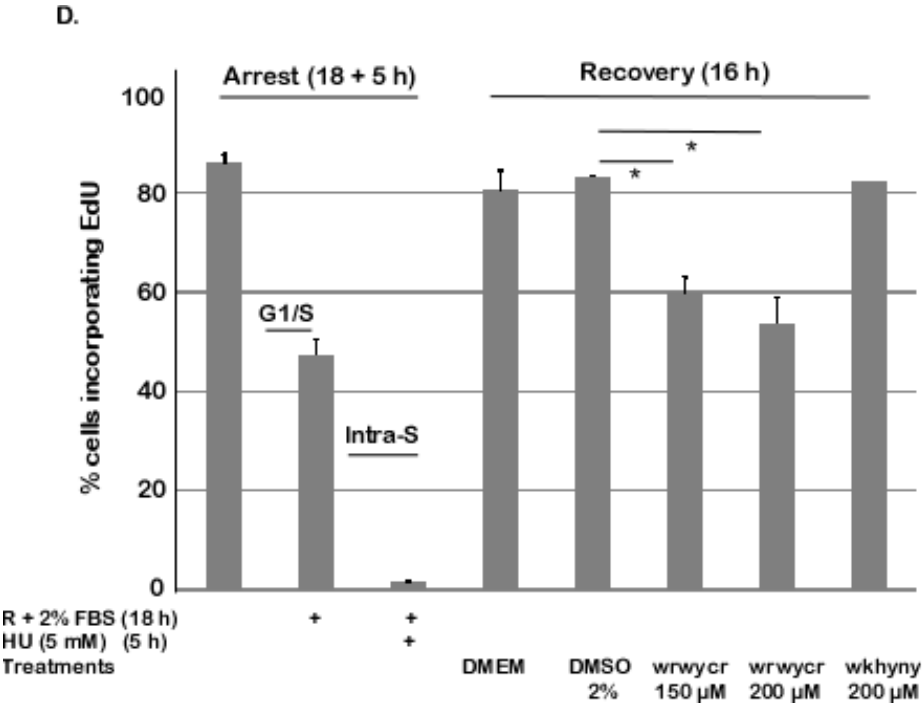

FigureII-9. Continued

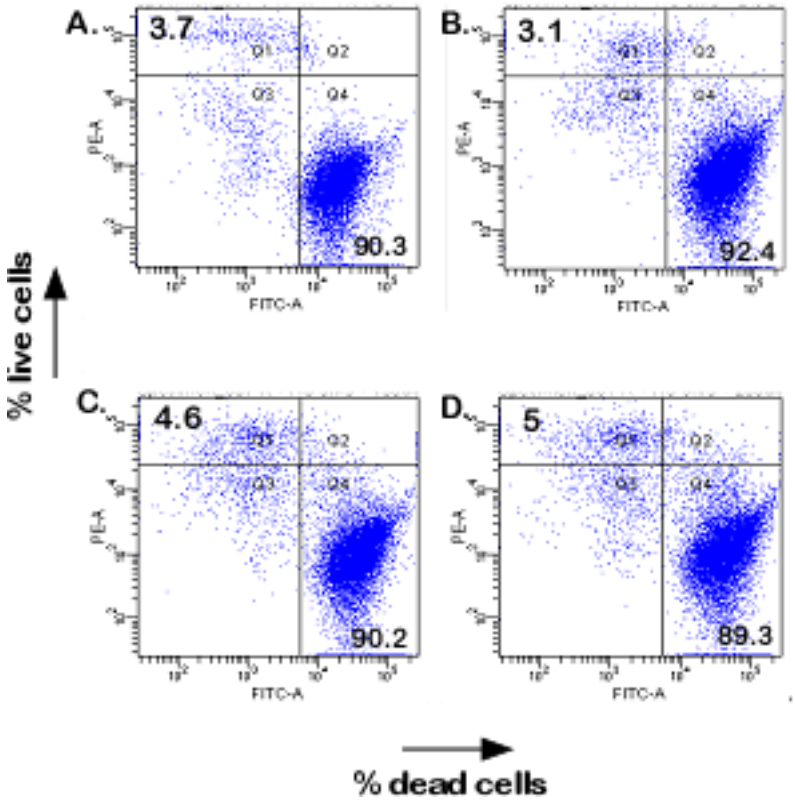

Figure II-10. DNA synthesis inhibition is not due to cell death.
Live / Dead assay was performed on U2OS cells arrested and recovered as in Figure II-9A. Shown here is the bivariate distribution of live vs. dead cells following Live / Dead staining of samples allowed to recover in presence of A. DMEM; B. 2% DMSO; C. 150 µM wrwycr and D. 200 µM wrwycr for 16 h. This is a representative of three independent experiments.

these transient repair proteins by several mechanisms (Rios-Doria et al, 2006; Chowdhury et al, 2005). In this study, we investigated the accumulation of three central sensors of DNA damage, γ-H2AX, ATR and phospho-ATM (Paull et al, 2000; Zhao and Piwnica-worms, 2001), in conditions where we see a negative effect on DNA synthesis. γ-H2AX co-operates with ATR (Ward and Chen, 2001) and ATM (Kurose et al, 2005; Agarwal et al, 2006) depending on the nature of DNA damage and the primary repair pathways and plays an active role in homologous recombination repair (Paull et al, 2000). ATM is involved in Double Strand Break repair (van Gent et al, 2001) whereas ATR plays active role in restarting stalled replication forks (Paulsen and Cimprich, 2007). Our synchronization regime was thus expected to involve ATR with or without γ-H2AX. However, our results are not exactly as predicted. Following intra-S arrest, we see profuse γ-H2AX foci formation, suggesting that the stepwise cell cycle arrest has generated DNA damage that needs to be repaired. ATR redistribution at the sites of damage is not evident. Samples containing increasing doses of wrwycr in the recovery media have more γ-H2AX foci than the DMSO (solvent) treated control (Figure II-11) suggesting that recovery from HU-mediated arrest is less efficient in presence of wrwycr. Surprisingly, ATR redistribution between DMSO and wrwycr treated samples is indistinguishable. On the other hand, we see a much more pronounced wrwycr effect on phospho-ATM foci formation (Figure II-12A). Counting the number of foci per nucleus for 50-60 cells per treatment shows a trend where increasing dose of wrwycr increases number of phospho-ATM foci per nucleus (Figure II-12B). This provides supporting evidence that wrwycr interferes with recovery from HU-mediated DNA damage. More detailed investigation of downstream repair proteins like Chk2, Chk1, Brca1, etc following this arrest-recovery regime will throw more light towards the predominant pathway wrwycr is involved in.

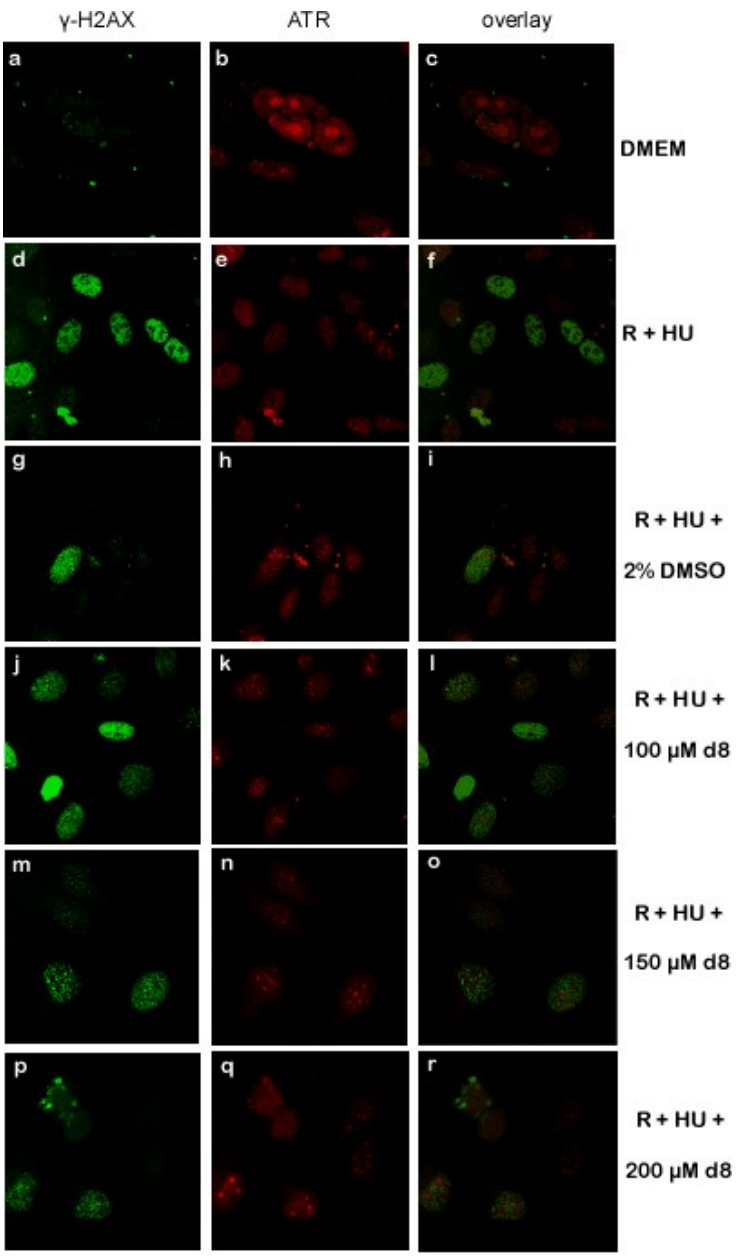

Figure II-11. Upregulation of ATR vs. γ-H2AX during recovery from HU-mediated damage.
The left column shows γ-H2AX foci (green), the middle column represents ATR distribution (red) and the right column is an overlay of the red and the green channel. Panel a-c designates the media only control. Panels d-f, R+HU represent the arrested cells after RPMI (18 h) + 5 mM HU (5 h) at 0 h recovery. Panels g-r shows samples after 16 h of recovery in presence of 2% DMSO (g-i), 100 µM d8 (j-l), 150 µM d8 (m-o) and 200 µM d8 (p-r).

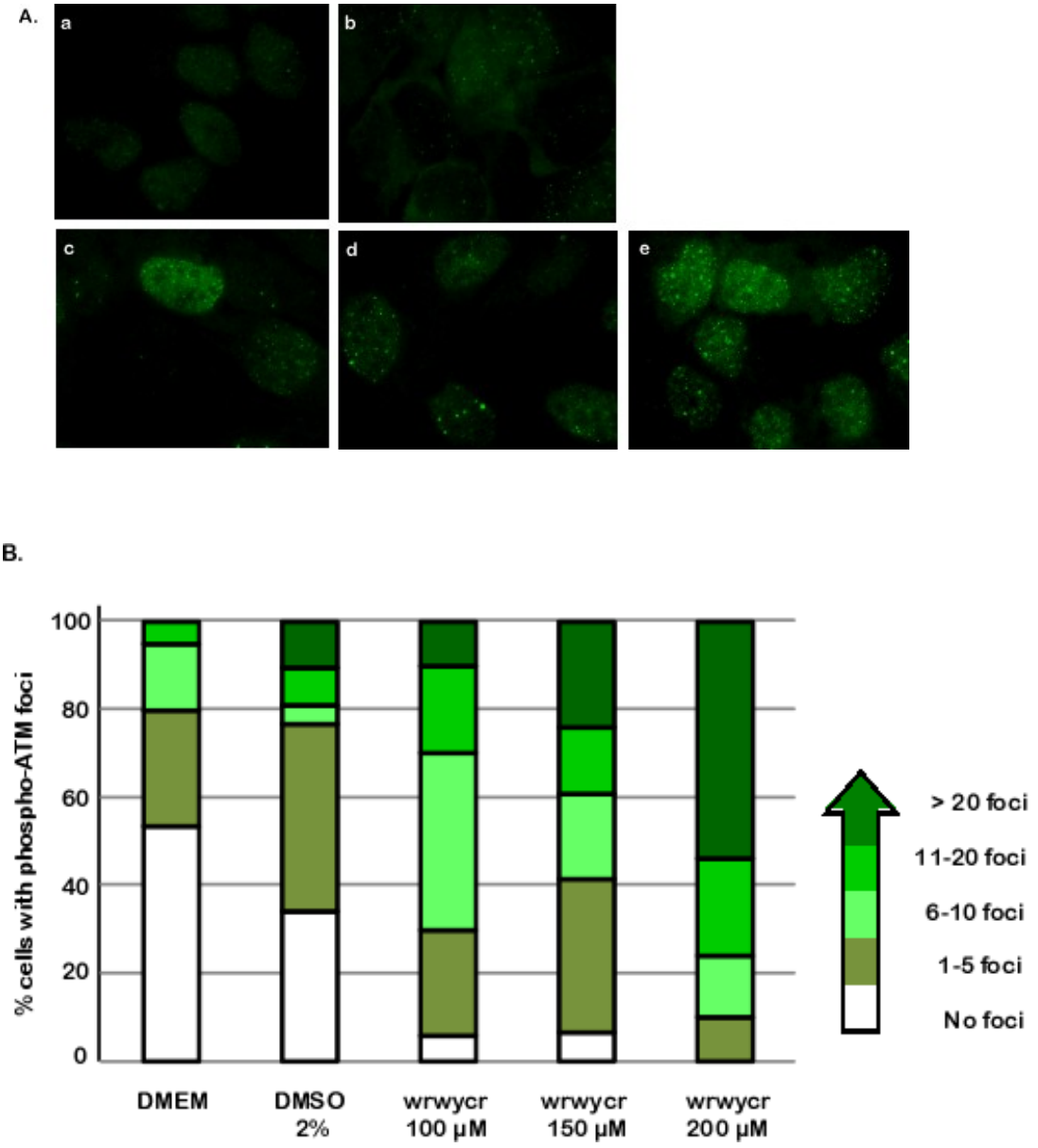

Figure II-12. Upregulation of phospho-ATM during recovery from HU-mediated arrest.

A. Representative images of phospho-ATM foci upon recovery from HU-mediated damage in presence of (b) 2% DMSO, (c) 100 µM wrwycr, (d) 150 µM wrwycr and (e) 200 µM wrwycr for 16 h. It should be noted that DMSO concentration is equalized (2% final) in all the three wrwycr treatments. Panel (a) is the unarrested DMEM (media) treated sample.

B. Quantitation of number of phospho-ATM foci per nucleus as color coded. At least 50 nuclei are counted per treatment. Each colored bar in the graph represents the % of cells generating that particular range of p-ATM foci.

IMR-90 cells, a slow-growing non-cancerous cell line, are resistant to wrwycr

In order to understand whether replication rate plays any role in wrwycr-mediated cytotoxicity and DNA damage, we tested effects of the peptide in a slow-growing, low passage lung fibroblast cell line and found that they are resistant to wrwycr-induced damage at conditions where U2OS cells are sensitive. The trend follows upon co-treatment of wrwycr with DNA damaging agents like etoposide and HU. Uptake of wrwycr in these cells is also minimum when compared to U2OS cells. Less entry inside these cells could be a plausible reason for the resistance towards wrwycr-induced cytotoxicity and DNA damage. Preliminary studies with several classes of cancer cell lines and two other primary cell lines (peritoneal macrophages, cardiac myocytes) also suggest that faster dividing cancer cells are better targets of wrwycr than primary cells (data not shown). More detailed investigation on this aspect is needed before it can be concluded that cancer cells are more sensitive to wrwycr than non-cancer cells.

Discussion

Cell penetrating, cationic peptides (CPPs) often have antibacterial (Boman, 1995; Zasloff, 2002; Pistolesi et al, 2007) and anticancer effects (Papo and Shai 2003, 2005). Natural antibacterial peptides are usually at least 20 amino acids long (Jenssen et al, 2006). Defensins, for example, were isolated from numerous insects as 43-mers. However, several smaller peptides (including 7-, 8- and 9-mers) designed based on the structure of insect defensins (with sequence VTCDLL SFEAKG FAANHS LCAAHC LALGRR GGSCER GVCICRR, having 6 highly conserved cysteine moieties followed by 4 arginines and 5 lysines, Miyanoshita et al, 1996) were subsequently synthesized and tested for antimicrobial activity, and shown to have the same mechanism of action as the parent compound (Saido-Sakanaka et al, 1999) with higher potency and broader spectrum of activity (Saido-Sakanaka et al, 2004).

Several of these cationic peptides are not cytotoxic to normal mammalian cells, probably because of their inability to bind to and permeate the zwitterionic mammalian cell membrane compared to the anionic bacterial cell membrane (Shai Y, 1999; Matsuzaki K, 1999). Cancer cell membranes, on the contrary, contain 3-9% more negative charge than normal cells (Zwaal R. F. A. et al, 2005). It is possible that cancer cells are more permeable and consequently more sensitive to these peptides. In this study, we have explored the anticancer potential of an antimicrobial peptide molecule, wrwycr, by investigating its effects on a human osteosarcoma cell line, U2OS. Our results are consistent with earlier findings about the anticancer potential of cationic antimicrobial peptides. wrwycr induces dose dependent cytotoxicity in U2OS cells. Interestingly, IMR-90 cells, a slow growing non-cancerous lung fibroblast cell line, show resistance to wrwycr-mediated cytotoxicity and DNA damage. We have also tested several other cancer cell lines and found them hypersensitive to wrwycr (data not shown) when compared to normal cell lines like primary peritoneal macrophages, primary cardiomyocytes, etc (data not shown).

The mechanism of antibacterial action of wrwycr is unique. Unlike cell penetrating antimicrobial peptides, wrwycr does not kill bacteria by cell lysis (Gunderson and Segall, 2006). Although they have some membrane perturbation effects (Yitzhaki et al, manuscript in preparation), the antibacterial action is due to its ability to interfere with DNA damage repair and cause accumulation of persistent DNA breaks inside bacterial cells (Gunderson and Segall, 2006, Gunderson et al, 2009). The fact that probable bacterial targets of wrwycr, namely branched DNA intermediates like HJ, are also produced in human cells led us explore the effects of this peptide in human cells.

In this study, we tested effects of wrwycr on a human cancer cell line, U2OS cells and compared it to two other peptides of similar size. Peptide wrwycr enters the U2OS cell cytoplasm, and to a lesser extent, the nucleus (Figure II-1A). The intracellular distribution of

the peptide is non-uniform. The vesicular pattern of distribution (Figure II-1g) is typical of a 6 amino acid long cell penetrating peptide and endocytosis is a plausible mechanism of uptake (Holm et al, 2006). There are regions of overlap with an endoplasmic reticulum protein, GRP78 (Appendix A.3, Figure A.3-2). HPLC-based quantitation of intracellular wrwycr concentration indicates that peptide uptake is co-operative (Table II-1, compare the fold change in intracellular peptide concentration between 100 μM, 150 μM and 200 μM wrwycr). This finding is consistent with the study which suggests that CPP uptake is often co-operative and the mechanism of uptake varies with the peptide input such that endocytosis is the predominant route at lower input concentration and is replaced by direct translocation at higher concentration (Fretz et al, 2007).

The first step in exploring the efficacy of a molecule as an anticancer agent is to test its capacity to induce cell death in the cancer cell population. Here we addressed acute cytotoxicity using Live/Dead assay after 24 h of wrwycr treatment and found that wrwycr exhibits a dose-dependent (Figure II-2A and 2B) decrease in cell viability in U2OS cells. In contrast, the control peptides wkhyny and WRWYAR and solvent DMSO had negligible effect.

wrwycr-induced cytotoxic effect is permanent but does not accumulate over time once the peptide is removed. This suggests that peptide wrwycr can be washed away. This is in contrast to etoposide treatment where 24 h of exposure is sublethal, but the treatment cannot be washed away and none of the cells can recover from the damage to form colonies. This indicates that etoposide interaction with its *in vivo* targets is irreversible (data not shown). It is worth mentioning here that we did not pursue our study in several other cancer cell lines due to the high cytotoxicity of DMSO alone, which made it more difficult to distinguish the wrwycr effect versus DMSO effect. In our hands, U2OS cells are the most resistant to DMSO-

induced cytotoxicity among the several cancer cell lines tested. The only assay where DMSO at its highest concentration (2%) showed some effect was the colony forming assay. There are two potential explanations for this observation. DMSO is known to have an anti-proliferative effect in different human cells (Eter and Spitznas, 2002; Rebourcet et al, 2004) and 24 h long treatment of cells with DMSO probably has a cytostatic effect. Thus, even after removal of the treatment, a fraction of the affected cells may be unable to reenter the cell cycle to form colonies. A second explanation may be that DMSO induces delayed damage to a subpopulation of U2OS cells, such that the effect is not evident after 24 h but the damage is irreversible and may eventually cause cell death. Either way, since we measure wrwycr effects mostly at or before 24 h, a delayed effect of DMSO, if any, is almost certainly not contributing to the wrwycr effect observed. The control peptides, resuspended in similar concentration of DMSO, do not have any significant effect in any of the assays performed. This provides additional evidence that wrwycr rather than DMSO is the main contributor to the reduction in viability.

U2OS cells, unlike other osteosarcoma cells, have wild type p53 and a functional apoptotic machinery (Allan et al, 1999). We tested for early (Annexin V-PI) and late apoptosis (caspase-3) and found that wrwycr induces some apoptosis in U2OS cells (Figure II-4 and Table II-2). However, preliminary results do not suggest any active role of p53 in this process. Upon wrwycr treatment, the p53 total protein is not stabilized (Appendix A.4, Figure A.4-1) or increased significantly on top of basal level (Appendix A.4, Figure A.4-1 and Figure A.4-2). Interestingly, p53 null variant of U2OS cells, Saos-2, is hypersensitive to wrwycr-induced apoptosis (Apendix A.4, Figure A.4-3). So far, our data suggest that wrwycr induced apoptosis is p53-independent. One interesting finding here, though, is that wrwycr treatment causes a mild up-regulation of p44 protein (a short isoform of p53 often referred to as hyper p53) that

increases significantly upon concurrent treatment of hydroxyurea (HU) (Appendix A.4, Figure A.4-1, Figure A.4-2). p44 is DNA damage inducible and causes premature aging either by triggering apoptosis or senescence or both (Tyner et al, 2002; Maier et al, 2004). This suggests that wrwycr-induced cell death might have a co-relation with DNA damage.

The *in vitro* and *in vivo* (bacteria) results with wrwycr intimates the possibility that wrwycr might be involved in DNA damage repair in mammalian cells (Boldt et al, 2004, Gunderson and Segall, 2006, Gunderson et al, 2009) since the primary target of wrwycr is generated in mammalian cells as well. We tested the potential first by performing wrwycr-mediated assays in the presence of DNA damaging drugs. Etoposide treatment primarily activates the ATM-Chk2 pathway and mimics γ-irradiation whereas hydroxyurea causes an intra-S phase arrest that gets repaired by ATR-Chk1 via a G2/M arrest. Since these are the two main repair pathways that involve homologous recombination and Holliday Junction formation, the results should suggest whether peptide-induced damage has any relation with DNA damage repair. Secondly, it might indicate which pathway(s) are more likely to create peptide targets in human cells.

We first checked the effect of the combination treatment in cell viability and found that the combination treatment was significantly more lethal than either alone. (Figure II-5A and B). Parallel estimation of DNA damage hallmarks like γ-H2AX foci induction (Figure II-7) and DNA fragmentation (TUNEL+ cells in presence of caspase family inhibitor) also showed similar trends (Figure II-6; Table II-3; Figure II-7). Between the two combination treatments, co-treatment of wrwycr with etoposide is more severe in causing cell death than inducing DNA breaks; DSBs (compare Figure II-5B with Figure II-7A) or single strand breaks (Figure II-6; Table II-3). Co-treatment with HU, however, induce more DNA breaks and γ-H2AX foci than cell death (compare Table II-3, Right panel with Left panel; Figure II-7B). These results

suggest that DNA synthesis might create more targets for wrwycr than direct DNA damage repair.

A major drawback of such analysis is that we are unable to analyze a significant fraction of treated cells because our treatment conditions induce cell death. Synchronization of cells at particular stages of the cell cycle should delay the doubling time and peptide-mediated cell death. Also, since a majority of cells would be arrested in a particular phase of the cell cycle, cell cycle specific peptide effect (like Homologous Recombination Repair) would not be underestimated. We synchronized U2OS cells in S phase and found that peptide wrwycr interferes with DNA synthesis during recovery from such arrest without inducing cell death (Figure II-9C and D; Figure II-10). This was corroborated by persistence of repair proteins like γ-H2AX and phospho-ATM at the end of the recovery phase, indicating the presence of unrepaired DNA lesions in cells.

Involvement of ATM and the minimal apparent involvement of ATR in the recovery from HU-mediated arrest was surprising since HU-induced damage is expected to trigger ATR redistribution (Wu et al, 2006). This observation can be explained by a few possibilities. First, this stepwise synchronization regime generates significant double strand breaks (DSB) inside cells that involves γ-H2AX-ATM for repair. This could be direct DSB formation or indirect due to the presence of stalled replication forks that never got restarted. Second, there is a possibility that ATR co-operates with ATM to repair the HU-mediated damage. Involvement of ATM in processing stalled replication forks has already been reported (Ewald et al, 2008). In fact, recent studies have demonstrated that these upstream PI(3)Ks have significant overlapping action. In the future we will perform more co-localization studies with several downstream proteins (like Chk1, Chk2, Brca1) and ATM/ATR to understand if wrwycr targets are generated preferentially in either of these pathways.

From this study we can conclude that DNA damage response processes generate some wrwycr targets. The non-linear increase in acute cytotoxicity with increasing dose of the peptide is probably due to the peptide action on other cellular targets at high intracellular concentration. Use of control peptides that share some characters of wrwycr but are different in all the different assays performed indicate that wrwycr effects in U2OS cells are sequence-specific events. We have preliminary evidence that at high concentration, wrwycr affects U2OS cell membrane (Appendix A.6, Figure A.6-1). Focused microarrays targeting particular processes should unravel more targets of wrwycr inside human cells.

Chapter II, in full, is being prepared for a future publication. The dissertation author is the primary investigator and author of this work. Co-authors are Nathan Authement and Anca Segall. I would like to acknowledge Nathan for his great assistance in performing the microscopy experiments under constant supervision of the primary author.

CHAPTER III

UPTAKE AND EFFECTS OF WRWYCR IN HELA CELLS AND A HELA CELL VARIANT

Introduction

Background

The effect of wrwycr on human cells was preliminarily explored by another member of the Segall laboratory, Leo Su, using HeLa cells as the prototype. Hela cells were isolated from a cervical carcinoma patient in 1951 (Gey et al, 1952). Several advantages of using HeLa cells included : (1) their widespread use in the study of mammalian cell processes (Masters 2002) especially in DNA repair studies (Hardt et al, 1981; Morita et al, 2001), (2) ease of maintenance in culture and (3) no requirement of gentle handling. This was the first attempt towards understanding if there is any co-relation between the effects of wrwycr *in vitro* and in prokaryotes and its effects in eukaryotes. This was reasonable since the *in vitro* and bacterial target(s) of wrwycr are HJs and some other branched DNA substrates generated and resolved during replication, recombination and DNA repair of both prokaryotes and eukaryotes (Guy et al, 2005; Li and Heyer, 2008; Friedberg et al, 2006). However, eukaryotic DNA is generally less accessible to external agents than bacterial DNA. First, the nuclear and mitochondrial DNAs are surrounded by an additional membrane, which are only selectively permeable (Ribbeck and Gorlich, 2001; Sun et al 2007). Second, eukaryotic nuclear DNA is largely present as chromatin, composed of DNA wrapped around a core of histone proteins (Park et al, 2002; Bårtová et al 2008). The DNA structure is somewhat relaxed during replication or repair to provide access to the relevant proteins. Branched DNA intermediates and Holliday Junctions in particular, would be produced only transiently, when the DNA is actively being repaired.

Hypothesis and previous study

The hypothesis for this study was that wrwycr exerts its effects in eukaryotic cells (as it does in bacteria) via binding to DNA repair intermediates like HJ produced during replication, fork reversal and recombination dependent repair (Kepple et al, 2005, 2008; Gunderson and Segall, 2006, Gunderson et al, 2009). The first attempt to test this was indirect. It was predicted that administration of sublethal concentrations of exogenous DNA damaging agents would produce several DNA lesions that would induce DNA repair, thereby producing transient intermediates like HJ. These intermediates would be stabilized in the presence of peptide wrwycr, resulting in the disruption of DNA repair and persistence of DNA damage. The effects of treating cells with a combination of peptide and sublethal dose of etoposide or hydroxyurea (HU) were tested to inquire about the cellular metabolic state (MTT), generation of DNA breaks (TUNEL) and their dependence on apoptosis (TUNEL in the presence of the caspase family inhibitor, Z-VAD) and more specifically DSBs (γ-H2AX up regulation). Etoposide and HU produce double strand break (DSB) via distinct mechanisms. Etoposide (VP-16) is a poison of topoisomerase II that interferes with the DNA cleavage-religation reaction of this mammalian enzyme and stabilizes a cleavable protein-DNA complex, thus producing double stranded breaks (Chen et al, 1984, Maanen et al, 1988; Tanabe et al, 1991, Treszezamsky et al, 2007). Hydroxyurea (HU) inhibits ribonucleotide reductase function, depleting dNTP pools and blocking DNA synthesis. Prolonged exposure or high concentration of HU can produce DSBs (Saintigny et al, 2001; Lundin et al, 2003) and cause ATR-dependent phosphorylation of H2AX (Ward and Chen, 2001; Ward et al, 2004; Chanoux et al, 2009). In some of the synergy assays, cycloheximide, a protein synthesis inhibitor with no direct relation to DNA, was used as a negative control.

Summary of results with HeLa cells

From the above studies it was concluded that rhodamine-tagged WRWYCR can enter HeLa cells and is non-uniformly distributed inside them (Figure III-1). Peptide wrwycr caused a dose-dependent reduction of metabolic activity in HeLa cells, measured by the activity of lactate and succinate dehydrogenases, a reduction that was more severe upon addition of etoposide but not cycloheximide. By itself, wrwycr generates DNA breaks only in a small (12%) subpopulation of the treated cells. This subpopulation increases to 60 and 80 % upon co-treatment with etoposide or hydroxyurea respectively. The DNA fragmentation observed was not a result of late apoptosis, since the same extent of fragmentation was observed with or without a caspase family inhibitor. Finally, wrwycr treatment generated γ-H2AX positive cells which are potentiated when administered in conjunction with etoposide or hydroxyurea. These results, summarized in Table III-1, suggested a causal relationship between wrwycr-induced cytotoxicity and DNA damage which supported, although did not prove, the predicted mechanism of action of wrwycr.

Limitations and current research outline

A much more detailed analysis of each of the questions is necessary before anything conclusive can be inferred from the above study. In this chapter, I reinvestigated the hypothesis by addressing the above questions from a slightly different perspective, analyzed and interpreted the overall results.

Specifically, I tried to clarify the following points. First, I quantifed the intracellular wrwycr concentration and determined the monomer versus dimer concentration by performing High Pressure Liquid Chromatography (HPLC). Secondly, to assess whether the dose-dependent decrease in

Table III-1. HeLa cell previous assay summary

Treatments	**MTT** (% loss in metabolic activity)	**TUNEL** (% cells with DNA breaks)	**caspase-3** (RFU / µg) protein	**% γ-H2AX + cells**
DMEM	100	0	1.5	7
DMSO (1%)	NT[c]	NT[c]	2	6
eto[a] (1.3 µM)	39.4	1	4	15
eto[a] (51 µM)	NT[c]	NT[c]	38	36
cyclo[b]	24.3	0	1.4	
HU (10 mM)	NT[c]	1.5	3.5	
Sorbitol (400mM)	NT[c]	75[d]	34	
wrwycr (µM)				
50	14.1			21
100	21.2	12		51
150	34.4			50
200	45.5			
eto[a] (1.3µM) + wrwycr (µM)				
50	44.5			49
100	54.6	60[e]	3.5	78
150	68.7			69
200	77.8			
cyclo[b] + wrwycr (µM)				
50	20.2			
100	33.3			17
150	61.4	16	1	35
200	54.6			45
HU (10 mM) + wrwycr (µM)				
50				72
100		80[e]	5.8	73
150				58

[a]eto = etoposide; [b] cyclo = cycloheximide; [c]NT = Not tested
[d] Indicates DNA fragmentation as a result of apoptosis
[e]Indicates non-apoptotic DNA breaks (compare TUNEL and caspase-3 signal)

metabolic activity in the wrwycr-treated population was due to cell death, I performed the Live / Dead assay to directly count live and dead cells by flow cytometry. In order to understand whether HeLa cells can recover from wrwycr-induced damage once the peptide is removed, I performed the colony forming assay (CFA). Finally, I assessed wrwycr-induced apoptosis in greater detail. Previous results indicated that 24 h of wrwycr treatment either by itself or with a sublethal dose of etoposide (1.3 μM) does not induce apoptosis. However, the only apoptotic parameter tested was caspase-upregulation, which is one of the latest events of apoptosis (Luthi and Martin, 2007, Walsh et al, 2008). If the majority of the affected population of cells is in earlier stages of apoptosis, the caspase assay would underestimate the outcome. Therefore I used a Hela cell variant, Htog1 (Goldstein et al, 2000, details of the construct in Materials and Methods) in which cytochromeC is tagged with GFP. Release of cytochrome C from the mitochondria can be easily tracked in this cell line. These cells have been used to study mitochondrial morphological changes during various stages of apoptosis (Sun et al, 2007). We used confocal microscopy with Htog1 to address the following hallmarks of apoptosis: (a) cytochrome C release from mitochondria. (b) loss of mitochondrial membrane potential (MMP) using TMRE staining and (c) classic morphological features of apoptosis like spikes, blebs and nuclear condensation, etc. We also measured cell size of the population using Image J. Finally, we extended the analysis of γ-H2AX foci via flow cytometry further by using fluorescence microscopy. Flow cytometry analysis determines whether a particular cell has more or less than a threshold fluorescence intensity. It only crudely distinguishes between cells with more or fewer foci if mean fluorescence intensity per cell is calculated. The level of focus formation can be directly estimated using microscopy to observe individual cells in a heterogeneous population.

Results

Uptake of wrwycr in HeLa cells

Previously, confocal microscopy experiments were performed to determine the uptake of WRWYCR, using peptide WRWYCR labeled with Liss-rhodamine at the N terminus (for details of the construct, see peptides in Materials and Methods). Traces of peptide inside cells (evidenced by Z series images) were clearly visible within 30 min of incubation and the intensity of staining increased over time (Figure III-1, taken from L. Su, PhD dissertation).

The results of the microscopy indicated that Rho-WRWYCR enters HeLa cells and concentrates in specific regions of the cell rather than distributing uniformly throughout the cell (Figure III-1, L. Su, PhD dissertation). The pattern of distribution was somewhat similar to that of mitochondrial cytochromeC oxidase, suggesting that the peptide might have a preference towards mitochondria (Nakagawa and Miranda 1987; Varlamov et al, 2002). In contrast, the nucleus is stained much less. There are several limitations to this approach. First, the Rhodamine tag is almost 60% the size as the peptide and may influence the uptake. Second, it is not easy to quantify the exact amount of intracellular peptide from the microscopy data. Third and the most important, it is impossible to evaluate the relative amount of active intracellular peptide (peptide dimer) using microscopy.

An HPLC based method was developed to directly quantify the presence of unlabeled monomer and dimer wrwycr inside cells. A standard curve was generated by running 0.2, 0.5 and 1 nanomoles of wrwycr via HPLC and integrating the area under the curve of the peptide-dependent peaks (monomer + dimer) (Figure III-2). The dimer and monomer peaks were confirmed by using DTT to reduce the dimer peak and

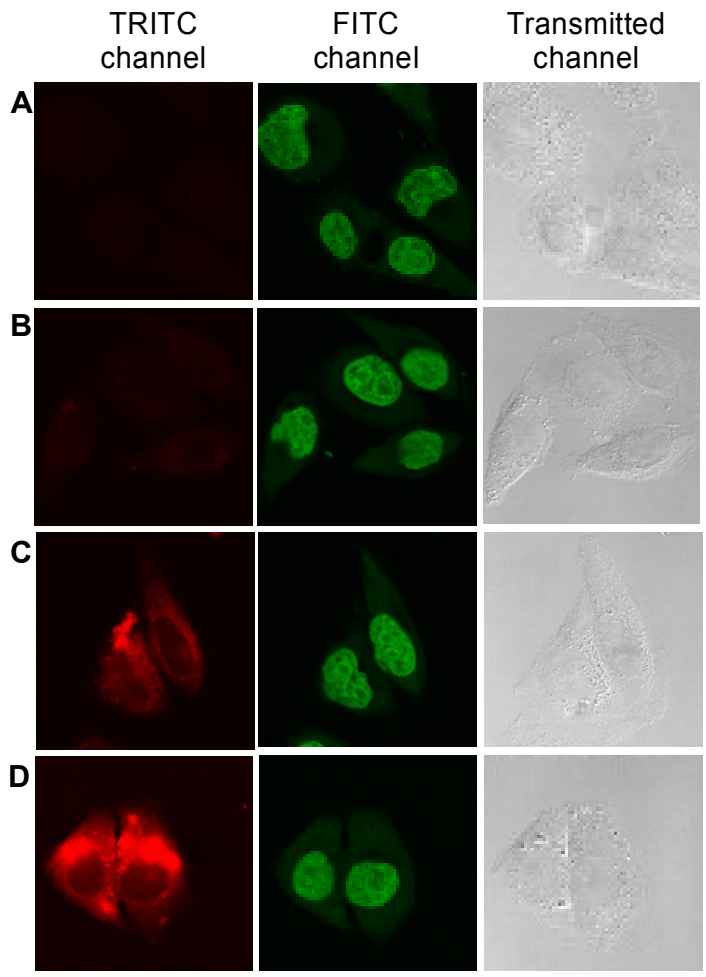

Figure III-1. Uptake of Rho-WRWYCR in Hela cells by confocal microscopy.
Hela cells were either incubated with (A) no peptide or 1μM Rho-WRWYCR for (B) 10 min, (C) 30 min or (D) 5 h, counterstained with picogreen for 10 min at 37ºC and visualized by confocal microscope. Rho-WRWYCR is visible in the TRITC channel and Picogreen (DNA, nucleus) is visible at the FITC channel. Each image is an optical section near the center of the cell obtained by capturing Z series images through focus (data generated by L. Su, L. Su, doctoral dissertation)

correspondingly increase the monomer peak (data not shown). In the method used, the monomer peptide elutes at 19.05 min and dimer peptide elutes at 19.25 min (representative trace, Figure III-3). The presence of wrwycr in the peaks was confirmed by MALDI-TOF mass spectrometry (TSRI facility). Plotting input concentration versus intracellular concentration, we found that (a) the dimer concentration correlates linearly with the input dose, whereas the total intracellular wrwycr concentration reaches saturation after administration of 150 μM wrwycr (Figure III-4, Table III-2). and (b) wrwycr accumulates inside HeLa cells (Table III-2).

Etoposide potentiates wrwycr-induced dose-dependent cytotoxicity in HeLa cells

Previously, wrwycr-induced cytotoxicity was assessed using an MTT assay to measure lactate and succinate dehydrogenase activity (Mossmann, 1983). The results indicated that wrwycr causes a dose-dependent reduction in cellular metabolic activity that is potentiated by DNA damaging agents like etoposide but not by the protein synthesis inhibitor, cycloheximide (Su, Patra and Segall, manuscript in preparation; L. Su, dissertation, 2009). Although the MTT assay is widely used as a general test of cell viability (Plumb 2004, Burton 2005, Wang et al, 2006 and Kim et al, 2007), it is not a direct measure of cell death. First, it does not distinguish between cytostatic effects of a compound that can cause temporary growth arrest or permanent senescence and cytotoxic effects that cause cell death. Second, in this high throughput assay, the activity is measured at the population rather than the individual cell level, and does not discern whether the effect of the peptide is uniform.

In order to supplement the MTT assay, I performed the Live / Dead assay where live and dead cells are directly categorized based on serum esterase activity and loss of

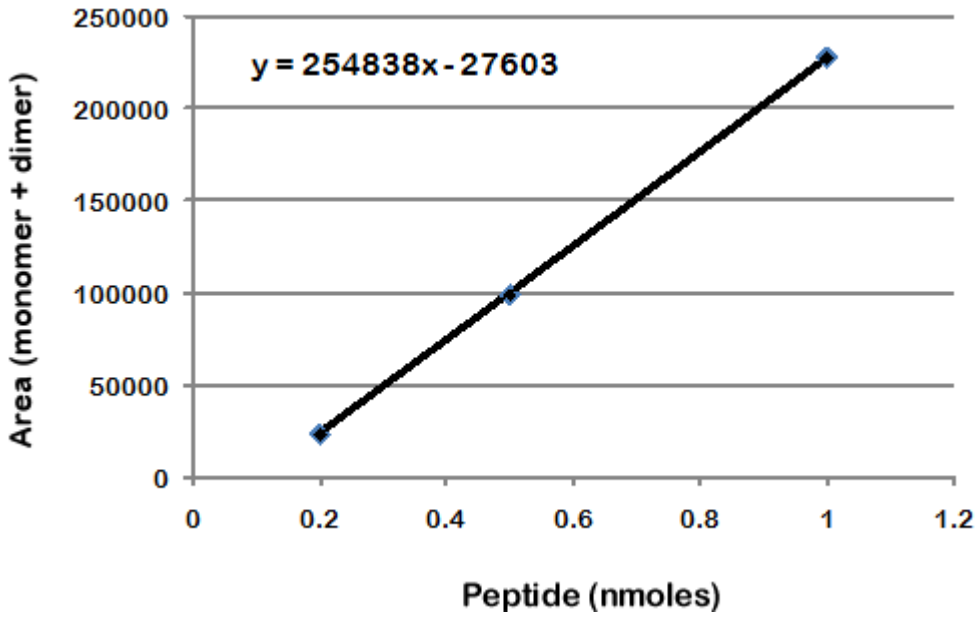

Figure III-2. Standard curve of wrwycr used to quantitate intracellular peptide concentration This is based on the area under the curve. 0.2, 0.5 and 1 nanomoles of standard wrwycr were run through HPLC and the total area under the peptide dependent peaks (monomer +dimer) were integrated and plotted against the corresponding wrwycr input concentration

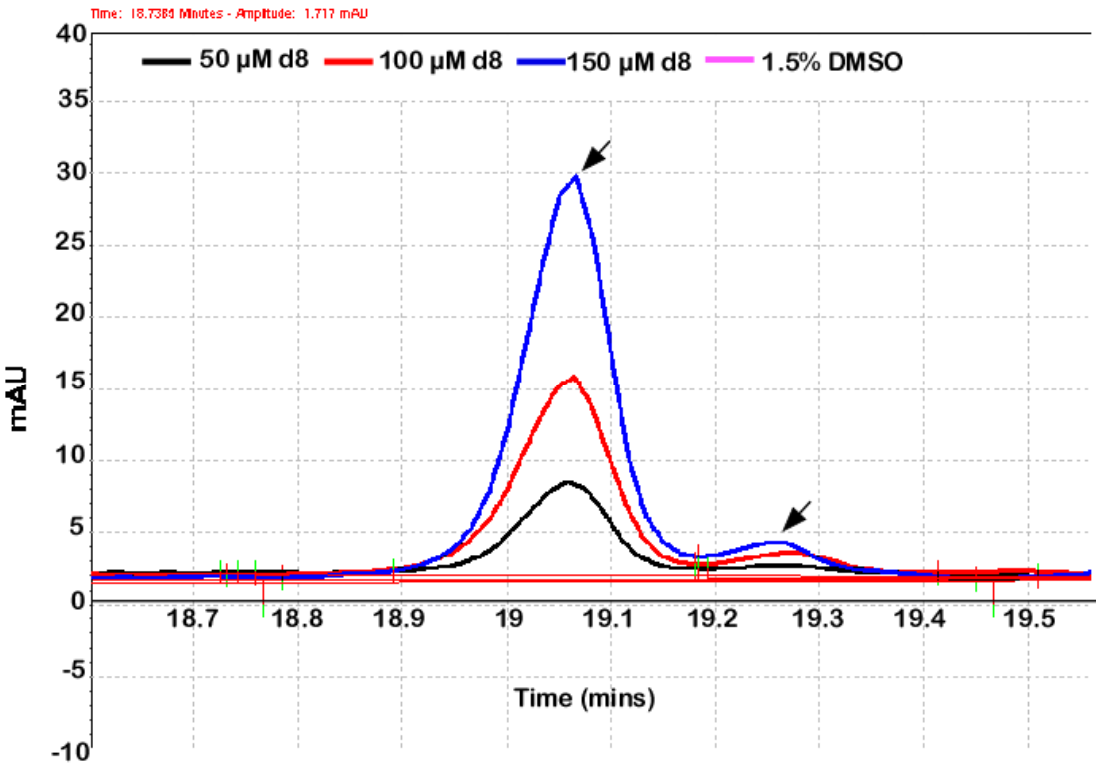

Figure III-3. Representative HPLC trace of Hela cells. Here 50 µM (black line), 100 µM (red line) and 150 µM (blue) wrwycr samples are overlaid on top of 1.5% DMSO (pink line). The arrowheads point to the monomer (left) and the dimer (right) peaks.

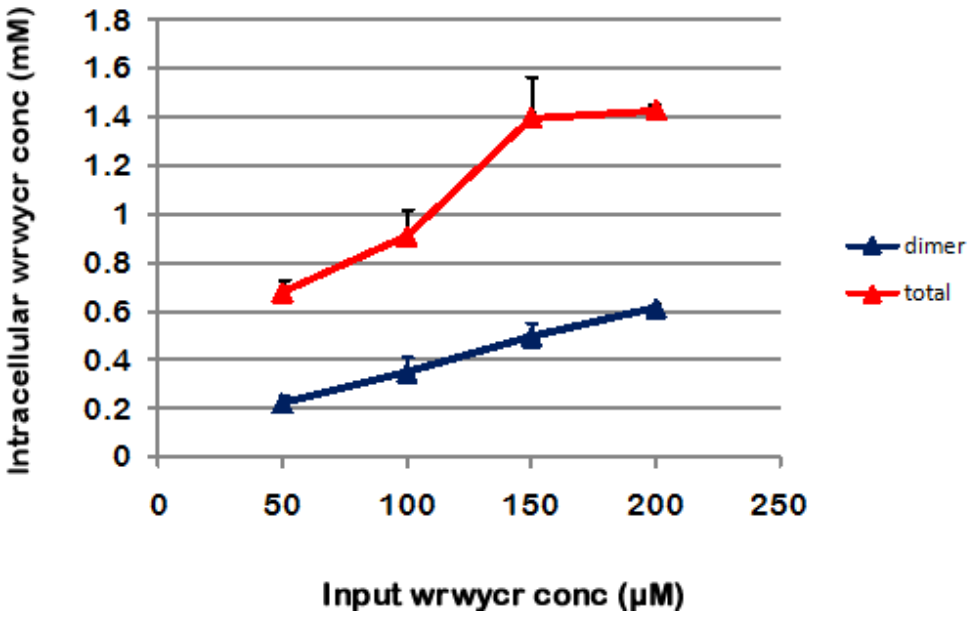

Figure III-4. Summary graph of HPLC quantitation in Hela cells.

Shown here is a line graph of intracellular wrwycr concentration versus. input concentration. The red line indicates the total intracellular peptide concentration [monomer + (dimer x 2)] and the blue line represents the intracellular dimer concentration. Each data point is a mean of at least 4 independent experiments, error bar represents standard error.

Table III-2. Quantitation of input vs. intracellular conc of wrwycr in Hela cells

Intracellular conc (mM)	Input monomer conc (μM)			
	50	**100**	**150**	**200**
monomer	**0.3** ± 0.06	**0.26** ± 0.08	**0.49** ± 0.2	**0.2**
dimer	**0.22** ± 0.03	**0.35** ± 0.06	**0.5** ± 0.06	**0.61** ± 0.01
fold change[b]	*1*	*1.6*	*2.23*	*2.77*
Total [a]	**0.68** ± 0.22	**0.91** ± 0.11	**1.4** ± 0.17	**1.43** ± 0.02
fold change[b]	*1*	*1.34*	*2*	*2.1*

[a] The input concentration (μM) as well as the final intracellular concentration (mM) are calculated as monomer concentration.
Thus, the total intracellular concentration = [monomer] + 2* [dimer]
[b] The fold change is calculated with respect to 50 μM wrwycr

membrane integrity, respectively, and counted individually using flow cytometry. Figure III-5A shows a representative bivariate distribution of live (Q4) vs. dead (Q1) cells after 24 h of 2% DMSO (Figure III-5A.i) or 200uM wrwycr (Figure III-5A.ii). The cells in Q2 and Q3 are considered sick because they have either lost membrane integrity but still have active serum esterase (Q2) or they do not have esterase activity but their membrane is still intact (Q3). Summarizing the assay results, we infer that wrwycr-dependent killing of HeLa cells is modest after 24 h treatment (Figure III-5B, lower panel). The fraction of live cells does decrease in dose-dependent fashion, suggesting that the cells may be experiencing difficulties in survival (Figure III-5B, upper panel).

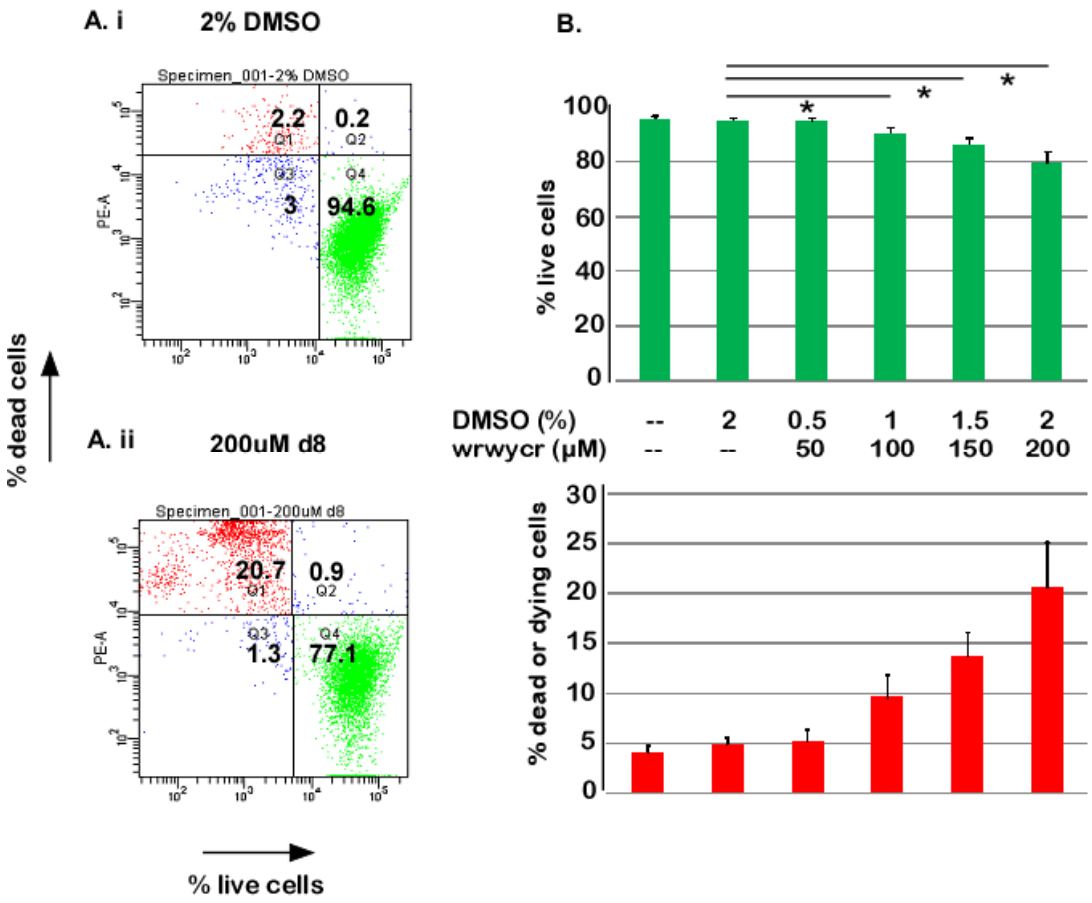

Figure III-5. 24 h of wrwycr treatment alone has a modest killing effect in HeLa cells. Panel A shows representative dot plots showing bivariate distribution of PE (dead) vs. FITC (live) cell population upon (i) 2% DMSO and (ii) 200 µM wrwycr treatment respectively. (B) The overall quantitation of % live cells (upper panel) and % dead cells (lower panel) following administration of increasing doses of wrwycr The mean is an average of at least three independent experiments

Table III-3. Comparison of MTT versus Live/Dead assay in HeLa cells

Treatments	MTT (% loss in metabolic activity	Live / Dead assay Dead	Sick	Live
DMEM	0	1.2	2.9	95.9
DMSO (2%)	NT[b]	2.2	2.7	95.1
eto[a] (1.3 μM)	39.4	3.5	10.7	85.6
wrwycr (μM)				
50	14.1	1.5	3.7	94.8
100	21.2	5.3	5.3	90.4
150	34.4	7.8	7.8	86.3
200	45.5	12.7	8	79.3
eto[a] (1.3 μM) + wrwycr (μM)				
50	44.5	NT[b]	NT[b]	NT[b]
100	54.6	NT[b]	NT[b]	NT[b]
150	68.7	13.1	16	70.9
200	77.8	21.1	9.5	69.4

eto[a] = etoposide
NT[b] = Not Tested

To check this, the sick cell population was sorted and allowed to grow in culture for about a week. None of the sorted cells recovered in culture, suggesting that wrwycr treatment does induce a dose-dependent cytotoxicity in HeLa cells but that the effect is delayed. We also found that administering a sublethal concentration of etoposide mildly potentiates wrwycr-mediated cell killing (Figure III-6A, Table III-3). Moreover, 24 h of etoposide treatment by itself increases the forward scatter (FSC, corresponding to cell size) and side scatter (SSC, corresponding to cell granularity) pattern of HeLa cells compared to the untreated sample, suggesting a problem in cell division (Figure III-6B, FSC vs. SSC dot plots, compare B.i, 1.3 μM etoposide, B.ii 150 μM wrwycr, and c. 1.3 μM eto + 150μM wrwycr, and Figure III-8D)

The two major conclusions of this study were that (a) The trend of results for the two assays (MTT and Live / Dead) were similar but showed that correlating wrwycr-mediated % reduction in metabolic activity with % loss of viability would have been an overestimation (Table III-3, compare the MTT results with the Live/Dead data). Also, results of the Live/Dead assay indicate that a fraction of the wrwycr-treated HeLa cell population that is not yet dead, shows signs of stress after 24 h (Table III-3). (b) Concurrent administration of etoposide and wrwycr increases the cell size in the population, a common sign of cell cycle arrest (Thiebut et al, 1994; Ruster et al, 2008).

Cytotoxicity induced by wrwycr is irreversible but not cumulative

One important question that arises here regards the fate of the wrwycr-treated cell subpopulation that has been arrested. Do cells recover after removal of wrwycr or are the cytotoxic effects permanent? A related question is whether the effect accumulates over time after withdrawing the treatment. This would give an insight to how transient the interaction of wrwycr is with its *in vivo* targets or whether the peptide may be effluxed via Multi Drug Resistant pumps (Brenwald et al, 2003). To test this, a colony forming assay (CFA) was performed. HeLa cells were treated for 24 h, then allowed to recover for several days in the absence of treatment. The results indicated that wrwycr exhibits a dose-dependent cytotoxicity that is irreversible (compare the % live cells in Figure III-5B, upper panel versus % cells forming colonies in Figure III-7B). For example, after 24 h of treatment with 150 μM wrwycr, 86.3% cells retained esterase activity and membrane integrity, but only ~ 66% were able to form colonies. This suggests that a subpopulation of cells that appeared healthy after 24 h of treatment could not form colonies. This could either be due to late manifestation of wrwycr-induced damage or a cytostatic effect of the peptide.

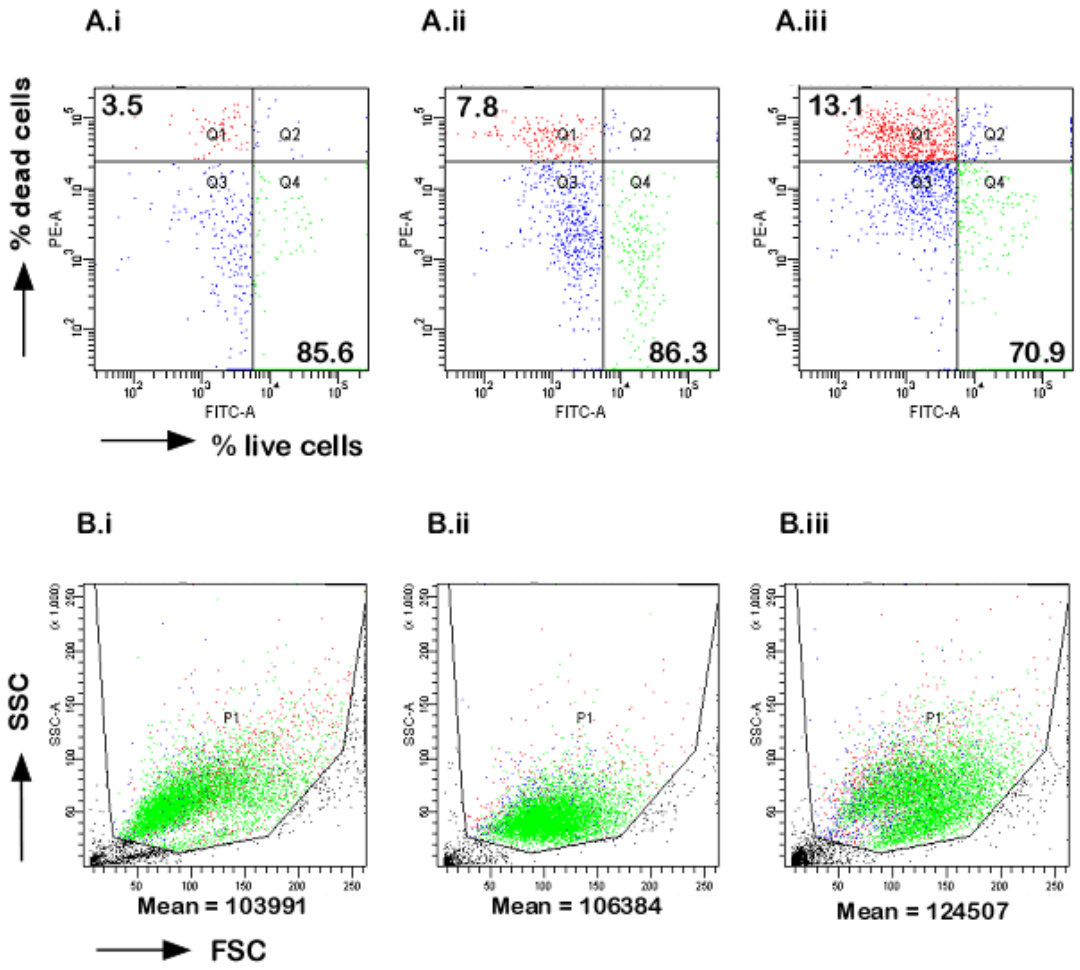

Figure III-6. Etoposide mildly potentiates wrwycr-induced killing of Hela cells.
Representative dot plots of A. live vs. dead cells and B. Size versus. granularity (SSC vs. FSC) after 24 h of (i) 1.3 µM etoposide, (ii) 150 µM d8 (wrwycr) and (iii) 1.3 µM etoposide + 150 µM d8 treatment. The number labeled as Mean in the plots of Panel B represents the Mean FSC value of the gated population.

Solvent DMSO also demonstrates a modest but significant reduction in viable colonies (Figure III-5A & B, 95% live cells versus Figure III.7B 86% colony forming cells). Thus a fraction of the delayed response in around 20% cells may be that of contributed by the solvent. The control peptide wkhyny does not show any toxicity above DMSO.

Significant fraction of wrwycr treated cells can form colonies after removal of wrwycr treatment indicating that wrwycr can be washed away. This suggests that wrwycr interaction with its targets in HeLa cells is transient. *In vitro* binding assays of wrwycr suggest that wrwycr stably interacts with its target DNA structures like HJs, but the interaction is not irreversible (Boldt et al, 2004, Kepple et al, 2005, 2008). These DNA substrates could thus be potential targets of wrwycr in HeLa cells. One interesting observation is that etoposide treatment at a concentration that is considered sublethal, 1.3 μM, failed to produce any colonies. Two plausible explanations of this phenomenon are (1) etoposide is stably bound to the topoisomerase II – DNA complex and is hard to wash away, causing damage to accumulate over the subsequent 6-7 days; the damaged cell does not recover and form colonies. This, however, is contrary to the previous findings (Long et al, 1985, Long et al, 1986) reporting that etoposide interacts with its *in vivo* targets in a reversible manner, and depending on the time of exposure, the lesions are reversible. (2) Another possibility is that the affected cells recover late and are not able to divide fast enough to form colonies.

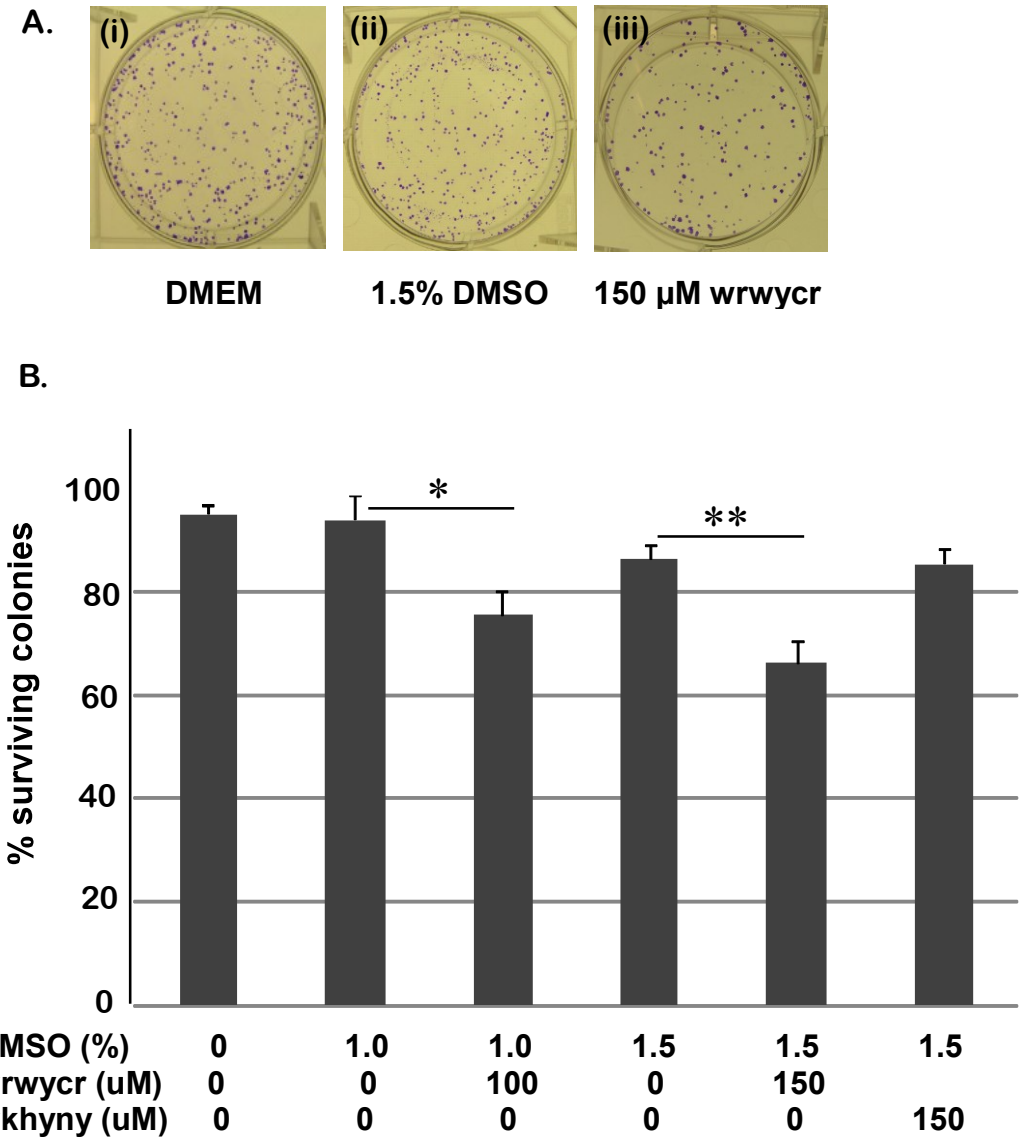

Figure III-7. wrwycr-induced Hela cell damage is completely irreversible.
Hela cells are treated for 24 h and allowed to recover and form colonies in the absence of treatment for 5-6 days.
A. Representative colony pictures after treatment with (i) DMEM, (ii) 1.5% DMSO and (iii) 150 µM wrwycr.
B. Overall quantitation of the experiment normalizing the number of colonies to % surviving colonies considering media only sample to be 100%. Statistical analysis was performed using student's t test. $P<0.05$ (*) and $P<0.005$ (**) indicates significant and highly significant difference between the two data points respectively.

Treatment with wrwycr does not induce significant apoptosis but increases cell size

The results of Leo Su's study indicated that 24 h of wrwycr treatment, alone or in combination with DNA damaging drugs like etoposide or hydroxyurea, generated DNA breaks (TUNEL positive cells, Table III-1) that are caspase-independent (Table III-1, compare caspase-3 upregulation with induction of % TUNEL-positive cells in 100 μM wrwycr treatment alone or in conjunction with etoposide or hydroxyurea). For instance, 24 h concurrent treatment of 10 mM HU and 100 μM wrwycr produces only 5.8 units of caspase-3 up regulation but 80% of cells were marked TUNEL-positive.

Since caspase-3 (or other members of caspase family) is activated only at very late stages of apoptosis, cells in earlier stages of apoptosis would score negative in the assay used and the conclusion will be misleading. Therefore, we used the Htog1 variant of HeLa cells containing the cytochromeC-GFP construct (Goldstein et al, 2000; Goldstein et al, 2005) which shows the intracellular distribution of this critical protein during various stages of apoptosis (Goldstein et al, 2005, Sun et al, 2007). Parallel use of a fluorescent probe, TMRE, that partitions into the mitochondrial matrix in response to the creation of $\Delta\psi_m$ helped us detect the status of the mitochondrial membrane potential, MMP (Loew, 1996). Loss of MMP (loss of TMRE staining) and release of cytochromeC are two important mitochondrial events of apoptosis that precede caspase induction (Goldstein et al, 2000; Goldstein et al, 2005). We used epifluorescence microscopy to assess these two hallmarks and, in parallel, searched for classical apoptotic features like nuclear and cytoplasmic condensation, spikes, or blebs after treatment with wrwycr with or without a sublethal dose of etoposide. Assessment of mitochondrial features may also provide insight into the general health of mitochondria after

the various treatments. This is relevant to our study because we have confocal microscopy evidence from that Rho-WRWYCR distribution does overlay with mitochondria (Appendix A.3, Figure II-1, Figure III-1 and Figure IV-1).

The results correlate well with Leo Su's previous findings that little apoptosis occurred in cells receiving peptide treatment alone or in combination with etoposide at the doses tested here (Figure III-8A, III-8B graph, compare ~70% of cells with apoptotic features in 150uM etoposide with all the other treatments each affecting only ~20% of cells). The majority (~80%) of the treated cells retained cytochromeC within the mitochondria (green channel) and punctuate TMRE staining (red channel) indicating that they have not initiated the apoptotic program. This is even more evident by the tight overlay of the two channels. A higher concentration of etoposide reported to cause apoptosis via DNA damage in HeLa cells (150uM etoposide for 16 h, Sun et al, 2007) was used as the positive control in this study.

Another finding using the Live / Dead assay supporting our preliminary observation from the FACS analysis of HeLa cells was that etoposide-treated samples that showed no signs of apoptosis appeared significantly larger in size than the untreated samples. (Figure III-8A, 1.3 μM etoposide treated sample). This enlargement is even more pronounced upon co-treatment with 100 μM wrwycr (Figure III-8A, 1.3 μM etoposide + 100 μM wrwycr). To follow up on this observation, we determined the cell size distribution for each treatment using the Image J program and found a significant increase, (almost doubling) in cell size upon treatment with etoposide and wrwycr (Figure III.8C, compare 1% DMSO vs. 100 μM wrwycr and 1.3 μM etoposide vs. 1.3 μM etoposide + 100 μM wrwycr). This suggests that the cells are unable to divide efficiently, probably due to cell cycle arrest.

Figure III-8. wrwycr treatment with or without etoposide does not induce significant apoptosis but interferes with cell division.

A. Confocal microscopy images showing transmitted channel (1st (leftmost column), cytochromeC-GFP (2nd column), TMRE (3rd column) and the overlay of GFP and TMRE channel (4th column) followed by 24 h treatment.

B. Quantitation of apoptotic cells by scoring release of cytochromeC (green bar), loss of TMRE (red bar) and typical morphological features of apoptosis like spikes, blebs, etc (grey bar) as % of total cells. # of cells counted for each treatment are labeled.

C. Estimation of cell size distribution using Image J analysis. The scatter plot shows the spread of size within the population. The difference is considered significant if $p<0.05$ (*) and highly significant if $p<0.005$ (**). The statistical analysis is performed using Student's t test and two tail analysis.

D. Flow cytometry analysis of the microscopy samples as an independent measurement of cell size. Shown here is the % increase in FSC (top panel) and SSC (bottom panel) taking 1% DMSO treated sample as 100%.

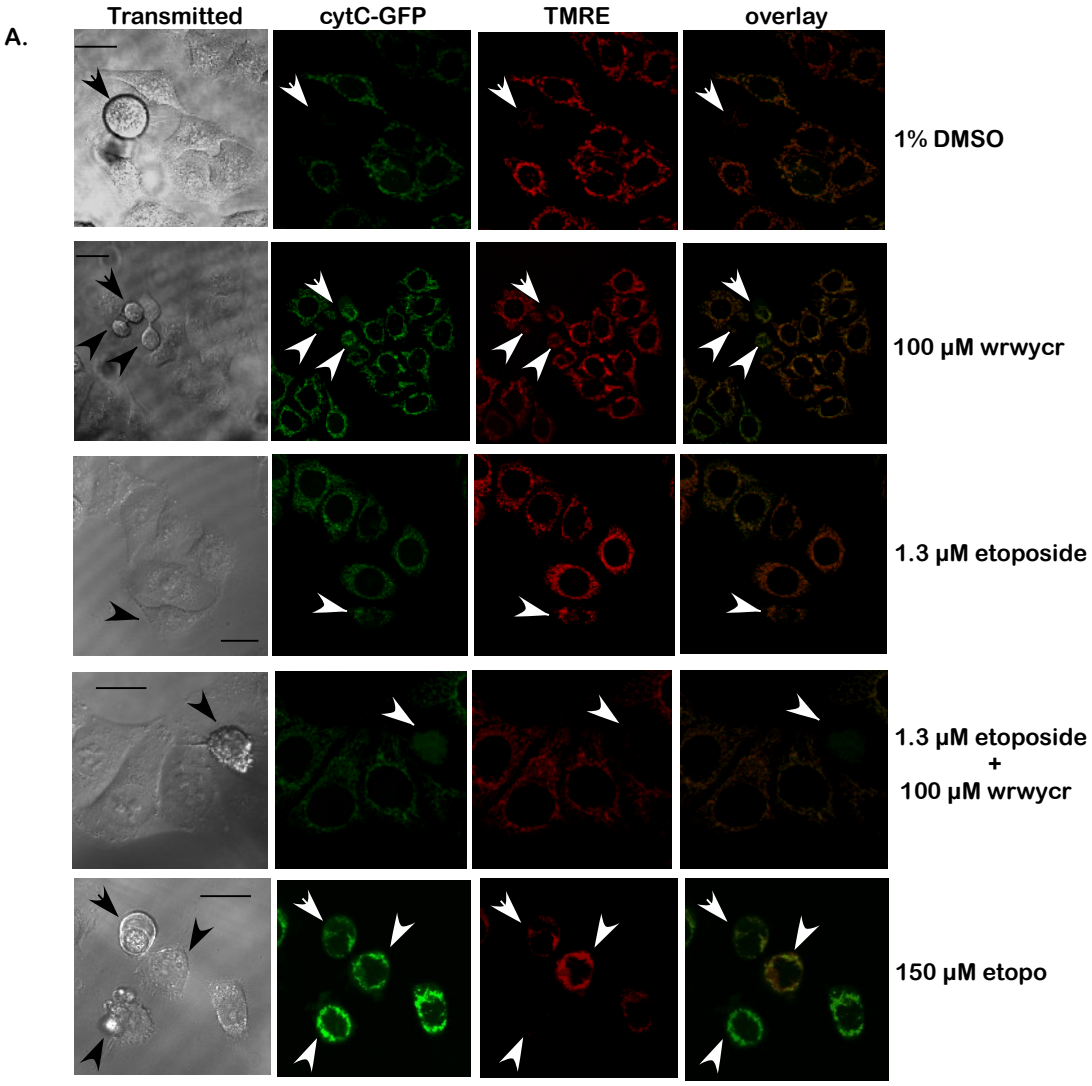
A.
Transmitted
cytC-GFP
TMRE
overlay
1% DMSO
100 µM wrwycr
1.3 µM etoposide
1.3 µM etoposide
+
100 µM wrwycr
150 µM etopo

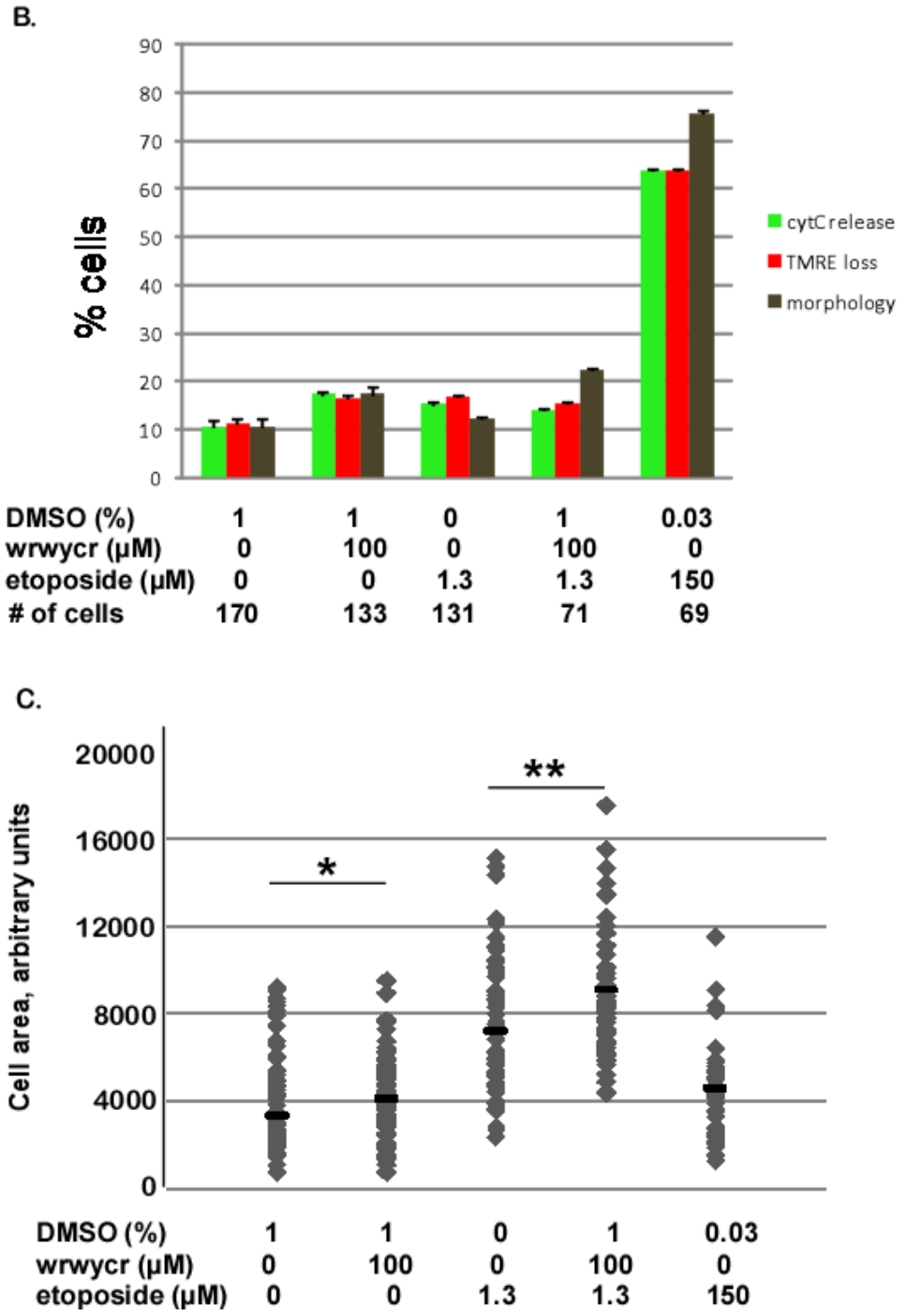

Figure III-8. Continued

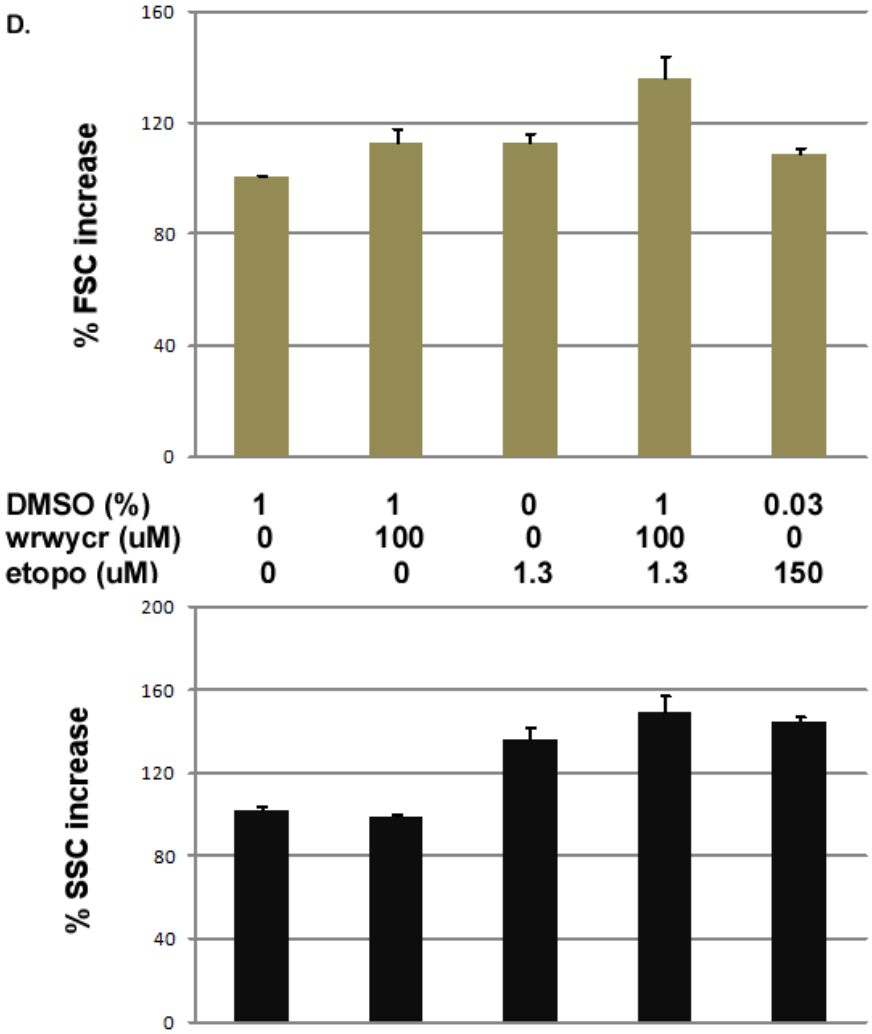

Figure III-8. Continued

There is a possibility that cell enlargement is an artifact of sample preparation for microscopy. To test this, we performed FACS analysis of the Htog1 cells treated in the same manner and calculated the forward scatter (FSC) vs. side scatter (SSC). FSC measures cell size. Thus increase in FSC indicates that the cell has increased in size. The flow cytometry results corroborate the microscopy data: a significant subpopulation of Htog1 cells treated with 1.3 μM etoposide and 100 μM wrwycr for 24 h showed a significant increase in FSC and a corresponding increase in SSC (Figure III-8D.a & III-8D.b).

From this study, we conclude that wrwycr treatment with or without etoposide induces only modest signs of early apoptosis in HeLa cells. This provides additional evidence towards inferring that the observed DNA fragmentation is due to the direct DNA damage activity of the peptide, presumably in preventing repair of DNA breaks. Concurrent administration of sublethal doses of wrwycr and etoposide increased cell size, probably by interfering with cell division.

wrwycr initiates DNA DSB response by generating γ-H2AX foci

H2AX, a histone variant becomes phosphorylated at Ser139 to produce γ-H2AX within minutes of DNA DSB formation (Rogakou et al, 1998). It recruits several repair proteins like Rad50, ATM, ATR, Brca1 and others to fix the damage (Paull et al, 2000). Only after the damage has been successfully repaired and the cell is ready to reenter the cell cycle, the foci disappear following dephosphorylation of γ-H2AX catalyzed by specific phosphatases (Chowdhury et al, 2005; Keogh et al, 2006). Leo Su's study used FACS analysis to quantitate the fraction of cells with γ-H2AX foci following the different treatments. Although flow cytometry is a convenient method of quantitating thousands of cells in a population, it does

not provide information on the number of foci per nucleus. Therefore, we wanted to follow up on the flow cytometry with a microscopy-based analysis of γ-H2AX focus formation.

Our results indicate that wrwycr by itself produces a few foci per nucleus (Figure III-9, Panel c). Sublethal dose of etoposide (1.3 μM) produces more distinct foci than HU (5 mM, Figure III-9, compare Panel d versus Panel e). This increases even more upon co-treatment of wrwycr (100 μM). However, microscopy gives us additional information that although 51% of wrwycr alone treated samples scored positive in FACS (Table III-1), each cell only had a few foci (Figure III-9, Panel c). On the other hand, only 18% of cells scored γ-H2AX positive after etoposide (1.3 μM) treatment in the flow cytometry assay, however, microscopy revealed that many cells had numerous foci per nucleus (Figure III-9, Panel d). Interestingly, we see significant increase in size of the nucleus in etoposide (1.3 μM) and HU (5mM) treated HeLa cells (Figure III-9, Panel d and Panel e) which increases significantly more upon co-treatment with wrwycr (50 μM and 100 μM; Figure III-9, Panel f, g and h). This suggests problem in nuclear division and DNA segregation, a third evidence of problem in cell division and cell cycle arrest.

Discussion

In this chapter, we expanded a previous effort to understand the effect of wrwycr in HeLa cells. In particular, we tried to resolve several questions: (1) to quantitate the amount of intracellular total peptide concentration and determine the dimer concentration; (2) to investigate wrwycr-induced cytotoxicity and its possible potentiation by other DNA damaging agents; (3) to discern direct DNA damage from apoptotic events; (4) to investigate the relationship between cytotoxicity and DNA damage; and (5) to test directly whether a marker specific for the DNA DSB response, γ-H2AX, was induced by the peptide treatment.

wrwycr uptake in Hela cells is linear

wrwycr is a cationic, hydrophobic, hexameric peptide molecule that dimerizes through the cysteine residue. Thus the effective chain length is 12. It is reasonable to expect that this molecule with ~50% of aromatic residues belongs to the class of cell penetrating peptides (CPPs) and traverses through the HeLa cell membrane without the help of transporters or other proteins. (For more details on CPPs refer to Chapter II). Intracellular total wrwycr concentration increases dose dependently with input concentration but the linear pattern plateaus off at 200uM (~1.43mM; Table III-2, total wrwycr concentration). Active wrwycr concentration (dimer), however, continues to increase linearly upto 200 μM input concentration. This is different than the non-linear pattern of uptake we see in U2OS cells (Chapter II). This difference in uptake could be a plausible reason for the difference in 24 h of cytotoxicity that we see in the two cancer cell lines, HeLa and U2OS. We will further discuss the possible correlation between uptake and cytotoxicity of wrwycr among the different cell lines tested in the overall Discussion chapter (Chapter V).

wrwycr-induced damage is irreversible but does not accumulate over time

Combining Leo Su's findings and the current results, we can conclude that 24 h of wrwycr treatment initiates a dose-dependent decrease in the metabolic activity (MTT) of HeLa cells and a corresponding but lesser decrease in the healthy cell population, as measured by the Live / Dead assay (Table III-3). However, the % cell death at 24 h is low,

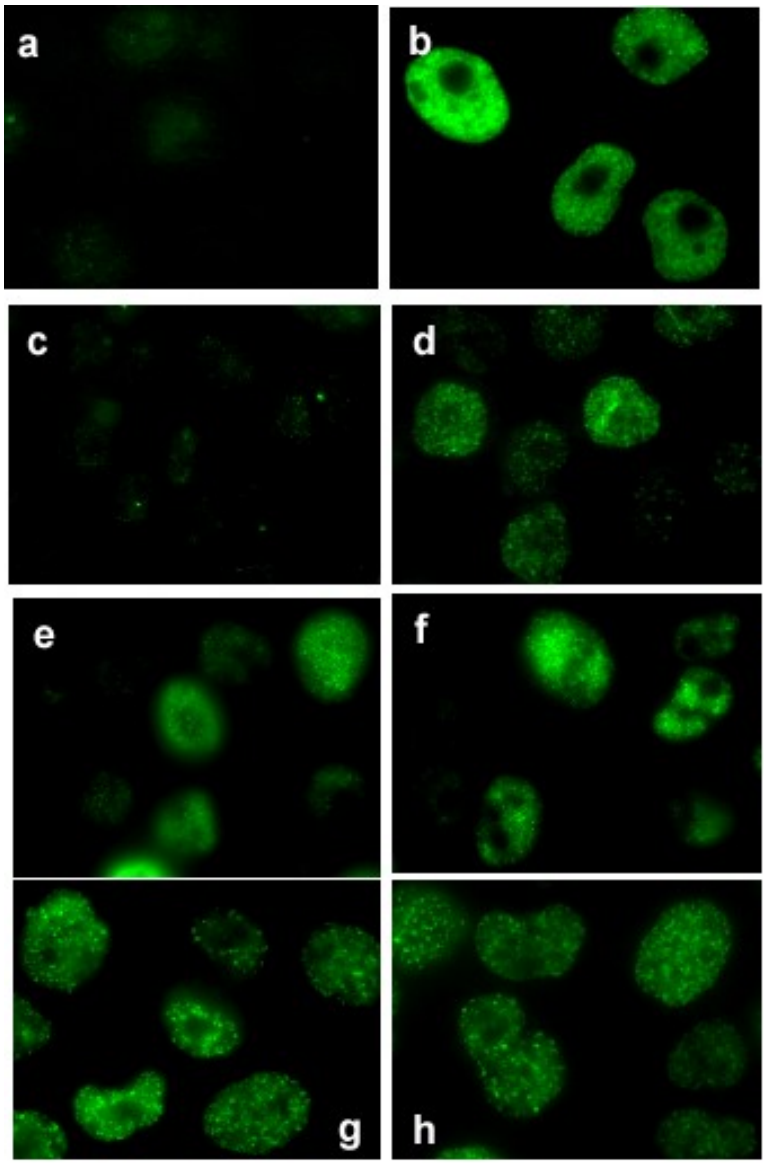

Figure III-9. Immunofluorescence microscopy of HeLa cells for upregulation of γ-H2AX foci.

Shown here are representative images of HeLa cells after 24 h of treatment with (a) DMEM, (b) 150 μM etoposide, (c) 100 μM wrwycr, (d) 1.3 μM etoposide, (e) 5 mM HU, (f) 5 mM HU + 100 μM wrwycr, (g) 1.3 μM etoposide + 50 μM wrwycr and (h) 1.3 μM etoposide + 100 μM wrwycr

indicating that wrwycr-induced damage reduces the active metabolic rate in a subpopulation of treated cells without killing them right away. Depending on the severity of the damage, a cell may have several possible fates: (a) It may repair the damage efficiently, recover, and start replicating once the peptide is washed away; (b) the repair process may be delayed such that the cell survives but cannot divide (premature senescence); or (c) the cell may not be able to repair the damage and will eventually die. If wrwycr interacts with its in vivo target(s) irreversibly, (d) the effect may be cumulative and a significant increase in killing may occur even after withdrawing the treatment. To distinguish among these possibilities, we further examined viability using a colony forming assay, where we exploited the capacity of individual cells to divide and form distinct colonies.

The results suggest that wrwycr-induced damage cannot be repaired and the cells affected within 24 h are unable to recuperate in the absence of the peptide. Sorting the sick population from the Live/Dead assay using flow cytometry supported this observation. None of the sick cells could survive in the plate. Around 15% of the population seems to be affected after 24 h (compare ~20% cells affected at 24 h of treatment [dead + sick], Figure III-5, Panel B; to ~35% of cells unable to produce colonies, Figure III-7). Some of this effect may be due to the DMSO solvent: around 15% of the DMSO-treated population is unable to produce colonies (Fig III.3B) showing that DMSO induces a cytostatic effect on HeLa cells (as it does in other cancer cells, Civoli et al, 1996), which is irreversible. This could contribute to the more severe effect of wrwycr observed in CFA assay than live dead assay. The wrwycr induced damage, however, is not cumulative and the majority of the cells unaffected in 24 h could proliferate upon withdrawal of treatment. This indicates that either (1) wrwycr interaction with its *in vivo* target(s) is transient and / or (2) wrwycr is actively effluxed out by Hela cells. This observation is in clear opposition to what we see with etoposide treatment where a sublethal

treatment concentration (1.3 μM) after 24 h induces severe cumulative damage and is lethal to 100% of the population 6-7 days after removing the treatment (CFA, data not shown).

Concurrent administration of etoposide and wrwycr induces non-apoptotic DNA damage

The earlier study relied on the upregulation of caspases during apoptosis. In this chapter, we studied the early hallmarks of apoptosis in HeLa cells with particular emphasis on mitochondrial structure and function. This is particularly interesting for our purpose because the peptide distribution inside HeLa and other cells correlates well with mitochondrial cytochrome oxidase and is less prominent in the nucleus (Figure III-1). Thus studying apoptotic markers residing in mitochondria might be more sensitive about the nature of action of wrwycr. According to our hypothesis, in vivo targets of wrwycr are branched DNA intermediates, which are generated both in the nucleus (Heyer, 2003; Li and Heyer, 2008) and in the mitochondria (Kajander et al, 2001). Hence mitochondrial DNA repair substrates might also be plausible targets of wrwycr. Much more detailed investigation on peptide uptake in mitochondria is necessary before expecting that the peptide targets mitochondrial DNA repair. Based on the results, the fluorescence microscopy approach can be extended to correlated electron microscopy and tomography studies (Sun et al, 2007, where the same cell can be sorted by fluorescent microscopy and processed for electron microscopy using a grid plate) to understand effect of wrwycr with or without DNA damaging agents on mitochondrial health and mitochondrial DNA repair.

Both earlier and current results indicate that the increase in DNA breaks upon co-treatment of cells with sublethal doses of etoposide and wrwycr is not a secondary event due to apoptosis, but rather is a direct DNA damage response. However, the fraction of cells with mitochondrial hallmarks of apoptosis is marginally more than the cells with caspase

upregulation (compare 100 μM wrwycr treatment with or without etoposide in Table III-1 versus Figure III-8B). This might be an indication that a subpopulation of cells are in the early stages of apoptosis. Another effect observed here is an increase in cell size upon etoposide administration that is significantly exacerbated upon co-administration of wrwycr. This is probably due to problems in cell division. In the future, we will perform the cell cycle analysis with the different treatments to try to understand if and at which stage the cells are being arrested.

Based on our data so far, we propose a model for the mode of action of wrwycr specifically in HeLa cells. Administration of sublethal doses of chemotherapeutic agents activates cell cycle check points and causes cell cycle arrest. This allows the cells time to repair the damage. Upon concurrent peptide treatment, the peptide dimers bind to the transient repair intermediates as they are generated, stabilize these intermediates, inhibit repair and enhance the delay in cell cycle, thereby triggering the DNA damage response. If this problem persists, a significant fraction of the affected population will die or enter permanent senescence. In either case, they will not be able to form colonies. In the absence of any external DNA damaging agents, the situation will be similar, but less severe because endogenous damage may be less extensive. Thus wrwycr treatment alone also shows dose-dependent cytotoxicity in the CFA assays to a greater extent than measures of acute toxicity (Live/Dead assay, microscopy or MTT).

Chapter III, in full, is being prepared for future publication. The dissertation author is a co first author of the work. Only the part performed by the dissertation author is presented in chapter III. The primary author in this paper is Leo Su and the corresponding author is Anca Segall.

CHAPTER IV

IMR-90 CELLS ARE RESISTANT TO WRWYCR-MEDIATED CYTOTOXICITY

Abstract

A major limitation to successful cancer treatment is the undesirable side effects of available cancer chemotherapeutics (Smith, L, 2000). In this dissertation we focused our work mainly on investigating the effects of a peptide molecule, wrwycr in a osteosarcoma cell line, U2OS and found that 24 h of wrwycr treatment caused dose-dependent cytotoxicity in these cells presumably by causing DNA damage. (more details in chapter II). Our results suggest that DNA damage is a contributing factor to cell death. In this chapter we explored the effect of wrwycr in a low passage lung fibroblast cell line, IMR-90 to understand its role in slow growing non-tumor cells. Our results indicated that IMR-90 cells are resistant to wrwycr-induced cytotoxicity by itself or in combination with sublethal doses of etoposide and hydroxyurea. While little or no acute cytotoxicity or apoptosis was observed after 24 h of wrwycr treatment, combination treatment with hydroxyurea affected the cell cycle and a small subpopulation of cells had subG_0 DNA content. This prompted us to inquire the possibility that concurrent administration of wrwycr and DNA damaging agents induces a similar but late DNA damaging effect in IMR-90 cells as they do in cancer cells. We also measured accumulation of DNA damage and phosphorylation of H2AX (γ-H2AX), a marker of double strand DNA breaks, after 24 h of wrwycr alone or in combination with etoposide and hydroxyurea, and found that the response is minimum. This finding is in agreement with the results of another study in which primary peritoneal macrophages were more resistant than a macrophage-like cancer cell line, J774A.1. Understanding the possible differences in peptide uptake and/or DNA repair may explain the

different sensitivity of U2OS, HeLa and IMR-90 cells to wrwycr treatment.

Keywords IMR-90, wrwycr, DNA repair, apoptosis, Holliday junction

Introduction

Cancer is the second leading cause of death in the US, after heart disease causing 23.1% of deaths (American Cancer Society, ACS, 2006). The fact that in the last 15 years only 16% reduction in cancer-related deaths is observed as compared to almost 36% reduction in heart disease related deaths (American Cancer Society and Center for Drug Control) suggests that cancer is still an ailment that needs extensive research both for early detection and improved therapy. An effective anticancer drug should be cytotoxic to cancer cells while not harming normal cells. Significant cancer research led to the discovery of several classes of anticancer drugs molecules effective in killing cancer cells. Finding a safe therapeutic window within which normal cells are resistant but cancer cells are sensitive, is facing more challenges. Most available chemotherapeutic agents induce significant cytotoxicity to non-cancerous cells. This reduces their therapeutic efficacy to a large extent. In addition, many chemotherapeutics exhibit off-pathway toxicity, causing liver and kidney damage at their effective doses. We are studying a peptide molecule that is cytotoxic to cancer cells (described in detail in chapter II and chapter III). In this chapter, we investigated its effect in a low passage non-cancerous cell line, IMR-90.

IMR-90 cells are fetal lung fibroblasts isolated 16 weeks after gestation (Nichols et al, 1977). Like normal human diploid fibroblasts, they are very slow growing and behave almost like primary cells. No mutation has been identified in these cells. IMR-90 cells are not an immortalized and have a limited doubling potential in culture (Hayflick and Moorhead, 1961; Nichols et al, 1977; and Hayflick, 1979). Senescence after ~ 20 passages in culture is probably

due to lack of DNA synthesis initiation, a hallmark of cellular aging (Pang and Chen, 1993). More recently, IMR-90 cells have been used to study interactions between different DNA repair proteins (Dolganov et al, 1996).

Slow growth rates are due to fewer rounds of replication and should require less DNA repair compared to cancer cells (Willers et al, 2002). Repair in slow-replicating cells appears to occur mostly by Non-homologous end joining, NHEJ (Harrington, 1992). Thus anticancer drugs targeting DNA substrates, like HJ, generated mostly in HR, may not target these cells. Since the peptide molecule we are testing targets HJ *in vitro* (Boldt et al, 2004, Kepple et al, 2005, 2008) and in bacteria, and is cytotoxic in osteosarcoma (U2OS) and a cervical (HeLa) cancer cells, it would be useful to explore its effect on IMR-90 cells. We tested whether we see any differences in sensitivity and / or uptake of wrwycr in IMR-90 versus U2OS or HeLa cells. The results will help to assess correlation between replication and repair activity of cells and their sensitivity to wrwycr.

Results

WRWYCR (wrwycr) entry in IMR-90 cells is less efficient than U2OS cells

Normal human cells are less permeable to small, cationic peptides belonging to the class of Cell Penetrating Peptides (CPPs) compared to cancer cells. We tested whether and to what extent WRWYCR (wrwycr) is able to enter IMR-90 cells, how similar is the intracellular distribution to other human cancer cells tested, and how the intracellular concentration of active wrwycr (dimer) compare with that in cancer cells under similar input conditions.

Confocal laser microscopy was performed using Rhodamine-tagged WRWYCR and detected the presence of peptide inside cells (Z series images taken, for more details see Materials and Methods section). The punctate, non-uniform distribution pattern was very similar to that seen

in the cancer cells (Figure IV-1, a-c). Z-series images throughout the thickness of the cell provide evidence that the peptide is inside the cells and not stuck outside. Counterstaining with a nuclear stain PicoGreen, followed by an overlay of the red and green channels, reflects the relative peptide distribution inside the nucleus. As with the other cell lines tested, the peptide enters the nucleus less efficiently than the cytoplasm of IMR-90 cells.

The intracellular peptide concentration was measured using HPLC. The intracellular dimer concentration was proportional to the input concentration (Table IV-1, 0.14, 0.25 and 0.39 mM for 100, 150 and 200 μM input respectively). Uptake, however, was less efficient in these cells compared to the U2OS cells (Table V-1) at all the concentrations tested. The difference is more pronounced at higher input concentrations. For instance, at 200 μM input concentration (the highest concentration used in the study), the total intracellular [wrwycr] is over 8 fold greater in the U2OS cells than in the IMR90 cells (Table V-1).

IMR-90 cells are resistant to wrwycr-mediated acute cytotoxicity

Based on our hypothesis, slower growing IMR-90 cells should generate fewer targets for wrwycr than cancer cells and thus should be more resistant to wrwycr-induced cytotoxicity. To test this directly, we used the Live / Dead assay (details in Materials and Methods and Chapter II, Results section). As expected, 24 h of wrwycr treatment alone or in combination with DNA damaging agents like etoposide or hydroxyurea did not induce any significant cell death (Figure IV-2A and Figure IV-2B). Interestingly, a small subpopulation of cells appeared sick in wrwycr-treated cells; this subpopulation increased in the combination treatment (note

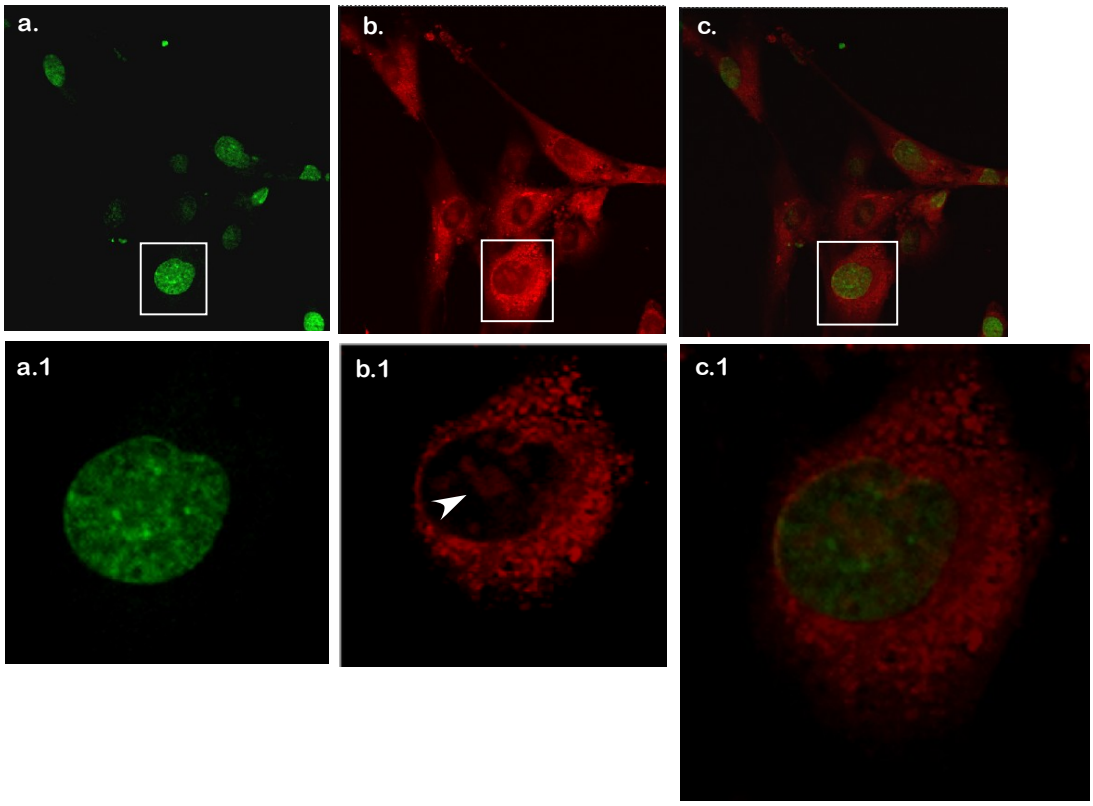

Figure IV-1. Rho-WRWYCR can enter IMR-90 cells.
IMR-90 cells were incubated with 10 μM Rho-WRWYCR at 37°C for 3 h and 1 μM picogreen for 10 min. The image shown is an optical slice near the center of the cell from a Z-series.
The top panel (a-c) represents a population of cells stained with (a) picogreen only, (b) Rho-WRWYCR and (c) overlay of red and green.
In the lower panel one cell in the field (marked by a square) is zoomed in with (a.1) picogreen only, (b.1) Rho-WRWYCR and (c.1) the overlay of the red and the green channel.

Table IV-1 Quantitation of intracellular wrwycr concentration in IMR-90 cells

Intracellular conc[a] (mM)	Input monomer conc (uM)		
	100	**150**	**200**
monomer	**0.4** ± 0.01	**0.44** ± 0.04	**0.49** ± 0.13
Dimer[b]	**0.14** ± 0.06	**0.25** ± 0.16	**0.39** ± 0.25
fold change	***1***	***1.8***	***2.8***
Total	**0.7** ± 0.14	**0.94** ± 0.28	**1.27** ± 0.37
fold change	***1***	***1.3***	***1.8***

[a] Total intracellular concentration of wrwycr is calculated as monomer
[b] wrwycr is active as a dimer *in vitro*
Shown here is the average of two independent replicate experiments.

the population of cells in Q2 & Q3, Figure IV-2A). This subpopulation may either suffer a temporary reduction or halt of metabolic activity or a transient loss of membrane integrity upon wrwycr treatment.

This observation was corroborated by phase contrast microscopy of the samples prior to processing for Live / Dead flow cytometry analysis (Figure IV-3A, Panels a-i). No sign of stress or cell death was evident after 24 h of wrwycr treatment. The treatment does not induce

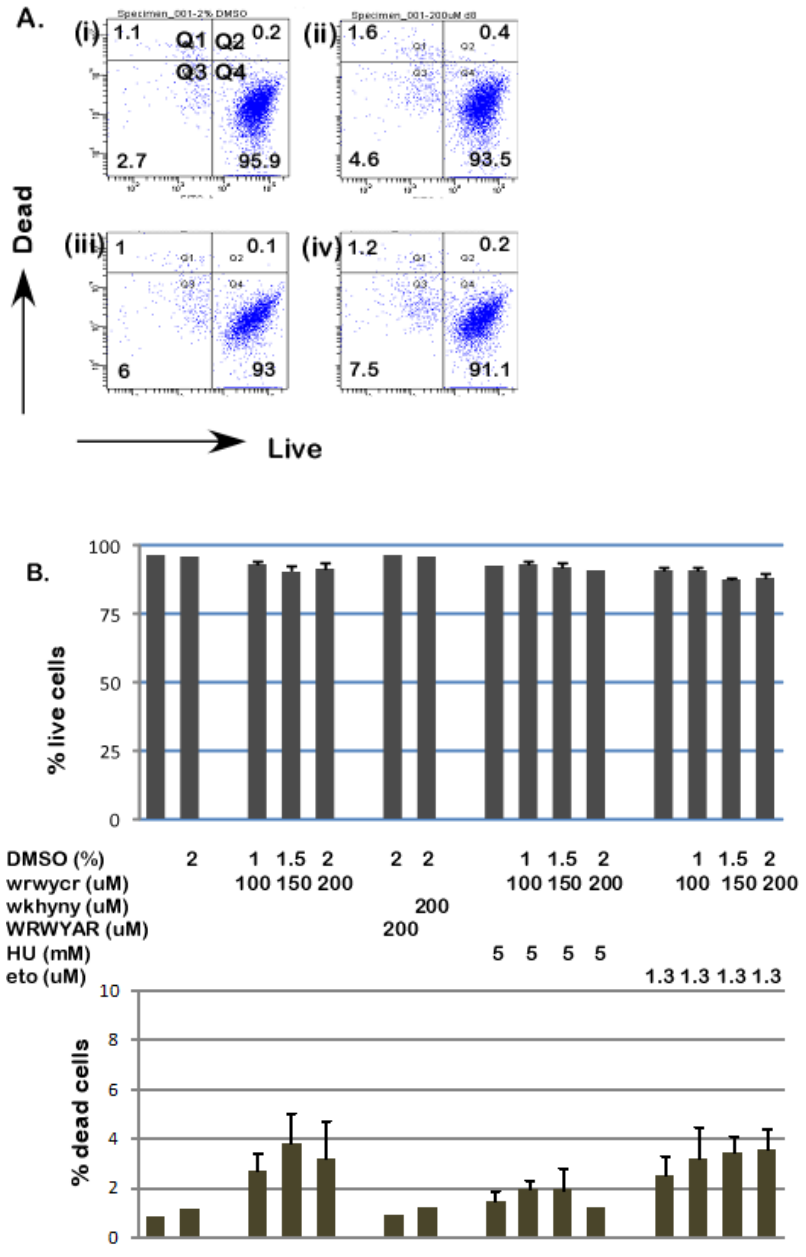

Figure IV-2. 24 h of wrwycr treatment with or without sublethal doses etoposide or HU does not induce any significant cell death in IMR 90 cells.

A. Representative FACS dot plots showing the relative distribution of live vs. dead cells after treatment with (i) 2% DMSO, (ii) 200 µM wrwycr, (iii) 5 mM HU and (iv) 5HU + 200 µM wrwycr. The numbers indicate the percentage of cells in that quadrant.

B. Bar graph representation of live (upper panel) and dead (lower panel) cells as percentage of total cells. Mean is the average between two experiments. Error bar represents the standard error

any significant effect on cell viability (Figure IV-3A). However, DMSO and wrwycr treatment probably affects the doubling time of the already slow dividing IMR-90 cells. (Figure IV-3A, compare Panels b & c to Panel a). Sublethal doses of hydroxyurea or etoposide also appeared to affect the rate of cell division; hallmarks of cell death or apoptosis, however, were rare (Figure IV-3A, Panels d & g). Interestingly, upon co-treatment of wrwycr (150 μM) and HU (5 mM), a small subpopulation of IMR-90 cells showed signs of stress (Figure IV-3A, compare Panels d & e with f).

To follow up on this, we calculated the doubling time (DT) of IMR-90 cells after 24 h of wrwycr treatment alone or in conjunction with etoposide or HU (Figure IV-3B). The results indicated that wrwycr induced a dose-dependent increase in the doubling time of the IMR-90 cells after 24 h of treatment (Figure IV-3B, compare 33.3 h in 2% DMSO to 37, 52.5 and 73.5 h in 100 μM, 150 μM and 200 μM). Etoposide (1.3 μM) and HU (5 mM) treatment, by themselves, also increased the doubling time of the IMR-90 cells to 90 h and 125 h respectively. This further increased upon concurrent administration of wrwycr with etoposide (184 h with 1.3 μM etoposide + 200 μM wrwycr, Figure IV-3) or HU (148 h with 5 mM HU + 200 μM wrwycr, Figure IV-3).

Concurrent administration of hydroxyurea and wrwycr reduces DNA content of IMR-90 cells

In order to further investigate the previous observations, cell cycle analysis was performed after 24 h of wrwycr treatment. It was observed that wrwycr by itself starts affecting the cell cycle of IMR-90 cells only at very high concentration (Figure IV-4A and Table IV-2). Again, no significant increase in the sub-G_0 population was observed, indicating no cell death upon wrwycr treatment alone (Table IV-2, %<G1).

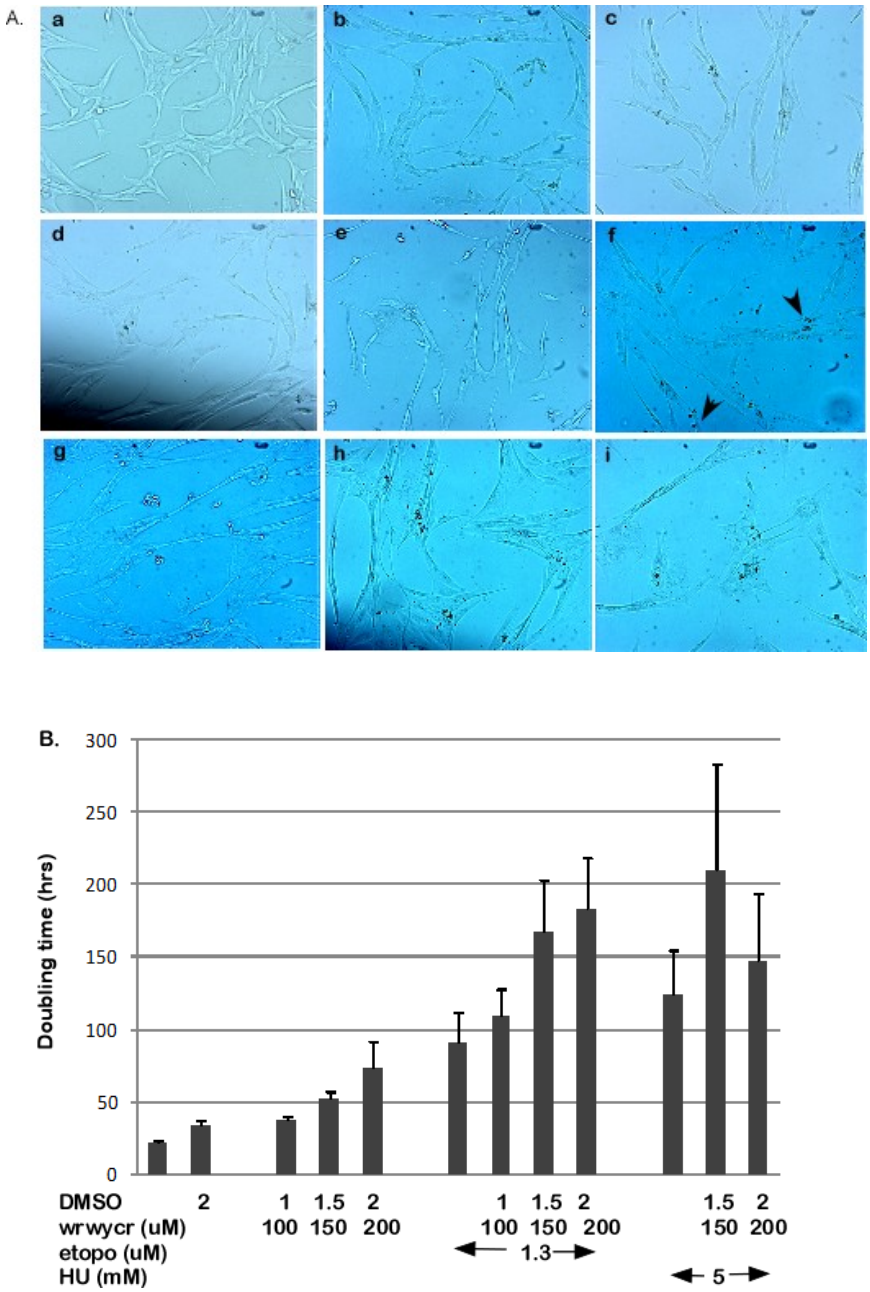

Figure IV-3. Doubling Time of IMR-90 cells increases upon co-treatment of wrwycr with HU or etoposide

A. Phase contrast pictures of a. DMEM, b. 1.5% DMSO, c. 150 µM wrwycr, d. 10mM HU, e. 10HU + 100 µM wrwycr, f.10HU + 150 µM wrwycr, g. 1.3 µM etoposide, h. 1.3 µM etoposide + 100 µM wrwycr and i.1.3 µM etoposide + 150 µM wrwycr

B. Doubling time calculation following 24 h treatment

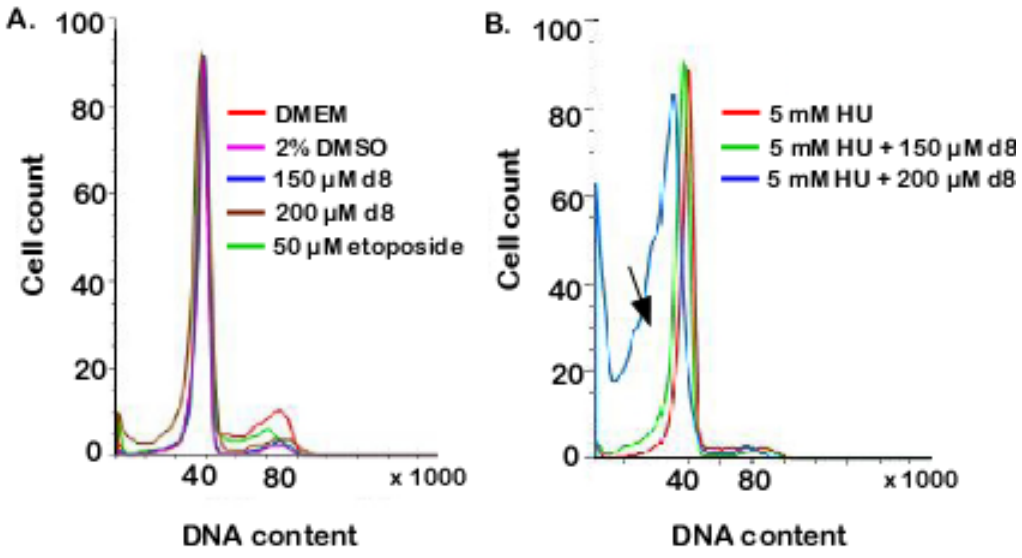

Figure IV-4. Effect of wrwycr on cell cycle with or without an Intra S blocker, HU

IMR-90 cells were treated for 24 h and analysed for DNA content. Histograms are overlaid on top of each other.

Panel A. Effect of increasing concentration of wrwycr alone on cell cycle of IMR-90 cells compared to the media control (DMEM) and the solvent control (DMSO).

Panel B. Effect of hydroxyurea by itself or in conjunction with wrwycr in IMR-90 cells. Shown here are representative histograms overlaid on top of each other.

The cells were sensitized upon co-treatment of wrwycr with HU. This included a reduction in the G2/M peak and a dose-dependent increase in sub-G_0 fraction of cells (Figure IV-4, right panel, compare 5 mM HU by itself with 5 mM HU + 150 µM d8 and 5 mM HU + 200 µM d8, the arrow points towards the sub-G_0 peak ; also compare the number

Table IV-2. Cell cycle analysis of IMR-90 cells

Treatments	%<G1[a]	% G1	% S	% G2 / M	%>G2
DMEM	7	62.5	4.8	27.5	0
2% DMSO	10.6	79.2	0	12.9	0
150 µM d8	7.7	77.4	18.7	0	0
200 µM d8					
5 mM HU + 1.5% DMSO[b]	7.2	86.4	2.3	0	
5 mM HU + 150 µM d8	16.9	77.3	0	7.5	2.3
5 mM HU + 200 µM d8	29.5	71.5	0	0	0

[a] This fraction of cells are considered apoptotic
[b] This sample is a control to test whether the solvent DMSO (1.5%) has any synergy with HU

of cells in <% G1 population in 5HU + 1.5% DMSO with 5HU + 150 µM d8 and 5HU + 200 µM d8, Table IV-2). Formation of sub-G_0 DNA content is used to detect apoptotic fraction of a population. (Bodo et al, 2006). Thus there is a possibility that co-treatment of HU and wrwycr induces apoptosis in a subpopulation of cells and the reduction in DNA content is due to loss of DNA in that fraction of cells.

wrwycr by itself does not induce apoptosis in IMR-90 cells

To address this possibility, we directly measured apoptosis using a late apoptotic marker, caspase-3 upregulation. Caspase-3 is a cysteine protease of the executioner caspase group, responsible for denaturing intracellular proteins by cleaving after specific aspartate residues during the late stages of apoptosis. We measured caspase-3 induction as a fraction of the total protein. The results indicate that wrwycr by itself does not cause any significant caspase-3 induction (compare 2% DMSO and 200 μM wrwycr in Figure IV-5b). However, as is evident in the DNA content analysis (Figure IV-4B, right panel), when IMR-90 cells are treated with wrwycr in conjunction with hydroxyurea, they show mild induction of caspase-3 (compare 5HU vs. 5HU + 200 μM wrwycr in Figure IV-4B). This effect is observed with etoposide, but the level of induction is even lower (1.3 μM etoposide + 200 μM wrwycr induce 4.9 RFU / μg total protein whereas 5HU + 200 μM wrwycr induce 7 RFU / μg total protein, Figure IV-4B).

These results demonstrate that IMR-90 cells are resistant to wrwycr- induced apoptosis at concentrations (150 μM, 200 μM) where several cancer cell lines are sensitive (Appendix A.4, Figure A.4-3).

One interesting finding here is that use of DNA damaging agents like etoposide under conditions that cause significant apoptosis in cancer cell lines (like U2OS, Saos-2, Appendix A.4, Figure A.4-3) generate much less caspase-3 in IMR-90 cells (24 h of 150 μM etoposide produces 7.5 RFU / μg protein in IMR-90 cells as compared to 67.8 RFU / μg protein and 30 RFU / μg protein in U2OS and Saos-2 cells, Figure A.4-3).

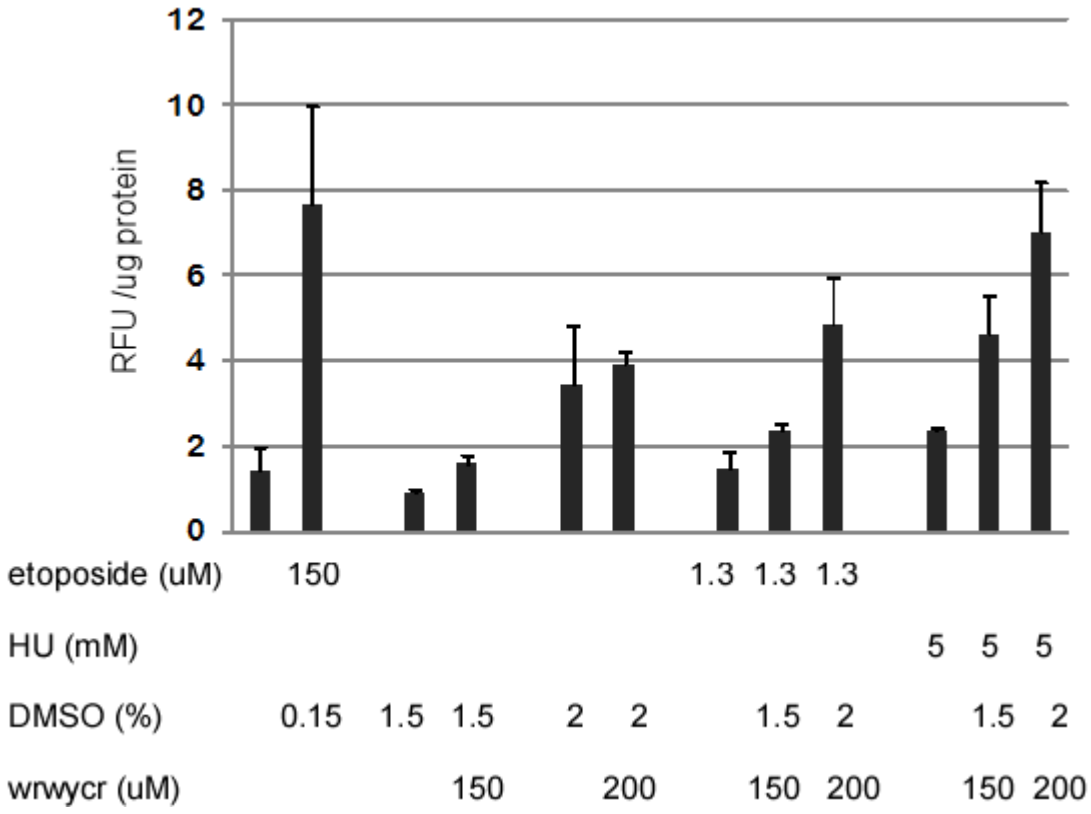

Figure IV-5. Co-treatment of wrwycr with HU or etoposide induces some apoptosis in IMR-90 cells.

caspase-3 activation is represented as RFU/ µg total protein in a sample

wrwycr treatment does not cause DNA breaks nor induce DSBR

Resistance to cell death could be due to several reasons, such as : (1) fewer wrwycr targets seen in 24 h due to slow replication, making IMR-90 cells refractory to wrwycr-induced damage; (2) wrwycr-induced damage is repaired by IMR-90 cells such that no significant death is observed after 24 h, although signs of damage are evident as cells repair the damage; or (3) wrwycr is unable to traverse non-cancerous cell membrane of IMR-90, hence these cells are unaffected by the peptide. HPLC excludes the third possibility and confirms that after 24 h wrwycr is detected inside IMR-90 cells. To discern whether the first or second option is correct, we performed two assays that measure fragmented DNA (TUNEL) and the presence of DSB that need to be repaired (γ-H2AX foci).

The TUNEL assay results indicate that either single treatment with etoposide, HU or wrwycr, or combination treatments produce very modest fraction of TUNEL positive cells (Table IV-4, 200 μM wrwycr produces 4.2%, 5HU by itself produces 2.2% whereas the combination produces only 5.8%). The TUNEL assay does not distinguish between single and double strand breaks.

The formation of γ-H2AX foci is an early marker of the double strand break repair (DSBR) (Vafa et al, 2002), an indication of cellular response to repair a DSB lesion. We tested whether DSBR is triggered in IMR-90 cells upon treatment with wrwycr in the presence or absence of sub-lethal doses of etoposide or HU by detecting % γ-H2AX positive cells via flow cytometry. This would clarify whether the resistance to cell death has any relation to DNA damage response. The trend is very similar to the TUNEL assay. Neither wrwycr by itself or in combination with HU or etoposide upregulate γ-H2AX significantly (Table IV-3, compare left versus right column). One intriguing difference between the two assay results is the response to HU. A sublethal dose of HU (5 mM) generates only a modest TUNEL response

(Table IV-3, only 2.2% of TUNEL positive cells) but a strong γ-H2AX (Table IV-3, 30.7% positive cells). Upon co-treatment with wrwycr, however, the response is not enhanced in either test. In fact, HU + wrwycr treatment induces fewer γ-H2AX positive cells than HU by itself (30.7% vs. 18.5).

Table IV-3. Comparison table of % TUNEL and % γ-H2AX positive IMR-90 cells

Treatments	% TUNEL + cells[c]	% γ-H2AX foci + cells[d]
DMEM	2.1 ± 1.9	1 ± 0.4
DNAse I	35.7 ± 15.2	nt[a]
51 μM etoposide	nt[a]	27 ± 3.2
2% DMSO	1.5 ± 0.05	2.8 ± 0.5
d8[b] (μM)		
150	1.8 ± 0.5	2 ± 0.5
200	4.2 ± 0.9	2.5 ± 0.9
etoposide (μM)		
1.3	3.1 ± 1.9	4.1 ± 0.07
1.3 + 150 μM d8	3.8 ± 1.1	7.6 ± 1.4
1.3 + 200 μM d8	3.5	nt[a]
HU (mM)		
5	2.2 ± 0.9	30.7 ± 2.5
5 + 150 μM d8	7.1 ± 3.6	18.5 ± 3.6
5 + 200 μM d8	5.8 ± 1.9	nt[a]

[a] nt = Not Tested
[b] d8 = wrwycr
[c] Average in the TUNEL assay is the mean of two independent experiments
[d] Average in the γ-H2AX assay is the mean of three independent experiments

Discussion

An essential milestone in promoting a successful anticancer drug is to minimize its side effects. Unfortunately, cancer cells do not always respond completely to any of the available classes of anti cancer drugs like antimetabolites (methotrexate), alkylating agents (chlorambucil, Melphalan) or natural products (vincristine, vinblastine) and often develop drug resistance. Most chemotherapeutics also affect normal cells and cause severe side effects (Smith, L 2000). Assessment of cytotoxicity in normal cells thus is an important step in investigating the potential anticancer efficacy and usefulness of a molecule. We are exploring the anticancer efficacy of an antibacterial peptide molecule that share features with Cell Penetrating Peptides (CPP), by comparing its relative cytotoxicity in cancer versus normal cells. In chapter II and chapter III, we investigated the effects of this peptide, wrwycr, in two cancer cell lines, U2OS and HeLa, and found that both are sensitive to wrwycr, albeit to different extents. In this chapter we tested uptake, cytotoxicity and DNA damage potential of peptide wrwycr in the low passage lung fibroblast cell line, IMR 90, as a first step to understand its effect in non-cancerous cells.

Plasma membrane composition of normal eukaryotic cells makes CPPs less permeable (Chan et al, 1998). Low membrane potential and a higher concentration of zwitterionic phospholipids in the outer leaflet of non-cancerous eukaryotic cells are the two major impediments towards CPP-mediated membrane disruption (Chan et al, 1998). We tested the uptake of wrwycr (and WRWYCR) via confocal microscopy and HPLC. Both microscopy and HPLC reveal that the peptide is able to get into IMR 90 cells, although to a lesser extent than the other two cell lines (Table V-1).

Lower intracellular wrwycr concentration is expected to induce lesser cytotoxicity. To test this directly, we performed Live / Dead assay after treating IMR-90 cells with wrwycr alone

or in conjunction with sublethal DNA damaging agents like etoposide or hydroxyurea and found that IMR-90 cells are mostly resistant to cytotoxicity of wrwycr even in the presence of chemotherapeutic agents. No significant apoptosis (caspase-3 upregulation) or hallmarks of DNA damage (TUNEL assay, γ-H2AX assay) are evident at these treatment conditions indicating that IMR-90 cells are resistant to peptide wrwycr-mediated cytotoxicity and DNA damage.

This is the first result that suggests that cancer cells are more sensitive to wrwycr treatment than non-cancerous cells. Although these data are preliminary, it is the first attempt to demonstrate that wrwycr is not cytotoxic to normal cells. This encourages us to pursue future studies in this direction with particular emphasis on cytotoxicity of wrwycr and wrwycr-induced DNA damage. For instance, the next logical question that needs to be addressed is whether wrwycr has any delayed effect upon prolonged exposure (48 h, 72 h) or after removal of peptide (doubling time experiment after 24 h of recovery in absence of the peptide). We also have preliminary evidence that primary macrophage cells (Su, L unpublished results).and mice (Naili I, unpublished results) are insensitive to wrwycr-mediated cell death.

CHAPTER V

DISCUSSION AND FUTURE WORK

The primary goal of this dissertation was to explore effects of wrwycr on human cells in culture and to investigate the anticancer potential of wrwycr alone or in combination therapy. In order to achieve this goal, (1) I quantified the relative intracellular wrwycr concentration in two cancer cell lines and one non-cancer cell line and compared peptide uptake with peptide-mediated cytotoxicity in these cells. (2) I evaluated DNA damage in response to the peptide and compared it with peptide-mediated cytotoxicity and (3) I developed a sensitive assay to measure DNA synthesis during recovery from intra-S arrest. In this section, I summarize the results and evaluate the similarities and differences in the response of U2OS, HeLa and IMR-90 cells upon exposure to wrwycr.

Characteristics of peptide wrwycr

1. Factors affecting intracellular wrwycr concentration

Before discussing the effects of peptide wrwycr in human cells, I want to explain the unique sequence of wrwycr. Peptide wrwycr has hydrophobic residues like tryptophan (W), tyrosine (Y) and two arginine residues. The arginine residue has both a hydrophilic charged head and a hydrophobic tail end. Taken together, this is a lipophilic molecule with a net positive charge of 2 units (1 unit per arginine) per monomer. The presence of a net negative plasma membrane potential ($\Delta\psi$, -60 mV, Nicholls and Budd, 2000) drives accumulation of these cationic molecules across the cell membrane. Inside the cell, peptide wrwycr might again partition into subcellular organelles with a higher negative membrane potential than

cytoplasm, like mitochondria, ($\Delta\psi$, -180 mV, Nicholls and Budd, 2000) and accumulate inside them. The cell, in turn will try to lower the cytoplasmic concentration of the peptide by an energy-dependent efflux system.

Thus, the net intracellular concentration of peptide wrwycr is a function of the net positive charge (depends on the equilibrium between peptide monomer and dimer), the membrane potential of the plasma membrane and membranes of subcellular compartments, the diffusion co-efficient through the membrane and the efficiency of active efflux of the peptide.

These factors will depend on replication status, genetic background and several other factors that vary with cell types. Thus, peptide uptake might also vary accordingly.

2. Relationship between uptake and cytotoxicity

Conventional HPLC methods measure peptide concentration relative to the total protein content in a sample (Holm et al, 2006). We modified this method and calculated intracellular concentration based on cell volume (in picoliters, details in Materials and Methods), quantifying the intracellular peptide concentration on a per cell basis. This method revealed that wrwycr is concentrated inside cells to mM levels when supplied at 100-200 μM in the medium (Table II-1). Since WRWYCR is a hydrophobic molecule with a net positive charge of 2 units (each contributed by one arginine molecule), it was expected that it would partition between lipid bilayers of the plasma membrane and even more within cell organelles having a negative membrane potential inside, like mitochondria. There is also possibility that wrwycr is not readily effluxed out, thus increasing the peptide concentration with respect to the cell volume. HPLC results indicate that wrwycr uptake is dependent on both the input concentration and time of incubation but it differs among the different cell lines. A caveat of this method is the accuracy in the determination of cell number, and the differences in uptake

between live and sick or dead cells. It should be noted that we are dealing with the population average rather than an individual cell.

I found a direct correlation between wrwycr-mediated cytotoxicity and the relative intracellular concentration in the three cell lines tested. IMR-90 cells were the most resistant to wrwycr-mediated cytotoxicity and the least permeable to the peptide, whereas U2OS cells were the most sensitive and accumulated the peptide to the highest levels. Specifically, intracellular peptide dimer concentration was often more informative than the total peptide concentration. Although the total intracellular concentration of wrwycr in HeLa cells was comparable to that in IMR-90 cells (Table V-1), the concentration of the wrwycr dimer, the active form inside cells, was 40-100% greater in HeLa cells compared to IMR-90 cells. Since we expect wrwycr to bind to its potential targets (Holliday junction and other branched DNA intermediates) as a dimer, this may partly explain the difference in wrwycr-mediated cytotoxicity observed between HeLa and IMR-90 cells.

3. Co-localization studies with WRWYCR

The vesicular pattern of rhodamine-tagged WRWYCR observed in all the cells tested suggests that the peptide is concentrated mostly in some perinuclear cell organelle, particularly in mitochondria (Appendix A.3, Figure A.3-1) and/or the endoplasmic reticulum. Since under normal conditions, both of these organelles generate a negative membrane potential inside ($\Delta\psi$), it is possible that cationic peptide wrwycr partitions preferentially into these cell organelles. Testing with antibody against an endoplasmic reticulum (ER) resident protein, GRP78, in U2OS cells indicated regions of overlap of Rh-WRWYCR and GRP78 (Appendix A.3, Figure A.3-2). More detailed analysis with antibodies against various subcellular markers and HPLC determination of the peptide concentration in subcellular compartments will

identify the regions where peptide WRWYCR concentrates inside cells. These studies will in turn permit a more focused search for the peptide's potential targets.

Evaluation of the DNA damage response and determining correlation with cytotoxicity

Possible mechanisms of cell death

Based on previous *in vitro* and *in vivo* data, we hypothesized that wrwycr stabilizes transient DNA repair intermediates like HJs and inhibits their resolution, causing cell death (Kepple et al, 2005, Gunderson and Segall, 2006, Gunderson et al, 2009). In order to test this hypothesis, we investigated the potential correlation between wrwycr-induced cytotoxicity and DNA damage in the cell lines tested. The results suggest that, like uptake, accumulation of DNA damage differs among the cell lines tested. In U2OS cells, only a subpopulation of the affected cells show signs of DNA fragmentation and double strand break repair, whereas in HeLa cells DNA damage is higher than wrwycr-induced cell death. This trend holds both in the presence and absence of sublethal doses of the DNA damage-inducing agents etoposide and hydroxyurea. One possible explanation for this would be that at higher concentrations wrwycr may also target non-specific substrates, and either that these targets are more abundant in U2OS cells or that U2OS cells are more sensitive to this off-target damage. The measurement of DNA synthesis during normal replication (Figure II-8B) and recovery from intra-S arrest (Figure II-9D) supports this possibility, because, unlike wrwycr-mediated cell death, wrwycr-induced decrease in DNA synthesis is linear, suggesting that DNA synthesis produces specific targets of wrwycr. One possibility is that translocation of wrwycr across the membrane, like the other CPPs, disturbs the membrane structure, e.g. the plasma and mitochondrial membranes, sufficient to activate the membrane repair response (Palm-Apergi,

2009). We have evidence that in bacteria, wrwycr generates both membrane and DNA damage (Yitzhaki, Rostron, Xu, Authement and Segall, manuscript in prep). Another potential target of peptide wrwycr may be mitochondrial DNA repair intermediates, and wrwycr may cause cell death via mitochondrial DNA damage. More detailed analysis is necessary to address these possibilities.

Table V.1. Comparison of wrwycr uptake in U2OS, HeLa and IMR-90 cells

Cell lines	**Input wrwycr concentration (μM) vs. intracellular concentration (mM)[b]**								
	100 μM			150 μM			200 μM		
	Mono[a]	Dimer	Total[c]	Mono[a]	Dimer	Total[c]	Mono[a]	Dimer	Total[c]
U2OS	1	0.2	1.4	2.2	0.4	3	6.9	1.8	10.4
HeLa	0.26	0.35	0.9	0.5	0.45	1.4	0.2	0.6	1.4
IMR-90	0.4	0.14	0.7	0.44	0.25	0.94	0.5	0.4	1.3

[a] Mono = monomer intracellular wrwycr expressed in mM concentration
[b] It should be noted that the wrwycr input concentration is in μM and the intracellular concentration is in mM indicating that the peptide gets concentrated inside cells
[c] Total intracellular concentration is calculated as Total = Monomer + (Dimer x 2)

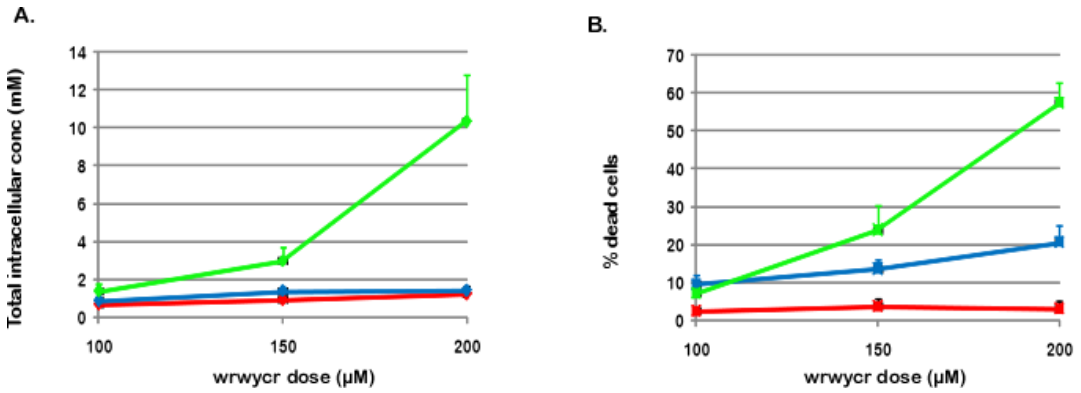

Figure V-1. Comparison of uptake and acute cytotoxicity of wrwycr in U2OS, HeLa and IMR-90 cells

IMR-90 cells are represented by the red line, HeLa cells by the blue line and U2OS cells by the green line.

Development of a sensitive assay to achieve stepwise synchronization of cells and to measure DNA synthesis

Serum and glutamine are the main growth factors required by immortal cell lines to replicate in culture. Complete absence of growth factors triggers apoptosis in mammalian cells (Savill J, 1999; Verzola et al, 2001). On the other hand, withdrawal of serum is used routinely to arrest cells at the G_1/S border for analysis of cell cycle parameters in synchronized cells (Jackman and O'Connor, 2003; Oya et al, 2003). However, there is a very delicate balance in the time of serum withdrawal that ensures cell cycle arrest but prevents induction of apoptosis.

Cell cycle arrest via serum deprivation takes 48-72 h to stop DNA synthesis in 100% cell population. Since cells are arrested at the G_0/G_1 or G_1/S border, they have to enter S phase before synthesizing DNA and this can take up to 12 h (Chou and Langan, 2003). It is common to lose a subpopulation of cells via apoptosis during such a prolonged procedure. Measuring DNA synthesis of synchronized cells in this way is thus time-consuming. Also, by the time the peptide effect becomes significant, a fraction of the affected population already shows signs of death (Figure II-8C, note the population with high SSC and low FSC that is outside the gate of analyzing population). This poses a big obstacle towards dissecting the mechanism of action of wrwycr.

Prolonging the time allotted for one round of cell division, might prevent cell death due to the triggering of cell cycle checkpoints by incomplete DNA synthesis. With this hypothesis, a rapid, stepwise synchronization and subsequent recovery process was designed specifically for the U2OS cells; using this protocol. 100% of cells stop synthesizing DNA and are arrested intra-S within 24 h (Figure II.9A). Moreover, during recovery from the arrest, cells start synthesizing DNA right away as they are already in S phase. Administration of increasing concentrations of peptide wrwycr (or an equivalent concentration of DMSO or control peptide wkhyny) during recovery from the intra-S phase arrest shows that wrwycr interferes with this

recovery without any significant killing of cells, at least by 16 h. This observation is supported by persistence of DNA repair foci suggesting problems in DNA repair. This provides evidence that wrwycr targets are generated in the pathway of recovery from replication fork stalling.

This synchronization strategy is a novel regime that can be used to reduce the rate of cell death by prolonging the cell cycle and can in principle be extended to any mammalian cells in culture with careful titration of serum concentration and time of arrest. Such a procedure will permit better dissection of mutations or inhibitors affecting recovery pathways without interference from cell death.

Discussion of the queries and suggestions for future work

1. Performing Microarray analysis

Human cells express and modulate the activity of many proteins in response to both endogenous and exogenous stresses. Since relatively little is known about the *in vivo* targets of wrwycr in human cells, a genome wide microarray analysis would provide some insight about the life processes wrwycr is interfering with. A more focused approach of testing whether wrwycr interferes with DNA damage repair, and which repair pathways are induced in response to peptide treatment, would be to perform pathway-specific microarray analysis for DNA damage repair in proteins in the presence and absence of DNA damaging agents. We could even extend this approach to explore other plausible targets of wrwycr by performing pathway specific microarray analysis for processes like membrane repair, ER stress response, mitochondrial DNA damage, etc. In either case, upregulation (or downregulation) of specific genes should be confirmed by performing qPCR experiments.

2. Understanding the mechanism of wrwycr uptake

The diverse mechanisms of uptake of CPPs are described in Chapter II. However, detailed investigation of mechanism of wrwycr uptake in the different cell lines has not been undertaken. Partial decrease in wrwycr uptake in Hela cells in presence of wortmannin, a PI(3)K inhibitor, along with a vesicular pattern of intracellular distribution suggests that endocytosis may play a role in peptide uptake in these cells (Figure III-1, panel D and data not shown,). In fact, a recent study has shown that both membrane potential and endocytosis play roles in uptake of CPPs in Hela cells (Zhang et al, 2009). Studies of wrwycr uptake in presence of an endocytosis inhibitor in U2OS cells would help discern whether the marked difference in uptake pattern of peptide wrwycr in these two cells is due to the fact that the mechanism of wrwycr uptake in these cells is distinct.

3. Studying repair protein upregulation at earlier time points of recovery from intra-S arrest

In the future, study of the upregulation and phosphorylation of DNA repair proteins that co-operate with ATM (and ATR) like Brca1, Chk1, Chk2, etc should be performed in order to dissect the predominant pathway that wrwycr is acting upon. Also, studying the formation of repair foci and activation of repair proteins at earlier time points could be very informative. For instance, after 16 h of recovery, we see a dose-dependent increase in phospho-ATM in wrwycr-treated cells but ATR foci did not increase prominently. Repeating the assay at 8 and 12 h will address whether the effect is ATR-independent or if ATR acts earlier and communicates the information to ATM via γ-H2AX. An alternative useful avenue will be to use other inhibitors, for example DNA-PK inhibitors that block non-homologous end joining (NHEJ), in conjunction with the peptides to determine the epistasis effects of the peptides on other pathways of DNA repair.

4. Testing wrwycr effect in mitochondrial DNA repair

It is interesting to note that agents that generate DSBs (etoposide) in mammalian cells also increase mitochondrial biogenesis and mitochondrial DNA content (Eliseev et al, 2003; Fu et al, 2008). However, the accompanying release of cytochrome C, loss of mitochondrial membrane potential and a reduction in ATP renders these newly generated mitochondria non-functional (Fu et al, 2008). Other agents that arrest the cell cycle at specific stages (e.g., aphidicolin, hydroxyurea) have direct effect on mitochondrial DNA synthesis (Bourdon et al, 2007, Thelander 2007) and cause mitochondrial DNA depletion (Bourdon et al, 2007). Asking specific questions regarding mitochondrial DNA synthesis during recovery from HU-mediated arrest in the presence of wrwycr would provide insights into the effects of wrwycr on mitochondrial DNA repair.

5. Detecting HJ accumulation *in vivo*

One direct test to detect accumulation of HJs upon wrwycr treatment would be to perform the 2D- Gel electrophoresis method in human cells treated with wrwycr in presence or absence of DNA damaging agents. This method allows direct visualization and quantitation of branched DNA structures generated *in vivo*.

6. Determinating wrwycr-HJ structure

One major obstacle towards elucidating mechanisms of action of wrwycr is the absence of its three dimensional structure. Both NMR and X-ray crystallographic studies are in progress to solve the atomic structure of the peptide molecule and its interactions with Holliday junction substrates (M. Rideout, G. York and A.Segall, unpublished results). Both biochemical and molecular modeling data (Ghosh et al, 2005, Kepple et al, 2008, R. Saha and A.Segall, unpublished results) suggest that wrwycr interacts with the center of the HJ in a

structure-specific (rather than sequence-specific) manner. The actual structure is expected to confirm this observation and, by highlighting the DNA-peptide interactions, may help predict the relative stability of wrwycr interaction with other DNA structures. In turn, this will perhaps permit the design of peptides that interact more stably (or even covalently) and/or more specifically with Holliday junctions and D-loops and less with replication forks. The structure may also hint at other potential intracellular targets of wrwycr.

Summary and model of wrwycr action

The goal of this dissertation was to explore the effect of wrwycr in cancer and non-cancerous cells with particular emphasis on DNA damage and the cause of cell death. To test our hypothesis, it was important to understand whether DNA damage was the cause of wrwycr-mediated cell death. In this study, we established that wrwycr can interfere with DNA damage repair pathway and wrwycr-induced DNA damage is at least partly contributing to the peptide-mediated cell death. More studies need to be performed to find out whether DNA damage is caused by wrwycr binding to the Holliday junction. Based on these results, I have generated a provisional model of wrwycr action in human cells. In this model, an actively replicating cell constantly undergoes endogenous DNA damage that gets repaired by recombination-dependent pathways. Peptide wrwycr accumulates inside cell organelles like mitochondria and nucleus, and their it stabilizes the branched DNA intermediates generated during repair and inhibits their resolution into repaired products. These stalled DNA intermediates initiate more DNA damage and generate cascades of DNA damage responses. Depending on the cell type and intracellular concentration of wrwycr, this could lead to immediate cell death and/or problems in cell division. The situation becomes more severe if the peptide is added during recovery from exogenous DNA damage. It is possible that

wrwycr-mediated cell death could partly be a result of wrwycr-induced off-target damage to other cellular processes.

CHAPTER VI

MATERIALS AND METHODS

Peptides, antibodies and cells: Peptide wrwycr, WRWYAR and wkhyny were synthesized with an amide at the C terminal tail by Sigma Genosys, dissolved in 100% DMSO and stored at -20°C. The primary antibodies against phospho-ATM (P at ser1981, Cat No 4526), ATR (Cat No sc 1887) and γ-H2AX (Cat No 05-636) were manufactured by Cell signaling Technology, Santa Cruz Biotechnology and Millipore respectively. Anti-phospho-ATM and anti-γ-H2AX-FITC were stored at -20°C. Anti-ATR was stored at 4°C.Dylight^{TM} 488-conjugated affinipure donkey anti-mouse (Cat No 715-485-150) secondary antibody was obtained from Jackson ImmunoResearch and stored in the dark at -20°C. Donkey anti-goat cy3 secondary antibody (Jackson ImmunoResearch, Cat No 705-165-003) was a gift from Chris Glembotski lab. The goat anti rabbit–Alexa 488 (Code No 715-485-151) secondary antibody was obtained from Jackson ImmunoResearch and stored in the dark at 4°C.

U2OS cells were a kind gift from Matthew Weitzman, Salk Institute, La Jolla. HeLa cells were kind gifts from Chris Glembotski (San Diego State University). Htog1 cells were a HeLa cell variant transfected with cytochrome C-GFP as described (Goldstein et al, 2000) and was kindly donated by Terry Frey (San Diego State University). IMR-90 cells were purchased from ATCC (Cat no CCL 186). U2OS, HeLa and Htog1 cells were propagated in 75cm^2 tissue culture flasks (Corning) in DMEM (Gibco 11995-065) supplemented with 10% FBS (Biowhittiker) and Penicillin-Streptomycin solution at 37^{o}C in a humidified atmosphere of 5% CO_2 / 95% air. IMR-90 cells were slow growing and needed 20% FBS to be kept in culture for 15-20 passages, after which they typically showed features of senescence. Cells were never kept in culture for more than 20 passages to avoid the chance of acquiring mutations due to serial passaging in serum-containing media. When confluent, cells were subcultured 1:6 to 1:8

by incubating the cell monolayer with 0.05% Trypsin-EDTA at 37ºC for 5 min to release them from the culturing flask. For IMR-90 cells, the subculturing ratio was 1:4 to 1:5 instead.

Confocal microscopy: U2OS cells were seeded in 8-well (LabTek-II) chamber slides at 40,000 cells per well, and incubated at 37°C with 5% CO_2 overnight to allow adhesion. The media was removed and replaced with fresh DMEM containing N-terminal rhodamine-labeled peptides (Sigma Genosys) or Rhodamine alone and incubated at 37°C for the indicated length of time. When indicated, Pico Green dsDNA reagent (Invitrogen) was added for the final 10 min of incubation. The media was removed and the cells were washed 3 times with PBS then fixed with 4% para-formaldehyde for 10 min. After removing the para-formaldehyde and washing the cells once more with PBS, the chambers were detached from the slide. Slow Fade® (Molecular Probes S2828) was added to minimize photo-bleaching. Z-series images were collected using a Leica TCS SP2 confocal microscope. Pico Green was excited using the 488nm line from an Ar/Kr laser attenuated to 35%. Rhodamine was excited using the 543nm line from an Ar/Kr laser unattenuated. The detector slits of the confocal microscope were adjusted to detect Pico Green emission between 497-553nm and rhodamine emission between 555-620 nm.

IMR-90 cells were seeded in 4-well (LabTek-II) chamber slides at 80,000 cells per well and incubated at 37°C with 5% CO_2 overnight to allow adhesion. The media was removed and replaced with fresh DMEM + 20% FBS containing 10 μM, 20 μM and 50 μM N-terminal rhodamine-labeled peptides (Sigma Genosys) or rhodamine alone and incubated at 37°C for the indicated length of time. Subsequent steps were the same as U2OS cells.

High performance liquid chromatography (HPLC): HPLC was used to detect and quantify the uptake of unlabeled peptide by U2OS, HeLa and IMR-90 cells. U2OS cells and

HeLa cells were seeded at a density of 300,000 cells per well in six well tissue culture plates and allowed to adhere overnight. IMR-90 cells were plated at 200,000 cells per well. The cells were incubated with unlabeled wrwycr or equivalent concentration of DMSO for 24 h at 37^{O}C. After removing the peptide-containing media, which were saved for analysis, the cells were gently washed with ice cold PBS. Cell lysates were prepared by incubating with 100µl lysis buffer (0.71% NP40, 71mM Tris (pH 7.5), 0.71mM EDTA, 212 mM NaCl) for 10 min on ice, followed by physical scraping. The lysates were centrifuged at 16.1 rcf for 3 min and the supernatants were collected for HPLC analysis. The samples were fractionated by reverse phase chromatography and analyzed on a HPLC (Beckman Coulter System Gold **BioEssential** 126/168) for the presence and abundance of the peptide. Samples were manually injected via a 300 µl loading loop and ran onto a Phenomonex Jupiter 4 micron Proteo 90Å C12 column, then eluted with 0.1% TFA (trifluoroacetic acid) in 100% acetonitrile at a flow rate of 1 ml per minute. The acetonitrile gradient was 0-30% from 5 to 13.5 min, 30-45% from 13.5 to 28.5 min, and up to 100% from 28.5 to 60 min. Peptide concentrations were determined by calculating the area under the peptide peaks, using the integration function of the HPLC's 32 Karat software (Beckman Coulter, Fullerton, California) and comparing it to a standard curve. Once the total peptide quantity per sample was determined, the intracellular peptide concentration was calculated by dividing that amount by the product of the number of cells per sample (300000) and the typical volume of a sarcoma cell (1 picoliter) for U2OS, 2.5 picoliter for HeLa cells (Wharton and Goz, 1978) and 2.1 picoliter for IMR-90 cells (Vasquez et al, 1982). It should be noted here that since % dimer peptide is not constant over time, all the calculations are performed as [wrwycr] and not [(wrwycr)2]. Unlike U2OS and HeLa cells, the media used to plate IMR-90 cells and resuspend the treatments was supplemented with 20% FBS.

Live-dead assay to measure acute cytotoxicity : U2OS and HeLa cells were seeded at 300,000 cells per well in 6-well tissue culture plates (Falcon 353046) in DMEM containing 10% FBS and allowed to attach overnight at 37^{O}C with 5% CO_2. IMR-90 cells, instead, were plated at 200,000 cells per well in DMEM containing 20% FBS. The media was removed and the cells were incubated with the appropriate treatments for 24 h. After 24 h, the treatments were removed and stored on ice and the cells were washed twice with PBS. The cells were incubated with 300 µl 0.05% Trypsin containing 0.2% EDTA (Gibco 15400) per well, at 37^{O}C for 5 min, to release them from the plate. DMEM (700 µl) with 10% FBS was added to each well to inactivate the trypsin and dislodge the cells. The detached cells were collected in 1.5 ml eppendorf tubes and centrifuged for 5 min at 0.8 rcf. Cell pellets were washed once with PBS and resuspended in 200 µl of solution containing either or both Live (Calcein AM) and Dead (ethidium homodimer) stain according to the manufacturer's protocol (Live/dead cytotoxicity kit for mammalian cells, Invitrogen, L-3224). The cells were stained for 20 min at room temperature in the dark, then diluted with 300 µl filtered PBS for analysis on the FACS Aria desktop cell sorter (Becton-Dickenson) using a 70 µm nozzle. Three controls were used for setting the gates on the flow cytometer. The cells were gated first by analyzing unstained and single color controls (green and red) and then by performing manual compensation to counteract the possible overlap of calcein and ethidium homodimer spectra (FACS dot plots not shown). Cells grown in DMEM with no other treatment were incubated with Calcein-AM only as the positive control for live cells (Calcein fluorescence detected in the FITC channel) and with PBS for the unstained control. Cells incubated in 70% methanol for 5 min at 37ºC, to permeabilize the cell membrane, served as the positive control for dead cells (ethidium homodimer fluorescence detected in the PE-Texas Red channel).All other samples were stained with both dyes. Data were collected and analyzed using the FACS Diva software (Becton-Dickenson).

Colony forming assay (CFA): U2OS and HeLa cells were seeded at 500 cells per well in 6-well tissue culture plates and allowed to attach overnight at 37^{O}C with 5% CO_2. The next day the cells were observed under the microscope to verify that they had adhered to the plate as a single cell (or a colony of two cells) and that there was sufficient space between two cells permitting formation of individual colonies. The media was then removed and replaced with fresh DMEM containing the appropriate treatments and incubated for 24 h. After the treatment, solutions were removed, the cells were washed once with PBS, fresh peptide-free medium was added and the cells were allowed to grow for 6-7 days (until individual colonies became visible under the microscope). Since Hela cells replicate faster than U2OS cells, the colonies were typically stained after 4-5 days instead of 6-7 days to avoid fusion of two adjacent colonies. Following removal of the media and washing once with PBS, the cells were stained with 1% crystal violet solution for 2 min at room temperature and rinsed immediately under running water until all excess stain was washed from the plates. Finally, the number of colonies was counted manually for each treatment and % survival was calculated using the media-treated culture as 100%. At least three independent experiments, each done in triplicate, were performed for each treatment condition.

It should be noted that it was not possible to perform the Colony forming assay (CFA) for the IMR-90 cells because the cells had long projections and it was difficult to count individual colonies.

Statistical analysis: The error bars in the graph represents standard error. Non-parametric test and student's t test (one tailed and two tailed analysis) were performed and the difference

between the two values were considered significant (*) if $p<0.05$ and highly significant (**) if $p<0.005$ in both the tests.

Apoptosis measurement assays:

Annexin V assay for measuring early apoptosis: This assay was performed only with U2OS cells. Cells were seeded at 150,000 cells per well in 12-well tissue culture plates (Costar 3513) and allowed to attach overnight at 37^{O}C with 5% CO_2. The media was removed and the cells were incubated with the appropriate treatments for the indicated time (6, 12 and 18 h). 150 µM etoposide treatment for 18 h was used to induce apoptosis. The treatments were removed and the samples were washed twice with PBS. The cells were incubated with 150 µl 0.05% Trypsin containing 0.2% EDTA (Gibco 15400) per well, at 37^{O}C for 5 min, to release them from the plate. DMEM (850 µl) with 10% FBS were added to each well to deactivate the trypsin and dislodge the cells. The detached cells were collected in 1.5 ml Eppendorf tubes and centrifuged for 5 min at 0.8 rcf. Methanol (70%) treatment at 37°C for 5 min was used to permeabilize the cells. All other samples were resuspended in 50 µl binding buffer (0.01M HEPES, pH 7.4, 0.14M NaCl, 2.5mM $CaCl_2$) by itself (unstained control), or containing 2.5 µl of Annexin V – APC or propidium iodide (PI, from stock of 1 mg/ml) or both. The samples were incubated in the dark at RT for 15 min. Data were collected and analyzed using the FACS Diva software (Becton-Dickenson).

Cytochrome C release assay for measuring central response to apoptosis: This assay was performed with a HeLa cell variant named Htog1. 2×10^5 Htog1 cells were seeded on glass coverslips glued to 35 mm microwell petri dishes (Mattek Corp. Ashland, MA) containing DMEM with 10% FBS and allowed to attach overnight. The media were removed from each well and replaced with 1 ml of the appropriate treatment and incubated for 24 h. 23

h after treatment addition, 1µl of 50 µM tetramethyl rhodamine ethyl ester, perchlorate (TMRE) solution was added to each well (final concentration 50 nM) and incubated at 37ºC in 5% CO_2 for the remaining hour. Cytochrome C release and loss of TMRE staining were determined in Z-series images that were acquired using a Leica TCS SP2 inverted confocal microscope. GFP was excited using a 488 nm line from a Ar/Kr laser attenuated to 33% and the fluorescence was detected at 497-553 nm. TMRE was excited using a 543 nm line from a Ar/Kr laser attenuated to 35% and the fluorescence was detected at 555-620 nm. Each cell was analyzed for evidence of the different hallmarks of apoptosis [release of cytochromeC (GFP channel), loss of mitochondrial membrane potential (TMRE loss) or morphological abnormalities] and the percentage cells positive for each hallmark was calculated for the various treatments.

Caspase-3 up regulation for measuring late apoptosis: Caspase-3 activity was measured using its fluorogenic substrate, DEVDAFC (Sigma). U2OS and IMR-90 cells were plated and treated exactly as described for Live/Dead assays. Following 24 h of treatment, cells were lysed on ice by lysis buffer (0.71% NP-40, 71 mM Tris pH 7.5, 0.71 mM EDTA, 212 mM NaCl) and centrifuged to remove cell debris. 50 µl of the resulting supernatant samples were mixed with 50 µl of the substrate solution (5mM DTT, 50 µM DEVD-AFC, 19mM HEPES pH7.4, 94mM NaCl) in a black-bottom 96-well titer plate in duplicate and incubated for 1 h at 37^{o}C. Caspase-3 mediated cleavage of DEVDAFC into free AFC was measured using a Spectra Max Gemini XS flourimeter plate reader with an excitation wavelength of 400 nm and an emission wavelength of 505 nm using Softmax Pro version 3.1.2 software. This experiment was replicated five times for U2OS cells, two of which were performed in duplicate and three times with IMR-90 cells. The fluorescence readings (RFU) were normalized to the total protein loaded in 50 µl of each sample as determined using the Bio-Rad protein assay system (Bio-Rad, 500-0006).

Cell size distribution measurement from confocal images (Image J analysis):

Cell size distribution Confocal images of the Htog1 cells used for determining the hallmarks of apoptosis were also used to determine the size of the cells. Cell size distribution for each treatment was calculated by determining the area of individual cells using the Image J software (NIH), taking into account the magnification of each image and using the simple formula

Actual area = Calculated area/zoom factor

Cell size distribution by FACS analysis

Htog1 cells were seeded at 300,000 cells per well in 6 well tissue culture plates (Falcon 353046) and allowed to attach overnight at 37^{O}C with 5% CO_2. The media was removed and the cells were incubated with the same treatments as confocal microscopy for 24 h. After washing away the treatments, the cells were incubated with 300 µl 0.05% trypsin containing 0.2% EDTA (Gibco 15400) per well, at 37^{O}C for 5 min, to release them from the plate. DMEM with 10% FBS (700 µl) were added to each well to inactivate the trypsin and dislodge the cells. The detached cells were collected in 1.5 ml eppendorf tubes and centrifuged for 5 min at 0.8 rcf. The cell pellets were resuspended in PBS and analyzed with the FACS Aria desktop cell sorter (Becton Dickenson) using a 70 µM nozzle. The forward scatter (FSC, size) versus side scatter (SSC, granularity) of samples was analyzed using FACS Diva software.

γ-H2AX foci formation:

FACS analysis: U2OS and IMR-90 cells were seeded at 300,000 and 200,000 cells respectively per well in 6 well tissµe culture plates (Falcon 353046) and allowed to attach overnight at 37^{O}C with 5% CO_2. The media was removed and the cells were incubated with

the appropriate treatments for indicated 24 h. etoposide treatment (51 μM) for 24 h was used as positive control. The cells were incubated with 0.05% trypsin (300 μl) containing 0.2% EDTA per well, at 37^{O}C for 5 min, to release them from the plate. 700 μl of DMEM with 10% FBS were added to each well to inactivate the trypsin and dislodge the cells. The detached cells were collected in 1.5 ml Eppendorf tubes and centrifuged for 5 min at 0.8 rcf. The cell pellets were fixed with 4% paraformaldehyde at RT for 30 min and permeabilized with 0.1% Triton X and 0.1% sodium citrate on ice for 3 min. The cells were washed once with PBS and resuspended either in PBS alone (unstained control) or PBS containing γ-H2AX–FITC antibody (1:500 dilutions, Upstate). The samples were incubated on ice in the dark for 30 min. Data were collected and analyzed using the FACS Diva software (Becton-Dickenson). FITC positive samples were considered γ-H2AX positive. A FITC-IgG control antibody was used to stain a 51 μM etoposide treated sample to check the specificity of the antibody.

Microscopy: U2OS cells and HeLa cells were plated on round cover slips, each placed in a well in 12-well tissue culture plates and allowed to adhere overnight at 37°C and 5% CO_2. The media was carefully replaced by the appropriate treatments and incubated for the indicated time points under the same incubator conditions. Cells were washed twice with PBS, fixed in 4% paraformaldehyde at RT for 30 min and permeabilized with 0.2 % Triton-X 100 on ice for 5 min. Cells were stained to detect γ-H2AX using a phospho-specific antibody (Millipore) against Ser139 of H2AX overnight (γ-H2AX) and counterstained with FITC-tagged secondary antibody at room temperature for 2 h with intermittent washing. After the final washing step, the cover slips were mounted on a glass slide containing the antifade agent and DAPI (nuclear stain) and observed under a fluorescent microscope. Since the number of foci per nucleus was too large to count manually, we used Image J to measure the total green fluorescence (FITC tagged secondary antibody is used to detect γ-H2AX foci) per nucleus per

treatment to estimate the number of foci per cell. For most of the treatments, 50 nuclei were counted and the mean calculated was the average of green intensity.

Replicative DNA synthesis measurement: U2OS cells were seeded at 200,000 cells per well in 12-well tissue culture plates (Costar 3513) and allowed to attach overnight at $37^{O}C$ with 5% CO_2. The media was removed and the cells were incubated with the appropriate treatments for 18h or 24h. EdU (10 μM) (freshly diluted from 10 mM stock, 1 μl added to a 1ml treatment) was added concurrently for the same amount of time. The rest of the procedure followed the manufacturer's protocol (Invitrogen C35002). Briefly, the cells were harvested by trypsinization (as described in the Live/Dead assay, Materials and Methods). Cells were fixed in 4% paraformaldehyde (RT for 15 min), washed with 1% BSA in PBS and permeabilized in Triton X based permeabilizing solution (supplied by the kit) on ice for 5 min. The cells were then incubated with the Click-iT reaction cocktail (containing reaction buffer, buffer additive, $CuSO_4$ and Alexa 488 - azide) at RT for 30 min in the dark to complete the in situ alkyne-azide reaction. The incorporation of EdU (corresponding to DNA replication) was measured by a corresponding increase in Alexa-488 signal as compared to the unstained control when data were collected in Becton-Dickenson FACSAria and analyzed using FACS DIVA software.

***Recovery from Intra-S arrest*:**

DNA synthesis: U2OS cells in culture were arrested intra-S in a stepwise manner as described in Figure II-9A. Briefly, cells were plated at a density of 200,000 cells per well in 6 well tissue culture plates with regular media (DMEM + 10% FBS + Pen/Strep) and allowed to settle overnight in standard incubation conditions (37°C, 5% CO_2). After approximately 18 h, the actively growing cells were arrested by replacing the high glucose DMEM with minimal

RPMI and 2% FBS (this is the minimum amount of FBS required for U2OS cells to survive in culture) and incubated for an additional 18 h. Now, the cells were released (by replacing RPMI again with DMEM + 10% FBS) in the presence of HU and arrested intra-S within 5-6 h (each step of arrest was checked using the EdU incorporation assay). HU was washed away and the cells were allowed to recover for different times 2 h, 4 h, 8 h, 12 h and 16 h in the presence or absence of wrwycr or control peptide. The cells were incubated with 10 μM EdU for the last 4 h of recovery to measure what fraction of cells is capable of restarting DNA synthesis except the 16 h time point where EdU was added at the time of HU washing. Data were collected using a Becton-Dickenson FACS Aria instrument and analyzed using FACS DIVA software. To confirm that the difficulty in recovery from HU-induced arrest is not an indirect consequence of cell death, we performed the Live/Dead assay with all the samples after the 16 h recovery phase (Figure II-10).

Microscopy: U2OS cells were plated on round cover slips, each placed in a well in 12-well tissue culture plates and allowed to adhere overnight at 37°C and 5% CO_2. The cells were arrested first in RPMI + 2% FBS for 18 h and then in HU (5 mM) for 6 h. Some arrested cells were processed for microscopy to assess the level of HU-mediated damage. Other arrested samples were allowed to recover for 16 h in the presence or absence of wrwycr and then processed for microscopy.

Cells were washed twice with PBS, fixed in 4% paraformaldehyde at RT for 30 min and permeabilized with 0.2 % Triton-X 100 on ice for 5 min. Cells were stained to detect γ-H2AX, ATR or phospho-ATM overnight and counterstained with FITC-tagged and/or cy3-tagged secondary antibody at room temperature for 2 h with intermittent washing. After the final washing step, the cover slips were mounted on a glass slide containing antifade agent and DAPI (nuclear stain) and observed under a fluorescent microscope.

Foci counting: Since the number of foci per nucleus was too large to count manually, we used Image J to measure the total green fluorescence due to γ-H2AX staining per nucleus per treatment. For most of the treatments, 50 nuclei were counted and the mean calculated was the average of green intensity.

Phospho-ATM foci were counted manually. Around 50-60 cells were counted per treatment. Individual cells were classified into five categories based on the number of foci per nucleus as follows; cells with no foci (0), 1-5 foci (1), 6-10 foci (2), 11-20 (3) and >20 foci (4). % cells in each category was calculated per treatment.

Phase contrast microscopy: IMR 90 cells were seeded at 300,000 cells per well in 6-well tissue culture plates (Falcon 353046) in DMEM containing 20% FBS and allowed to attach overnight at 37^{O}C with 5% CO_2. The media was removed and the cells were incubated with the appropriate treatments for 24 h. Several fields of pictures for the different treatments were taken to identify morphological features of stress.

DNA content measurement for cell cycle analysis: Cell cycle distribution was evaluated in IMR-90 cells using PI staining according to standard procedures. Briefly, 200,000 cells were plated per well in 6 well tissue culture plates and allowed to adhere overnight followed by 24 h of treatments. Cells were fixed with 4% paraformaldehyde for 30 min at room temperature and DNA was stained with PI solution (25 μg/ml final concentration containing RNAseA and 0.01% Triton X 100) at room temperature for 30 min in the dark and analysed by flow cytometry. Relative cell cycle distribution was assessed using Flow Jo software (Treestar Inc).

TUNEL assay: The In Situ Cell Death Detection Kit, Fluorescein (Roche, 11 684 795 910) was used to measure DNA breaks due to direct DNA damage or apoptosis and the

manufacturer's protocol was followed. Briefly, 300,000 cells (U2OS cells) or 200,000 cells (IMR-90 cells) were plated in six well tissue culture plates and allowed to attach overnight at 37°C with 5% CO_2. Cells were then incubated with appropriate treatments for 24 h. After harvesting, fixed and permeabilized cell pellets were either resuspended in the reaction buffer only (unstained control) or TdT (terminal deoxytransferase) enzyme to label 3' broken DNA ends with dUTP tagged FITC and incubated at 37°C for 30 min. Data to determine %TUNEL positive cells were collected and analysed as FITC positive particles using FACS Diva software (Becton-Dickenson). The mean is an average of 3 independent experiments.

APPENDIX A.1

Mass spectrometry (Maldi Tof reflectron) confirms presence of monomer and dimer in U2OS cell lysate

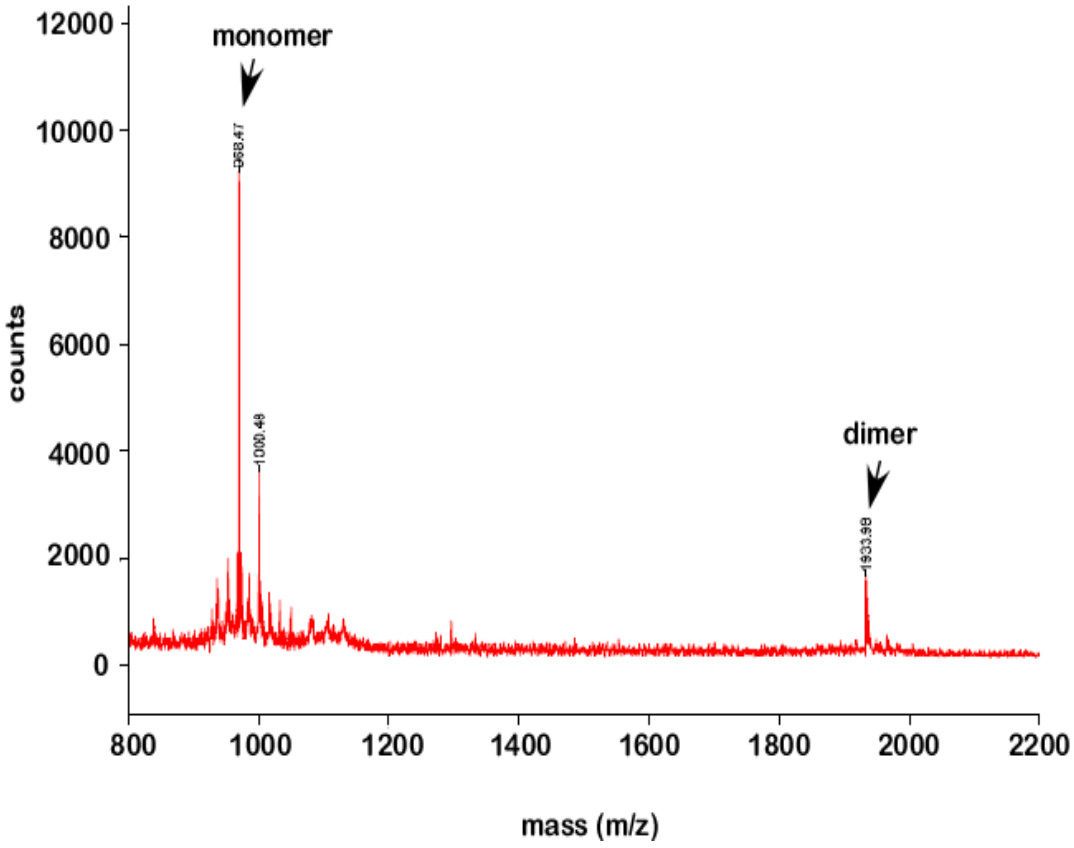

Figure A.1-1. Mass spectrometry of HPLC fraction containing peptide monomer and dimer

The peptide-dependent peaks (shown in arrows) confirm the presence of monomer and dimer wrwycr in peptide treated U2OS cell lysate. It should be noted that it is difficult to isolate the monomer and dimer dependent fraction of the HPLC eluent.

Intracellular distribution of high concentration of Rho-WRWYCR

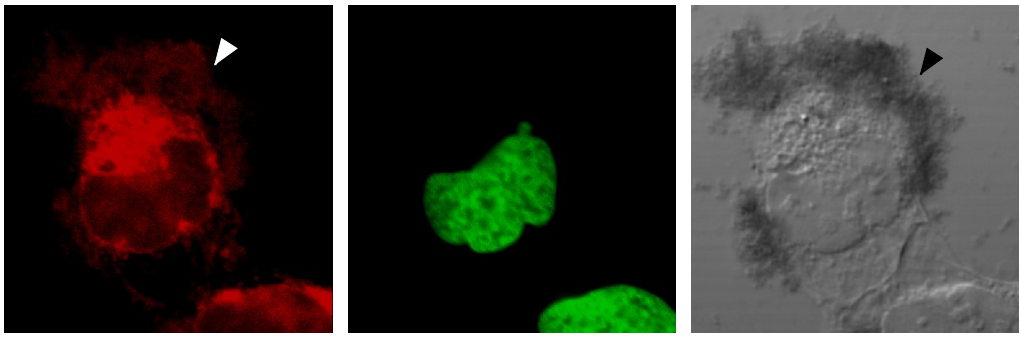

Figure A.1-2. Confocal microscopy of Rh-WRWYCR-treated U2OS cells

150 μM R-WRWYCR was incubated with U2OS cells for 24 h and counterstained with PicoGreen

Red : Rh-WRWYCR; Green : PicoGreen and Trans : Bright field image

APPENDIX A.2

Phase contrast microscopy of U2OS cells

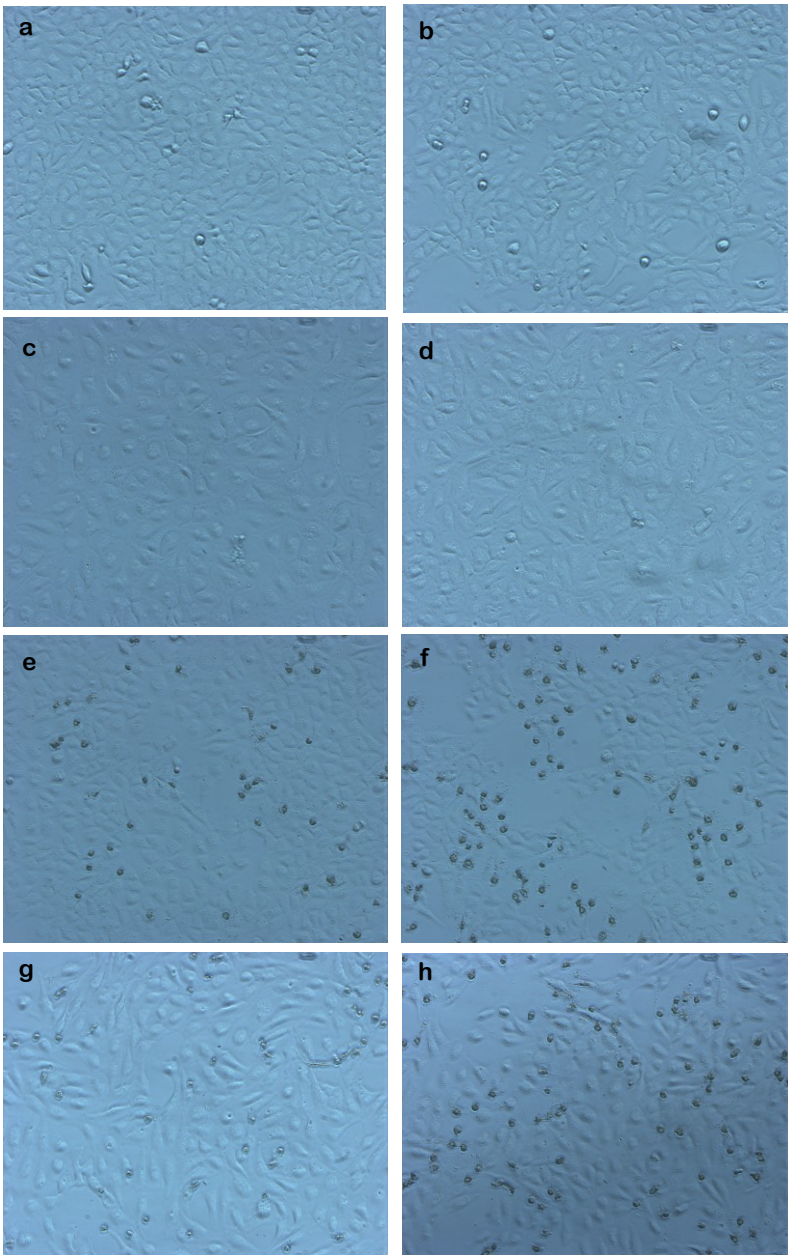

Figure A.2-1. Phase contrast microcopy of U2OS cells

Shown here are representative fields of U2OS cells after 24 h treatment with a. DMEM, b. 2% DMSO, c. 1.3 µM etoposide, d. 5 mM HU, e. 150 µM wrwycr, f. 200 µM wrwycr, g. 5 mM HU + 150 µM wrwycr and h. 5 mM HU + 200 µM wrwycr

APPENDIX A.3

Co-localization of WRWYCR in cell organelles

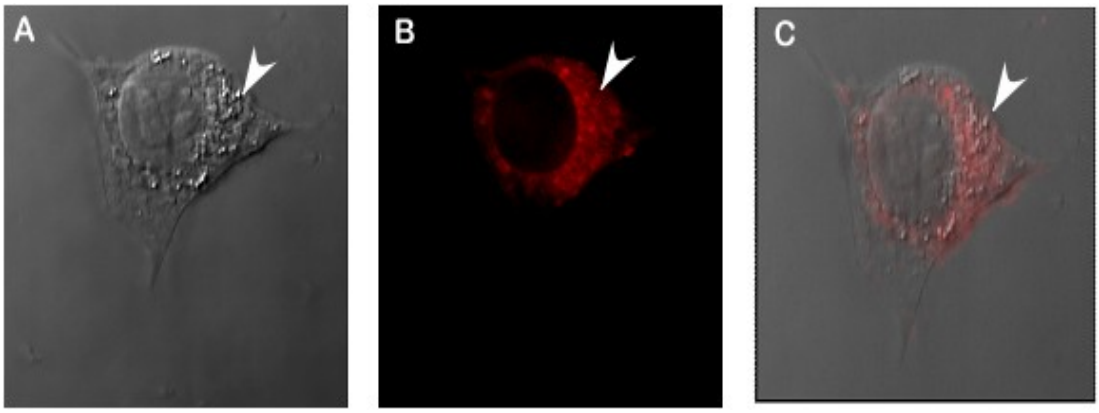

Figure A.3-1. Rh-WRWYCR localizes in or around mitochondria

Z section images of a Hela cell variant, Htog1, incubated with 10 μM Rho-WRWYCR for 3 h showing overlap of Rho-WRWYCR with mitochondria. Bright field image (A) the arrowhead points to mitochondria, TRITC channel (B) showing the Rhodamine-tagged WRWYCR distribution and overlay (C) of the two channels

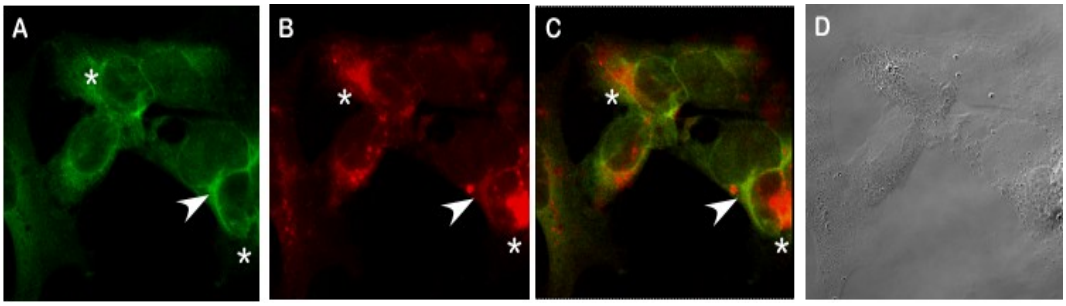

Figure A.3-2. Rh-WRWYCR have some co-localization with ER-resident GRP-78

U2OS cells incubated with 10 μM Rho-WRWYCR for 3 h, fixed and stained with antibody against GRP-78. A. green channel showing ER with GRP-78 staining, B. Rho-WRWYCR (10 μM) incubation for 3 h C. overlay of green and red channel and D. bright field image. The yellow regions (marked by arrowhead) in panel C mark areas of overlap indicating presence of Rh-WRWYCR in ER and the red regions are areas of no overlap indicating presence of WRWYCR in places other than ER.

APPENDIX A.4

Role of p53 in wrwycr-induced cytotoxicity

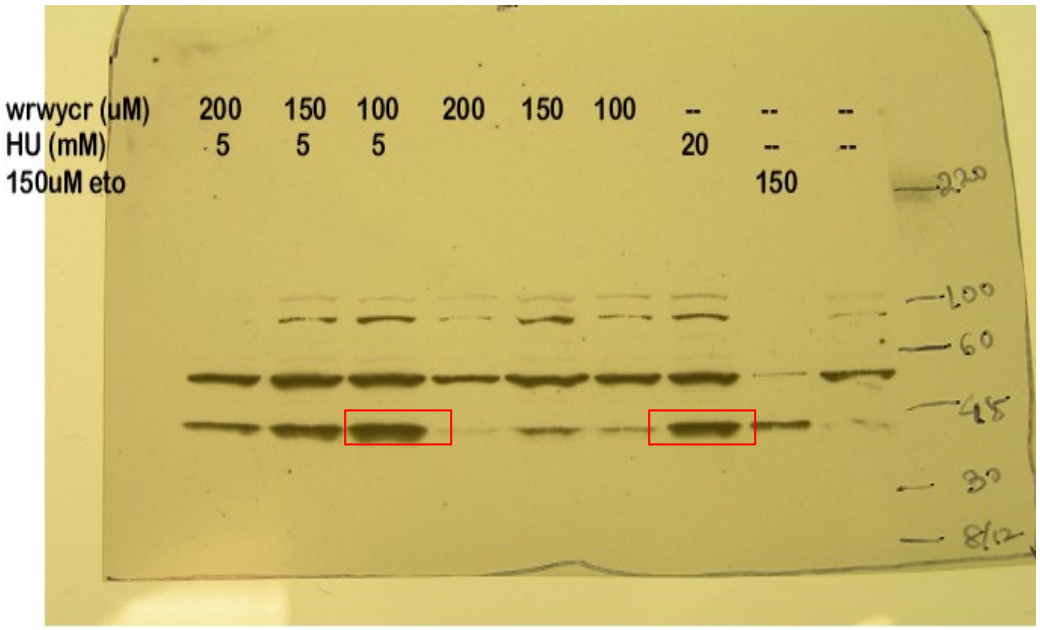

Figure A.4-1. wrwycr-treatment upregulates p44 protein in U2OS cells

Western blot analysis of U2OS cell lysates after 24 h incubation with the labeled treatments. Interestingly, a lower molecular weight p53 variant, p44 gets upregulated upon addition of DNA damaging agents like etoposide and HU which increases significantly more upon concurrent administration of increasing concentrations of wrwycr.

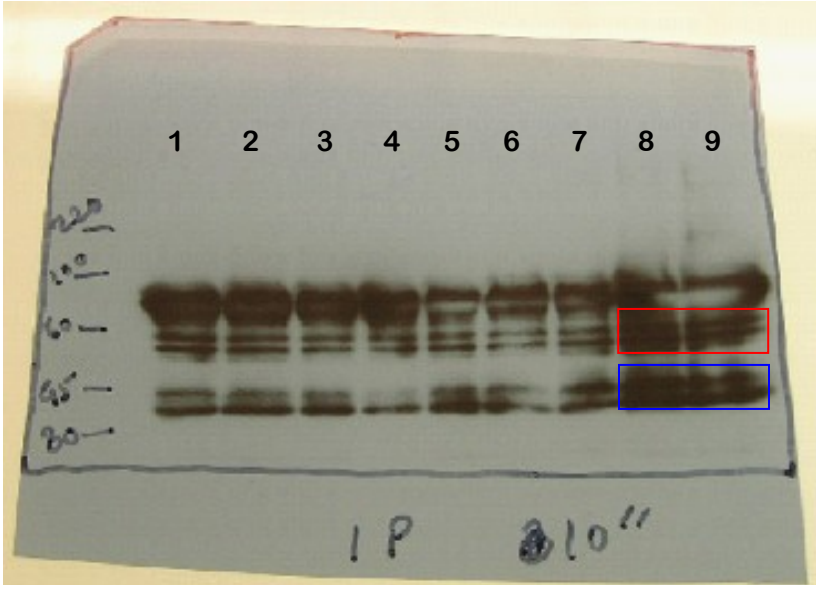

Figure A.4-2. Co-treatment with HU increases p44 accumulation in U2OS cells

Immunoprecipitation of U2OS cell lysates for total p53 protein followed by 24 h treatment with
1. DMEM, 2. 150 µM etoposide, 3. 20 mM HU, 4. 2% DMSO, 5. 100 µM wrwycr, 6. 150 µM wrwycr, 7. 20 HU + 150 µM wrwycr, 8. 200 µM wrwycr and 9. 20 HU + 200 µM wrwycr. The red rectangle represents the p53 protein and blue rectangle represents p44 protein. It should be noted that lane 8 and 9 shows up-regulation of both protein variants.

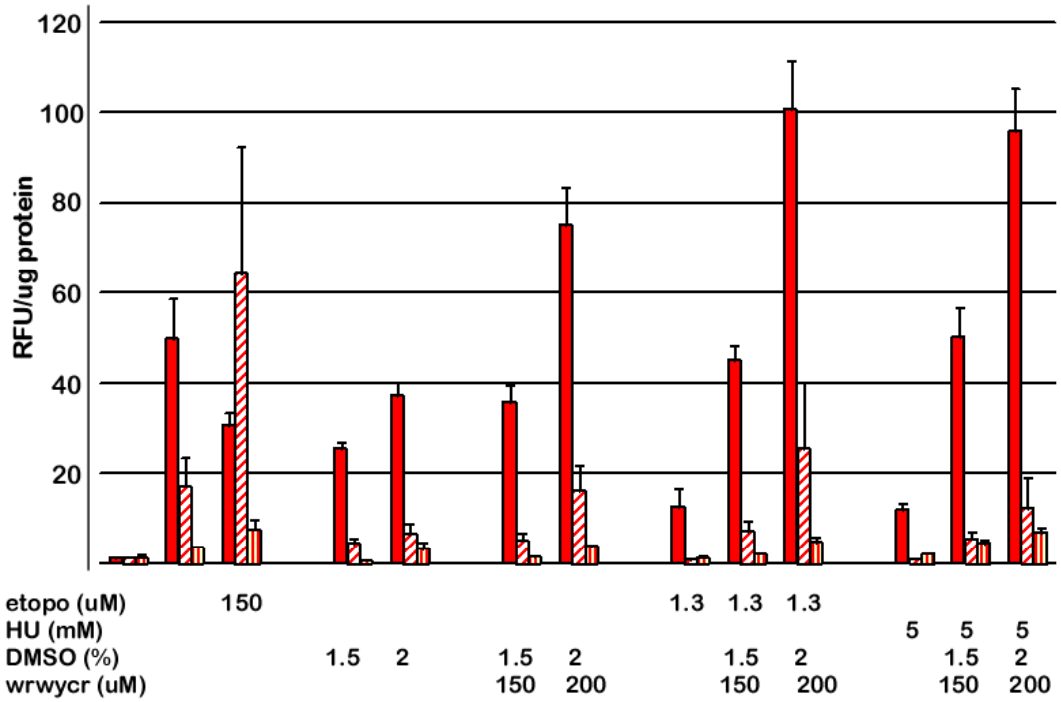

Figure A.4-3. wrwycr induces p53-independent apoptosis.

Comparative analysis of caspase-3 activity in p53 null Saos-2 (solid red bars) vs. wild type p53 containing U2OS (white bar with red hatches) and IMR90 (white bar with red stripes) after 24hrs incubation with the labeled treatments

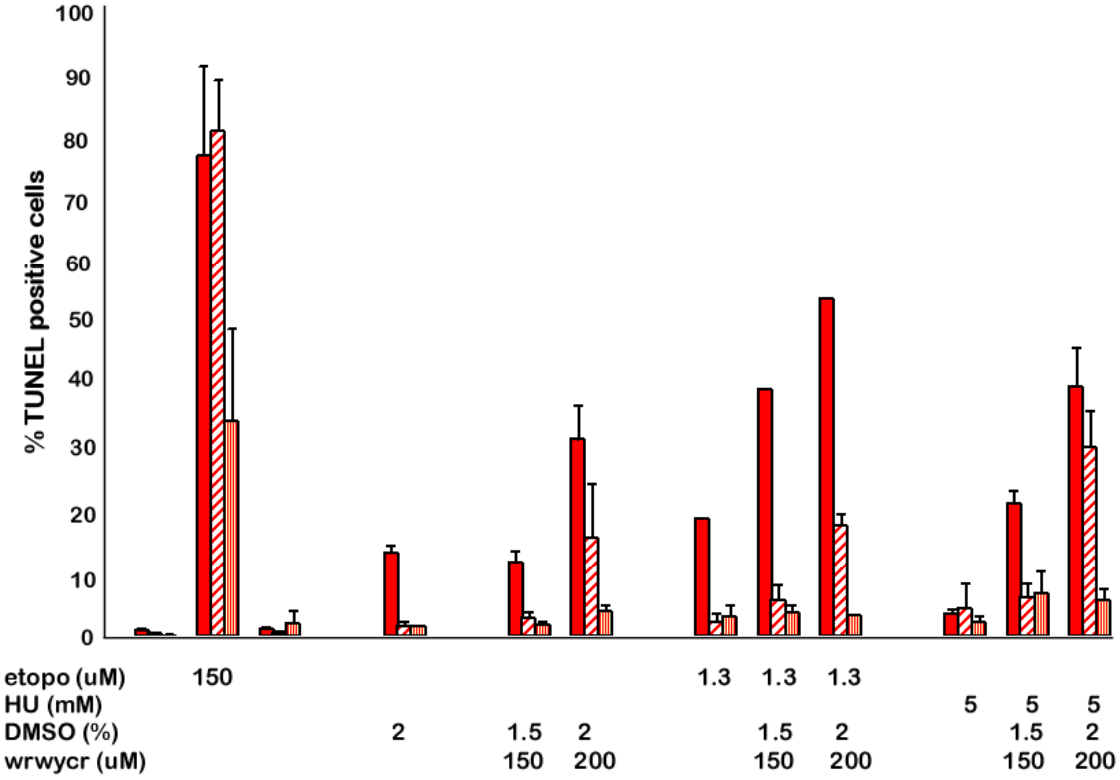

Figure A.4-4. Accumulation of DNA breaks is also p53 independent.

TUNEL assay performed to quantitate percentage of cells experiencing DNA breaks after 24 h incubation with the above mentioned treatments. p53 null Saos-2 cells (red solid bars) show maximum sensitivity towards accumulating DNA damage as depicted by % TUNEL positive cells as compared to p53 containing U2OS (white bars with red hatched lines) and IMR90 (white bar with red stripes) cells.

APPENDIX A.5

Effect of the dodecamer peptide, wrwyrggrywrw, in human cells

Abstract

Previous studies *in vitro* and in bacterial system and current study in human cells show that wrwycr is active as a dimer and it dimerizes via cysteine (Gunderson et al, 2009; Orchard et al, unpublished results; Patra et al, unpublished results). This is tested both by increasing sensitivity to DTT and complete loss of potency when cysteine is mutated to alanine to generate wrwyar (Gunderson et al, 2009). Subsequently a dodecamer peptide with sequence wrwyrggrywrw is synthesized by replacing the c5 cysteine molecule of wrwycr with glycine. Theoretically, this peptide should act as a dimer of wrwycr resistant to *in vivo* reduction. Use of wrwyrggrywrw in living system has a few advantages over wrwycr. (1) Since, effective peptide concentration in wrwyrggrywrw is twice as in wrwycr, same efficacy can be achieved upon administration of about half the dose. (2) Also, solvent toxicity induced by DMSO should be reduced accordingly.

In this study we tested effect of the dodecamer peptide in U2OS cells. Our results indicate that wrwyrggrywrw can enter U2OS cells (HPLC) and induces dose dependent acute cytotoxicity after 24 h of administration. The effect is more potent and linear in wrwyrggrywrw than wrwycr. Unlike wrwycr, apoptosis is not the major mechanism of cell killing. In fact, higher dose of wrwyrggrywrw (100 μM and 150 μM) has reduced caspase-3 activity than 75 μM wrwyrggrywrw. Our overall results indicate that the dodecamer is significantly more toxic than wrwycr but probably lack specificity of action. This is corroborated by the fact that wrwyrggrywrw imparts less specificity in HJ binding in vitro. (Boldt et al, unpublished results).

Results

Dodecamer wrwyrggrywrw can enter U2OS cells

I used HPLC to detect and quantitate the amount of intracellular dodecamer peptide inside U2OS cells. Specifically I used a differential centrifugation technique to enrich the mitochondrial fraction to test whether the dodecamer can enter the mitochondria of U2OS cells. Our results show that there is a linear increase in wrwyrggrywrw concentration in both cytoplasmic and mitochondrial fractions of U2OS cell lysates (Table A.5-1). However, cytoplasmic fraction is 4-8 times that of mitochondrial fraction depending on the input dose (Table A.5-1). Like wrwycr, dodecamer wrwyrggrywrw concentrates in U2OS cells (from μM to mM range).

wrwyrggrywrw exhibits dose-dependent acute cytotoxicity to U2OS cells

A careful titration of wrwyrggrywrw was performed using Live/Dead assay (described in detail in chapter II) after exposing U2OS cells to the dodecamer for 24 h. 2%DMSO, being the highest concentration of DMSO used in the experiment, (2% DMSO is used to dissolve 200 μM dodecamer) is used as the '0' peptide control and as the only solvent control. As expected, U2OS cells are marginally sensitive to 25 μM dodecamer (equivalent to 50 μM wrwycr) which increases with increasing concentration of the peptide. Unlike wrwycr response in U2OS cells, the dose response of wrwyrggrywrw is more linear in increasing % dead cells and a corresponding decrease in % live cells (Figure A.5-1, note the linearity of the green and red curves in the range from 50 μM to 150 μM).

Table A.5-1. Quantitation of intracellular dodecamer concentration in U2OS cells

Intracellular conc (mM)	Input monomer conc (μM)		
	50	**100**	**150**
Mitochondria	**0.32**	**0.51**	**1.1**
Cytoplasm	**1.24**	**4.8**	**9.4**
Fold inc on top of mitochondria	***4***	***9.4***	***8.5***

Differential centrifugation of U2OS cell lysates to isolate mitochondria-rich and cytoplasm-rich fractions followed by HPLC of the fractions.

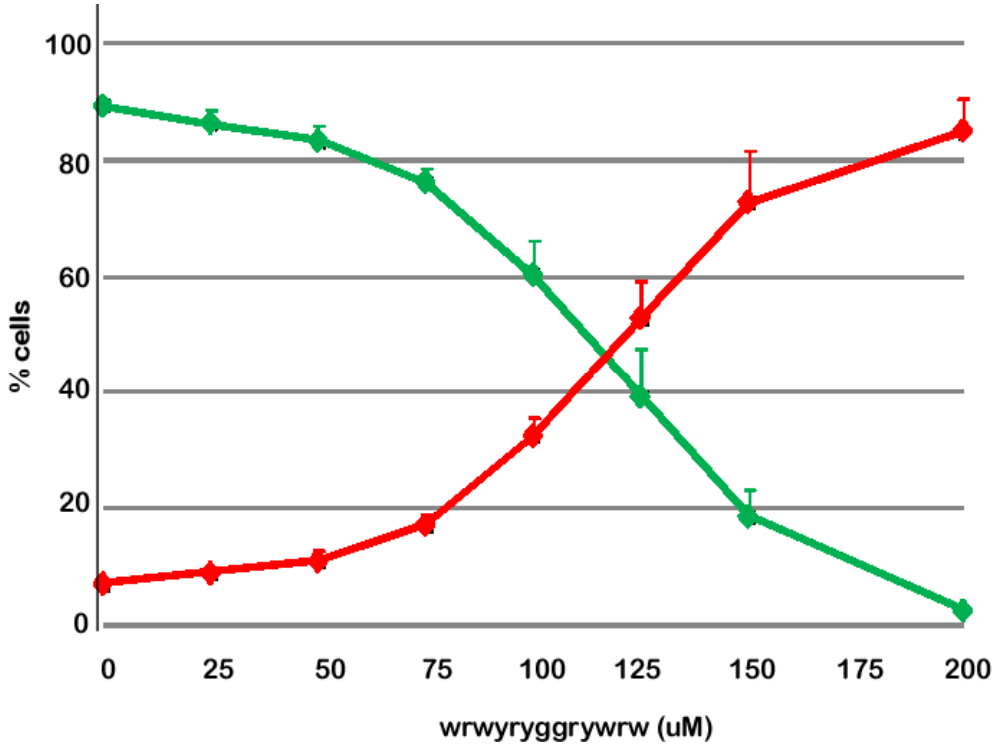

Figure A.5-1. **Dodecamer peptide wrwyrggrywrw induces dose dependent toxicity in U2OS cells.**

The graph represents line graph of % live (green) vs. % dead (red) cells after treatment with increasing doses of wrwyrggrywrw. Each data point represents mean of at least three independent experiments each done in duplicate. Error bar depicts the standard error.

APPENDIX A.6

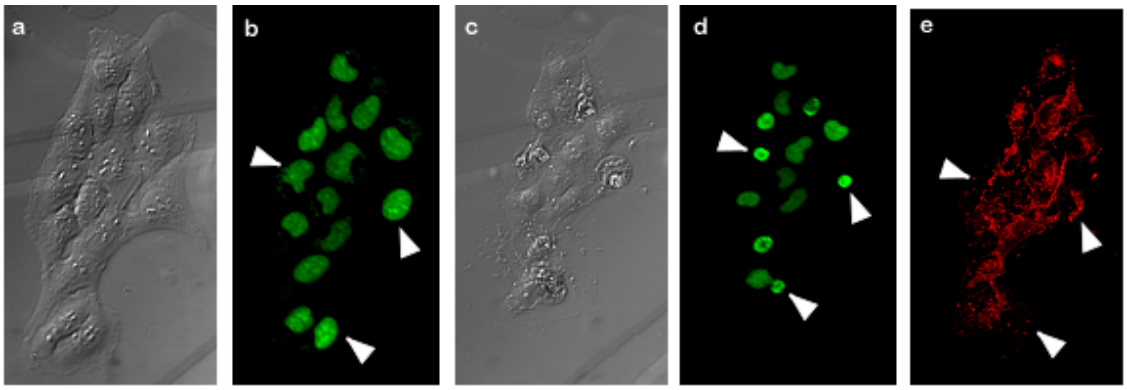

Figure A.6-1. wrwycr induces some nuclear condensation and membrane damage in U2OS cells

Panels (a) and (b) untreated; Panels (c)-(e) 200 μM wrwycr

Panels (a) and (c) bright field images ; Panels (b) and (d) PicoGreen staining and Panel (e) FM-464 staining

It should be noted that with the use of grid plate, we are tracking the same cell before and after treatment. The arrowheads point to three such cells.

REFERENCES

1. Acehan D, Xuejun J, Morgan D J, Heuser J E and Wang X Three-Dimensional Structure of the Apoptosome: Implications for Assembly, Procaspase-9 Binding, and Activation Molecular Cell. 2002;9:423–432

2. Agarwal C, Tyagi A and Agarwal R Gallic acid causes inactivating phosphorylation of cdc25A/cdc25C-cdc2 via ATM-Chk2 activation, leading to cell cycle arrest, and induces apoptosis in human prostrate carcinoma DU145 cells. Mol. Cancer Ther 2006;5(12)3294-3302

3. Allan L.A and Fried M p53-dependent apoptosis or growth arrest induced by different forms of radiation in U2OS cells: p21WAF1/CIP1 repression in UV induced apoptosis. Oncogene 1999 18: 5403 - 5412.

4. Alnemri E. S, Livingston D. J, Nicholson D. W, Salvesen G, Thornberry N. N. A, Wong W. W, and Yuan J Human ICE/CED-3 protease nomenclature Cell. 1996;87:171

5. Amor K. B, Breeuwer P, Verbaarschot P, Rombouts F. M, Akkermans A. D. L, De Vos W. M, and Abee1 T Multiparametric Flow Cytometry and Cell Sorting for the Assessment of Viable, Injured, and Dead Bifidobacterium Cells during Bile Salt Stress. Applied and Environmental Microbiology 2002;68(11):5209-5216

6. Arora A. S, de Groen P. C, Croal D. E, Emori Y, and Gores G.J Hepatocellular carcinoma cells resist necrosis during anoxia by preventing phospholipase-mediated calpain activation. J.Cell. Physiol. 1996;167:434-442

7. Bårtová E, Krejčí J, Harničarová A, Galiová G and Kozubek S Histone modifications and nuclear architecture : A Review Journal of Histochemistry & Cytochemistry 2008;56(8):711-721

8. Bell L, Byers B Separation of branched from linear DNA by two dimensional gel electrophoresis. Analytical Biochemistry. 1983;130(2):527-535

9. Berninghausen O, and Leippe M Necrosis versus Apoptosis as the Mechanism of Target Cell Death Induced by Entamoeba histolytica. Infection and Immunity 1997;65(9):3615–3621

10. Bielas J. H, and Heddle J. A Proliferation is necessary for both repair and mutation in transgenic mouse cells PNAS 2000**;**97(21):11391–11396

11. Bodo J, Jakubikova J, Chalupa I, Bartosova Z, Horakova K, Floch L, and Sedlak J Apoptotic effect of ethyl-4-isothiocyanatobutanoate is associated with DNA damage, proteasomal activity and induction of p53 and p21cip1/waf1. Apoptosis 2006;11:1299–1310

12. Boldt J. L, Pinilla C, and Segall A. M Reversible Inhibitors of λ Integrase-mediated Recombination Efficiently Trap Holliday Junction Intermediates and Form the Basis of a Novel Assay for Junction Resolution. J. Biol. Chem. 2004;279:3472-83

13. Boman, H. G Peptide antibiotics and their role in innate immunity. Annu. Rev. Immunol. 1995;13:61–92

14. Bourdon A, Minai L, Serre V, Jais J. P, Sarzi E, Aubert S, Chretien D, Lonlay P, Paquis-Flucklinger V, Arakawa H, Nakamura Y, Munnich A and Rotig A Mutation of RRM2B, encoding p53-controlled ribonucleotide reductase (p53R2), causes severe mitochondrial DNA depletion. Nature Genetics 2007;39(6):776-780

15. Bratton S. B, and Cohen G. M Apoptotic death sensor: an organelle's alter ego? Trends Pharmacol Sci 2001; 22:306–315

16. Brenwald N.P, Appelbaum P, Davies T and Gill M.J Evidence for efflux pumps, other than PmrA, associated with fluoroquinolone resistance in Steptococcus pneumonia. Clinical Microbiology and Infectious Diseases 2003;9:140-143

17. Bugreev D. V, Hanaoka F and Mazin A. V Rad54 dissociates homologous recombination intermediates by branch migration. Nat Struct Mol Biol 2007,14:746-753

18. Bugreev D. V, Mazina O. M and Mazin A. V Rad54 protein promotes branch migration of Holliday junctions. Nature 2006;442:590-593

19. Burton J.D The MTT assay to evaluate chemosensitivity. Methods Mol Med 2005;110:69-78

20. Carre V and Guilloton M DNA fragmentation attested by TUNEL in Saccharomyces cerevisiae subjected to photodynamic treatment J of Microbiological Methods 1997;29(3):185-190

21. Cassell G, Klemm M, Pinilla C, and Segall A Dissection of Bacteriophage λSite-specific Recombination using Synthetic Peptide Combinatorial Libraries. J. Mol. Biol. 2000;299:1193-1202

22. Cassell G. D, and Segall A. M Mechanism of inhibition of site-specific recombination by the Holliday junction-trapping peptide WKHYNY: insights into phage lambda integrase-mediated strand exchange. J. Mol. Biol. 2003;327(2):413-29

23. Chan S. C, Yau W. L, Wang W, Smith D. K, Sheu F. S, and Chen H. M J. Pept. Sci. 1998;4:413–425

24. Chanoux R, Yin B, Urtishak K. A, Asare A, Bassing C. H and Brown E ATR and H2AX co-operate in maintaining genome stability under replication stress. J Biol Chem. 2009;284(9)5994-6003

25. Chehab N. H, Malikzay A, Stavridi E. S and Halozonetis T. D Phosphorylation of ser-20 mediates stabilization of human p53 in response to DNA damage. PNAS. 1999;96(24):13777-13782

26. Chen G. L, Yang L, Rowe T. C, Halligan B. D, Tewey K. M, Liu L. F Nonintercalative antitumor drugs interfere with the breakage-reunion reaction of mammalian DNA topoisomerase II. J Biol Chem. 1984;259:13560-6

27. Chowdhury D, Keogh M. C, Ishii H, Peterson C. L, Buratowski S, Lieberman J gamma-H2AX dephosphorylation by protein phosphatase 2A facilitates DNA doublestrand break repair. Mol Cell 2005;20:801-9

28. Civoli F, Pauig S. B, and Daniel L. W Differentiation of HL-60 cells distinguishes between cytostatic and cytotoxic effects of the alkylphospholipid ET-18-OCH3. Cancer chemotherapy and pharmacology 1996;38(3):269-272

29. Danial N. N, and Korsmeyer S. J Cell death: critical control points. Cell 2004;116:205–219

30. Derossi D, Chassaing G, and Prochiantz A Trojan peptides: the penetratin system for intracellular delivery. Trends Cell Biol. 1998;8:84– 87

31. Derossi D, Joliot A. H, Chassaing G, and Prochiantz A The third helix of the *Antennapedia* homeodomain translocates through biological membranes. J. Biol. Chem. 1994;269:10444-10450

32. Derossi D, Calvet S, Trembleau A, Brunissen A, Chassaing G, and Prochiantz A Cell internalization of the third helix of the Antennapedia homeodomain is receptor-independent. J. Biol. Chem. 1996;271:18188-18193

33. Dolganov G. M, Maser R. S, Novikov A, Tosto L, Chong S, Breassan D. A and Petrini J. H. J Human rad50 is physically associated with human Mre11 : Identification of a

conserved multiprotein complex implicated in recombinational DNA repair. Mol and Cell Biol. 1996;16(9):4832-4841

34. Duchardt F, Fotin-Mleczek M, Schwarz H, Fischer R, and Brock R A comprehensive model for the cellular uptake of cationic cell-penetrating peptides. Traffic 2007;8:848–866

35. Edinger A. L, and Thompson C. B Death by design: apoptosis, necrosis and autophagy. Curr. Opin. Cell Biol. 2004;16:663–669

36. Eliseev R, Gunter K. K and Gunter T. E Bcl-2 prevents abnormal mitochondrial proliferation during etoposide-induced apoptosis. Exp. Cell Research. 2003;289:275-281

37. Eter N, and Spitznas M DMSO mimics inhibitory effect of thalidomide on choriocapillary endothelial cell proliferation in culture. Br J Ophthalmol 2002;86:1303–1305

38. Fadok V. A, Voelker D. R, Campbell P. A, Cohen J. J, Bratton D. L, and Henson P. M Exposure of Phosphatidylserine on the surface of Apoptotic Lymphocytes triggers specific recognition and removal by Microphages. The Journal of Immunology 1992;148(7):2207-2216

39. Fiore M, Zanier R, and Degrassi F Reversible G(1) arrest by dimethyl sulfoxide as a new method to synchronize Chinese hamster cells. Mutagenesis 2002;17:419– 424

40. Fretz M. M, Penning N. A, Al-Taei S, Futaki S, Takeuchi T, Nakase I, Storm G, and Jones A. T Temperature-, concentration- and cholesterol-dependent translocation of L- and D-octa-arginine across the plasma and nuclear membrane of CD34+ leukaemia cells. Biochem. J. 2007;403:335–342

41. Friedberg E.C, Walker G. C, Siede W, Wood R.D, Schultz R. A and Ellenberger T DNA Repair and Mutagenesis 2006; Second Edition, ASM Press

42. Friedman K. L and Brewer B. J Analysis of replication intermediates by two-dimensional gel electrophoresis. Methods in Enzymology 1995;262:613-627

43. Fu X, Wan S, Lyu Y. L, Liu L. F and Qi H Etoposide induces ATM-dependent mitochondrial biogenesis through AMPK activation. PLoS ONE. 2008;3:1-10

44. Fulda S, and Debatin K. M Extrinsic versus intrinsic apoptosis pathways in anticancer chemotherapy Oncogene 2006;25:4798–4811

45. Gatti L, Supino R, Perego P, Pavesi R, Caserini C, Carenini N, Righetti S. C, Zuco V, and Zunino F Apoptosis and growth arrest induced by platinum compounds in U2-OS cells reflect a specific DNA damage recognition associated with a different p53-mediated response. Cell Death and Differentiation 2002;9(12): 1352-1359

46. Gey G. O, Coffman W. D, Kubicek M. T Tissue culture studies of the proliferative capacity of cervical carcinoma and normal epithelium. Cancer research 1952;12:264-265

47. Giovanninia C, Matarreseb P, Scazzocchioa B, Sanchezc M, Masellaa R, Malornib W Mitochondria hyper polarization is an early event in oxidized low-density lipoprotein-induced apoptosis in Caco-2 intestinal cells. FEBS Letters 2002;523:200-206

48. Goldstein J. C, Munoz-Pinedo C, et al. Cytochrome c is released in a single step during apoptosis. Cell Death Differ 2005;12(5):453-62

49. Goldstein J. C, Waterhouse N. J, et al. The coordinate release of cytochrome c during apoptosis is rapid, complete and kinetically invariant. Nat Cell Biol 2000;2(3):156-62

50. Golstein P, and Kroemer G Cell death by necrosis: towards a molecular definition. Trends Biochem. Sci. 2006;32(1):37-43

51. Gray M. D, Shen J. C, Kamath-Loeb A. S, Blank A, Sopher B. L, Martin G. M, Oshima J, and Loeb L. A The Werner syndrome protein is a DNA helicase. Nature Genet. 1997;17:100–103

52. Green D. R, and Kroemer G The pathophysiology of mitochondrial cell death. Science 2004;305,626–629

53. Gunderson C. G, and Segall A.M DNA repair, a novel antibacterial target: Holliday junction-trapping peptides induce DNA damage and chromosome segregation defects. Molecular Microbiology 2006;59(4):1129–1148

54. Gunderson C. W, Boldt J. L and Segall A. M Peptide wrwycr inhibits the excisive recombination of several prophages and traps Holliday junctions inside bacteria. J Bacteriology 2009;191:2169-2176

55. Guy C. P, and Bolt E. L Archaeal Hel308 helicase targets replication forks in vivo and in vitro and unwinds lagging strands. Nucleic Acids Res. 2005;33:3678–3690

56. Hallbrink M, Oehlke J, Papsdorf G, and Bienert M. uptake of cell penetrating peptides is dependent on peptide-to-cell ratio rather than on peptide concentration. Biochim Biophys Acta 2004;1667:222-228

57. Hammill A. K, Uhr J. W, and Scheuermann R. H Annexin V Staining Due to Loss of Membrane Asymmetry Can Be Reversible and Precede Commitment to Apoptotic Death. Experimental Cell Research 1999;251:16-21

58. Hansen S. H, Olsson A and Casanova J. E Wortmannin, an inhibitor of phosphoinoside-3-kinase, inhibits transcytosis inpolarized epithelial cells. J. Biol Chem 1995;270(47)28425-28432

59. Hardt N, Pedrali-Noy G, Focher F and Spadari S Aphidicolin does not inhibit DNA repair synthesis in ultraviolet-irradiated HeLa cells. A radioautographic study. Biochem. J 1981;199:453-455

60. Harrington J, Hsieh C. L, Gerton J, Bosma G, and Lieber M. R Analysis of the defect in DNA end joining in themurine scid mutation. Mol Cell Biol. 1992;12(10):4758–4768

61. Hayflick L and Moorhead P. S The serial cultivation of human diploid cell strains Exp Cell Research 1961;25:585-621

62. Hayflick L, The cell biology of ageing. J. Invest. Dermatol 1979;73: 8–14

63. Heyer W. D Biochemistry of eukaryotic homologous recombination. Molecular Genetics of Recombination 2007;17:95-133

64. Heyer W-D, Ehmsen KT and Solinger JA Holliday junctions in eukaryotic nucleus : resolution in sight? Trends in Biochemical Sciences 2003;28:548-557

65. Hoeijmakers J. H Genome maintenance mechanisms for preventing cancer. Nature 2001;411:366–74

66. Holm T, Johansson H, Lundberg P, Pooga M, Lindgren M, and Langel U Studying the uptake of cell penetrating peptides. Nature protocols 2006;1(2):1001-1005

67. Iwasaki T, Ishibashi J, Saido-Sakanaka H, Tanaka H, Sato M, Asaoka A, Taylor D, and Yamakawa M Antibacterial and anticancer activity of diastereomeric 9-mer peptides derived from beetle defensins. Jackie Wilce (editor) on behalf of Australian Peptide Association. Proceedings of the 4th International Peptide Symposium in conjunction

with the 7th Australian peptide conference and the 2ns Asia-Pacific International Peptide symposium, 2007

68. Jackman J and O'Connor P. M Methods for synchronizing cells at specific stages of the cell cycle. Current protocols in cell biology. 2003;8.3.1-20

69. Jenssen H, Hamill P, and Hancock R. E Peptide antimicrobial agents. Clin. Microbiol. 2006;19:491–511

70. Johansson H J, El-Andaloussi S, Holm T, Mae M, Janes J, Maimets T and Langel U Characterization of a novel, cytotoxic cell-penetrating peptide derived from p14ARF protein Mol Therapy. 2007; 16:115-123

71. Joux F, and Lebaron P Use of fluorescent probes to assess physiological functions of bacteria at single-cell level. Microbes Infect. 2000;2:1523–1535

72. Kajander O.A, Karhunen P.J, Holt I.J and Jacobs H.T Prominent mitochondrial DNA recombination intermediates in human heart muscle. Embo Rep 2001;2:1007-1012

73. Kaplan I. M, Wadia J. S, and Dowdy S. F Cationic TAT peptide transduction domain enters cells by macropinocytosis. J Control Release 2005;102:247–53

74. Karow J. K, Constantinou A, Li J. L, West S. C, and Hickson I. D The Bloom's syndrome gene product promotes branch migration of Holliday junction. Proc. Natl Acad. Sci. USA 2000;97:6507–6508

75. Keogh MC, Kim JA, Downey M et al. A phosphatase complex that dephosphorylates γ-H2AX regulates DNA damage checkpoint recovery. Nature 2006;439:497-501

76. Keogh M. C, Kim J. A, Downey M, Fillingham J, Chowdhury D, Harrison J. C, Onishi M, Datta N, Galicia S, Emili A, Lieberman J, Shen X, Buratowski S, Haber J. E, Durocher D, Greenblatt J. F, Krogan N. J A phosphatase complex that dephosphorylates gammaH2AX regulates DNA damage checkpoint recovery. Nature 2005 (EPUB ahead of print, PMID:16299494).

77. Kepple K. V, Boldt J. L, and Segall A. M Holliday junction-binding peptides inhibit distinct junction-processing enzymes. PNAS 2005;102(19):6867-6872

78. Kepple K. V, Patel N, Salamon P, and Anca Segall A. M Interactions between branched DNAs and peptide inhibitors of DNA repair. Nucleic Acids Research 2008;36(16):5319–5334

79. Kerr J. F, Willie A. H Apoptosis: a basic biological phenomenon with wide-ranging implications in tissue kinetics. Br J Cancer 1972;26(4):239-257

80. Khanna K. K, Jackson S. P DNA double-strand breaks: signaling, repair and the cancer connection. Nat Genet 2001;27:247–54

81. Kim E, Jeon I.S, Kim J.W, Kim J, Jung H.S and Lee S. J An MTT-based method for quantification of periodontal ligament cell viability. Oral diseases 2007;13:495-499

82. Koopman G, Reutelingsperger C. P. M, Kuijten G. A. M, Keehnen R. M. J, Pals S. T, and van Oers M. H. J Annexin V for flow cytometric detection of phosphatidylserine expression on B cells undergoing apoptosis. Blood 1994;84**:**1415–1420

83. Kreuzer, K. N. Interplay between DNA replication and recombination in prokaryotes. Annu Rev Microbiol 2005; 59: 43-67

84. Kroemer G, El-Deiry W. S, Golstein P, Peter M. E, Vaux D, Vandenabeele P, Zhivotovsky B, Blagosklonny M. V, Malorni W, Knight R. A, Piacentini M, Nagata S, and Melino G, Classification of cell death: recommendations of the Nomenclature Committee on Cell Death. Cell Death Differ 2005;12(2):1463–1467

85. Kurose A, Tanaka T, Huang X, Halicka H. D, Troganos F, Dai W and Darzynkiewicz Z Assessment of ATM phosphorylation on ser-1981 induced by DNA topoisomerase I and II inhibitors in relation to ser-139-Histone H2AX phosphorylation, cell cycle phase and apoptosis. Cytometry Part A 2005;68A:1-9

86. Lee D. G, Hahm K. S, Park Y, Kim H. Y, Lee W, Lim S. C, Seo Y. K and Choi C. H Functional and structural characteristics of anticancer peptide Pep27 analogues. Cancer Cell International 2005;5:21

87. Levesque A**,** Paquet A**,** and Page M Measurement of Tumor Necrosis Factor Activity by Flow Cytometry. Cytometry 1995;20:181-184

88. Li Q, Dong C, Deng A, Katsumata M, Nakadai A, Kawada T, Okada S, Clayberger C, and Krensky A. M Hemolysis of erythrocytes by granulysin-derived peptides but not by granulysin. Antimicrob. Agents Chemother 2005;49:388–397

89. Li X and Heyer W. D Homologous recombination in DNA repair and DNA damage tolerance. Cell Research 2008;18:99-113

90. Lindgren M, Ha¨llbrink M, Prochiantz A., and Langel u¨ Cell-penetrating peptides, Trends Pharmacol. Sci. 2000;21:99– 103

91. Loew L. M. Determination of mitochondrial membrane potential in single living cells using confocal microscope images. SPIE 1996;2678:80-87

92. Lohner K, and Blondelle S. E Molecular mechanisms of membrane perturbation by antimicrobial peptides and the use of biophysical studies in the design of novel peptide antibiotics. Comb Chem High Throughput Screen 2005;8(3):241-56

93. Long B. H, Musal S. F, and Brattain M. G Single- and double-strand DNA breakage and repair in human lung adenocarcinoma cells exposed to etoposide and teniposide. Cancer Res 1985;45:3106-3112

94. Long B. H, Musal S. F, and Brattain M. G DNA breakage in human lung carcinoma cells and nuclei that are naturally sensitive or resistant to etoposide and teniposide. Cancer Res 1986;46:3809-3816

95. Lundberg M, and Johansson, M Positively charged DNAbinding proteins cause apparent cell membrane translocation. Bichem. Biophys. Res. Commun. 2002;291:367-371

96. Lundin S. L, Schultz N,Arnaudeau A, Mohindra A, Hansen L. T and Helleday T. RAD51 is involved in repair of damage associated with DNA replication in mammalian cells J. Mol. Biol. 2003;328:521-535

97. Lu¨ thi A. U, Martin S. J The CASBAH: A searchable database of caspase substrates. Cell Death Differ 2007;14:641–650

98. Maier B, Gluba W, Bernier B, et al. Modulation of mammalian life span by the short isoform of p53. Genes Dev. 2004;18:306-319

99. Martin R Cell suicide for beginners. Nature 1998;396:119-122

100. Masters, J. R. 2002. Hela cells 50 years on : the good, the bad and the ugly. Nat Rev Cancer. 2002;2:315-9

101. Matsuzaki K Biochim. Biophys. Acta 1999;1462:1-10

102. McGlynn, P, and Lloyd, R. G. Recombinational repair and restart of damaged replication forks. Nat Rev Mol Cell Biol (2002); 3: 859-870

103. Michel B, Grompone G, Flores M. J, and Bidnenko V. Multiple pathways process stalled replication forks. Proc Natl Acad Sci USA 2004;101:12783-12788

104. Miyanoshita A, Hara S, Sugiyama M, Asaoka A, Taniai K, Yukuhiro F and Yamakawa M. Isolation and characterization of a new member of the insect Defensin family from a beetle, Allomyrina dichotoma. Biochem Biophys Res Commun 1996;220:526-531

105. Morita E, Tada K, Chisaka H, Asao H, Sato H, Yaegashi N and Sugamura K Human Parvovirus B19 Induces Cell Cycle Arrest at G2 Phase with Accumulation of Mitotic Cyclins. Journal of Virology 2001; 75(16):7555-7563

106. Mosmann T. Rapid colorimetric assay for cellular growth and survival: application to proliferation and cytotoxicity assays. J Immunol Methods 1983; 65(1-2):55-63.

107. Nakagawa M and Miranda A. F Amonoclonal antibody against cytochrome c oxidase distinguishes cardiac and skeletal muscle mitochondria. Exp Cell Res 1987;168:44-52

108. Nakase I, Tadokoro A, Kawabata N, Takeuchi T, Katoh H, Hiramoto K, Negishi M, Nomizu M, Sugiura Y, and Futaki S Interaction of arginine-rich peptides with membraneassociated proteoglycans is crucial for induction of actin organization and macropinocytosis. Biochemistry 2007;46:492–501

109. Nicholls D. G and Budd S. L Mitochondria and neuronal survival Physiological Reviews 2000;80:315-360

110. Nichols W. W, et al. Characterization of a new human diploid cell strain, IMR-90. Science 1977;196:60-63

111. O'Driscoll M, and Jeggo P. A The role of double-strand break repair – insights from human genetics. Nature Reviews Genetics 2006;7:45-54

112. Oya N, Zolzer F, Werner F and Streffer C. Effects of serum starvation on radiosensitivity, proliferation and apoptosis in four human tumor cell lines with different p53 status. Strahlentherapie und Onkologie. 2003;179:99-106

113. Padari K, Sa¨a¨lik P, Hansen M, Koppel K, Raid R, Langel u¨, and Pooga M Cell transduction pathways of transportans. Bioconjug. Chem. 2005;16;1399–1410

114. Palffy R, Gardlik R, Behuliak M, Kadasi L, Turna J and Celec P On the physiology and pathophysiology of antimicrobial peptides. Mol. Med 2009;15(1-2):51-59

115. Palm-Apergi C, Lorents A, Padari K, Pooga M, and Ha¨llbrink M The membrane repair response masks membrane disturbances caused by cell-penetrating peptide uptake. FASEB J. 2009;23:214–223

116. Pang J. H, and Chen K. Y A Specific CCAAT-binding Protein, CBP/tk, May Be Involved in the Regulation of Thymidine Kinase Gene expression in Human IMR-90 Diploid Fibroblasts during Senescence. Issue of Febmam'5 1993;268(4):2909-2916

117. Papo N and Shai Y New lytic peptides based on the d, l amphipathic helix motif preferentially kill tumor cells compared to normal cells. Biochemistry 2003;42(31)9346-9354

118. Papo N and Shai Y A Molecular Mechanism for Lipopolysaccharide Protection of Gram-negative Bacteria from Antimicrobial Peptides. J Biol Chem 2005;280(11)10378-10387

119. Park J-H, Cosgrove M.S, Youngman E, Wolberger C and Boeke J. D A core nucleosomal surface crucial for transcriptional silencing. Nature Genetics 2002;32:273-279

120. Patel L. N, Wang J, Kim K-J, Borok Z, Crandall E. D and Shen W-C Conjugation with cationic cell-penetrating peptide increases pulmonary absorption of insulin. Mol. Therapeutics 2009; XXX(XX):A-L

121. Paull T. T, Rogakou E. P, Yamazaki V, Kirchgessner C. U, Gellert M, and Bonner W. M A critical role for histone H2AX in recruitment of repair factors to nuclear foci after DNA damage. Current Biology 2000;10(15):886-895

122. Paulsen R. D, and Cimprich C. A The ATR pathway: fine-tuning the fork. DNA repair 2007;6:953-966

123. Pistolesi S, Pogni R, and Feix J. B Membrane Insertion and Bilayer Perturbation by Antimicrobial Peptide CM15. Biophysical Journal 2007;93:1651–1660

124. Plumb J. A Cell sensitivity assays : the MTT assay. Methods Mol Med 2004;88:165-169

125. Pray L DNA replication and causes of mutation. Nature education 2008;1(1):

126. Raff M Cell suicide for begineers. Nature 1998;396(119-122)

127. Rajeev L, Segall A.M and Gardner J The bacteroides NBU1 integrase performs a homology-independent strand exchange to form a Holliday junction intermediate. J Biol Chem 2007;282(3):1228-1237

128. Rebourcet R, Mignot T. M, Robert B, Ferre F Endothelin-2 down-regulation occurs in parallel with the anti-proliferative effect of dimethylsulfoxide in BeWO human choriocarcinoma cell line. Cellular and molecular biology 2004;50:701-712

129. Renvoize C, Biola A, Pallardy M, and Breard J. Apoptosis: identification of dying cells. Cell Biol Toxicol 1998;14:111–120

130. Ribbeck K and Gorlich D Kinetic analysis of translocation through nuclear pore complexes. The EMBO Journal 2001;20(6)1320-1330

131. Richard J. P, Melikov K, Brooks H, Prevot P, Lebleu B, and Chernomordik L V Cellular uptake of unconjugated TAT peptide involves clathrin-dependent endocytosis and heparan sulfate receptors. J. Biol. Chem. 2005;280:15300–15306

132. Rios-Doria J, Fay A, Velkova A, Monteiro A. N DNA damage response: determining the fate of phosphorylated histone H2AX. Cancer Biol. Ther. 2006;5(2):142-4

133. Rogakou E.P, Pilch D.R, Orr A.H, Ivanova V.S, Bonner W.M DNA double strand breaks induce histone H2AX phosphorylation on serine 139. Journal of Biological Chemistry 1998;273:5858-5868

134. Rothkamm K, and Lo¨ brich M Evidence for a lack of DNA double-strand break repair in human cells exposed to very low x-ray doses. PNAS 2003;100(9):5057-5062

135. R¨uster C, Bondeva T, Franke S, F¨orster M, and Wolf G Advanced glycation end-products induce cell cycle arrest and hypertrophy in podocytes. Nephrol Dial Transplant 2008;23:2179–2191

136. Saido-Sakanaka H, Ishibashi J, Sagisaka A, Momotani E, and Yamakawa M Synthesis and characterization of bactericidal oligopeptides designed on the basis of an insect anti-bacterial peptide. Biochem. J. 1999;338:29-33

137. Saido-Sakanaka, H, Ishibashi, J, Momotani, E, Amano, F, and Yamakawa, M *In vitro* and *in vivo* activity of antimicrobial peptides synthesized based on the insect defensin. Peptides, 2004;25:19-27

138. Saintigny Y, Delacote F, Vares G, Petitot F, Lambert S, Averbeck D and Lopez B. S Characterization of homologous recombination induced by replication inhibition in mammalian cells. EMBO J 2001;20:3861-70

139. Savill J Regulation of glomerular cell number by apoptosis. Kidney Int, 1999;56:1216-1222

140. Scheller A, Oehlke J, Wiesner B, Dathe M, Krause E, Beyermann M, Melzig M, and Bienert M, Structural requirements for cellular uptake of alpha-helical amphipathic peptides. J. Pept. Sci. 1999;5:185– 194

141. Shai, Y Biochim. Biophys. Acta. 1999;1462:55-70

142. Shiozaki E. N, and Shi Y Caspases, IAPs and Smac/DIABLO: mechanisms from structural biology. Trends Biochem. Sci. 2004;29,486–494

143. Smith L. L, Brown K, Carthew P, Lim C. K, Martin E. A, Styles J, and White I. N Chemoprevention of Breast Cancer by Tamoxifen: Risks and Opportunities Crit. ReV. Toxicol. 2000;30:571-594

144. Soria G, Speroni J, Podhajcer O. L, Prives C, and Gottifredi V p21 differentially regulates DNA replication and DNA repair-associated processes after UV irradiation. Journal of Cell Science 2008;121:3271-3282

145. Sun M. G, Williams J, Munoz-Pinedo C, Perkins G. A, Brown J. M, Ellisman M. H, Green D. R, and Frey T. G Correlated three-dimensional light and electron microscopy reveals transformation of mitochondria during apoptosis. Nature Cell Biology 2007;9(9):1057-1065

146. Suttmann H, Retz M, Paulsen F, Harder J, Zwergerl U, Kamradt J, Wullich B Underteregger G, Stockle M and Lehmann J. BMC Urology 2008:8(5)

147. Takahashi A, Mori E, Somakos G. I, Ohnishi K, Ohnishi T Heat induces γ-H2AX foci formation in mammalian cells. Mutation Research 2008;656:88–92

148. Takata M, Sasaki M. S, Sonoda E, Morrison C, Hashimoto M, Utsumi H, Yamaguchi-Iwai Y, Shinohara A, and Takeda S Homologous recombination and non-homologous end joining pathways of DNA double-strand break repair have overlapping roles in the maintenance of chromosomal integrity in vertebrate cells. EMBO 1998;17(18): 5497–5508

149. Tanabe K, Ikegami Y, Ishida R, Andoh T Inhibition of topoisomerase II by antitumor agents bis (2, 6 dioxopiperazine) derivatives. Cancer Res. 1991;51:4903-8

150. Tavernarakis N Cardiomyocyte necrosis: Alternative mechanisms, effective interventions. Biochimica et Biophysica Acta 2007;1773:480–482

151. Terrone D, Sang S. L. W, Roudaia L, and Silvius J. R Penetratin and Related Cell-Penetrating Cationic Peptides Can Translocate Across Lipid Bilayers in the Presence of a Transbilayer Potential. Biochemistry 2003;42(47):13787–13799

152. Thiebaut F, Enns R, and Howell S. B Cisplatin Sensitivity Correlates With Its Ability to Cause Cell Cycle Arrest via a Wee1 Kinase-Dependent Pathway in Schizosaccharomyces pombe. Journal of Cellular Physiology 1994;159506514

153. Timmer J. C, Salvesen G. S Caspase substrates. Cell Death Differ 2007;14:66–72

154. Treszezamsky A. D, Kachnic L. A, Feng Z, Zhang J, Tokadjian C, Powell S. N Brca-1 and Brca-2 deficient cells are sensitive to etoposide-induced DNA double strand breaks via topoisomerase II. Cancer Res. 2007;67:7078-81

155. Tsaneva I. R, Muller B, and West S. C RuvA and RuvB proteins of Escherichia coli exhibit DNA helicase activity in vitro. Proc. Natl Acad. Sci. USA 1993;90:1315–1319

156. Tsukuda T, Fleming A. B, Nickoloff J. A, Osley M. A Chromatin remodelling at a DNA doublestrand break site in Saccharomyces cerevisiae. Nature 2005;438:379-83

157. Tyner S, Venkatachalam S, Choi J, Jones S, Ghebraniousk N, Igelmann H, Lu X, Soron G, Cooper B, Brayton C, ParkI S. H, ThompsonI T, Karsenty G, Bradley A & Donehower L p53 mutant mice that display early ageing-associated phenotypes. Nature 2002;415:45-53

158. Vafa O, Wade M, Kern S, Beeche M, Pandita T. K, Hampton G. M, and Wahl G. M c-Myc can induce DNA damage, increase reactive oxygen species, and mitigate p53 function: a mechanism for oncogene induced genetic instability. Mol. Cell 2002;9:1031–1044

159. van Gent D. C, Hoejimakers J. H. J and Kanaar R Chromosomal stability and the DNA-double stranded break connection. Nature Genetics;2:196-206

160. Van Maanen J. M. S, Retèl J, de Vries J, and Pinedo H. M Mechanism of Action of Antitumor Drug Etoposide: A Review J Natl Cancer Inst 1988;80:1526-1533

161. Varlamov D. A, Kudin A. P, Vielhaber S, Schroder R, Sassen R, Becker A, Kunz D, Haug K, Rebstock J, Heils A, Elger C. E and Kunz W. S Metabolic consequences of a novel missense mutation of the mtDNA CO I gene. Hum Mol Genet 2002;11:1797-1805

162. Vasquez B, Ishibashi F, and Howard B. V Measurement of Intracellular Volume in Monolayers of Cultured Cells. In Vitro Cellular & Developmental Biology – Plant 1982:18(7):643-649

163. Vermes I, Haanen C, Steffens-Nakken H, and Reutelingsperger C novel assay for apoptosis: Flow cytometric detection of phosphatidylserine expression on early apoptotic cells using fluorescein labelled Annexin V. J. Immunol. Methods 1995;184:39–51

164. Verzola D, Villagio B, Berruti V, Gandolfo M T, Deferrari G and Garibotto G Apoptosis induced by serum withdrawal in human mesangial cells. Exp Nephrology 2001;9:366-371

165. Walsh J. G, Cullen S. P, Sheridan C, Lüthi A.U, Gerner C and Martin S. J Executioner caspase-3 and caspase-7 are functionally distinct proteases. PNAS 2008;105(35):12815-12819

166. Wang X, Wang Ge. K, Qian J and Zou Y Evaluation of MTT assay for measurement of emodin-induced cytotoxicity. Assay Drug Dev Technol 2006;4:203-207

167. Ward I. M and Chen J Histone H2AX is phosphorylated in an ATR dependent manner in response to replication stress J Biol Chem 2001;276:47759-47762

168. Ward I. M, Minn K and Chen J UV-induced ATR activation requires replication stress. J Biol Chem 2004;279:9677-9680

169. Wen Q, Mahdi A. A, Briggs G. S, Sharples G. J, and Lloyd R. G Conservation of RecG activity from pathogens to hyperthermophiles. DNA Repair 2005;4:23–31

170. Wharton W and Goz B Induction of alkaline phosphatase activity in HeLa cells by choline chloride. Cancer Research 1978;38(11 Pt 1):3764-3748

171. Willers H, Xia F, and Powell S. N Recombinational DNA Repair in Cancer and Normal Cells: The Challenge of Functional Analysis. J Biomed Biotechnol. 2002;2(2):86–93

172. Wyman C, Kanaar R DNA double-strand break repair : All's well that ends well. Annu Rev Genetics 2006; 40:363-383

173. Yang D-S, Miaoa X-D, Ye Z-M, Feng J, Xub R-Z, Xin Huang, Gec F-F Bacterial redox protein azurin induce apoptosis in human osteosarcoma U2OS cells. Pharmacological Research 2005;52:413–421

174. Yano H, Nakanishi S, Kimura K, Hanai N, Saitoh Y, Fukoi Y, Nonumura Y and Matsuda Y Inhibition of histamine secretion by wortmannin through the blockade of phosphatidyl-inositol 3-kinase in RBL-2H3 cells. J. Biol. Chem, 1993 268:25846-25856

175. Zasloff, M Antimicrobial peptides of multicellular organisms. Nature 2002;415:389–395

176. Zhang J, Shideng B, Furumai R, Kucera K. S, Ali A, Dean N M and Wang X Protein phosphatase 5 is required for ATR-mediated checkpoint activation. Mol and Cell Biology. 2005;25(22):9910-9919

177. Zhang X, Jin y, Plummer M. R, Pooyan S, Guanaseelan S and Sinko P. J Endocytosis and membrane potential are required for HeLa cell uptake of R. I-CK Tat9, a retro-inverso tat cell penetrating peptide. Mol. Pharmaceutics. 2009;6(3):836-848

178. Zhao H and Piwnica-worms H ATR-mediated checkpoint pathways regulate phosphorylation and activation of human Chk1. Mol. And Cell. Biology. 2001;21(13):4129-4139

179. Zhou B. B and Elledge S. J The DNA damage response : putting checkpoints in perspective. Nature 2000;408(6811):433-439

180. Zou L, Cortez D and Elledge S. J Regulation of ATR substrate selection by Rad17-dependent loading of Rad9 complexes onto chromatin. Genes Dev. 2002;16:198-208

181. Zwaal R. F. A, Comfurius P, and Bevers E. M Surface exposure of phosphatidylserine in pathological cells. CMLS, Cell. Mol. Life Sci. 2005;62 :971–988.